Contribution of Calnexin to HIV-1 Nef effects on ABCA1

By Lucas Trent Jennelle

B.S. in Biochemistry, May 2003, Virginia Polytechnic Institute and State University
B.A. in Chemistry, May 2003, Virginia Polytechnic Institute and State University

A Dissertation submitted to

The Faculty of
The Columbian College of Arts and Sciences
of The George Washington University
in partial fulfillment of the requirements
for the degree of Doctor of Philosophy

May 19th, 2013

Dissertation directed by

Michael I. Bukrinsky
Professor of Microbiology/Tropical Medicine and Biochemistry/Molecular Biology

The Columbian College of Arts and Sciences of The George Washington University certifies that Lucas Trent Jennelle has passed the Final Examination for the degree of Doctor of Philosophy as of March 21st, 2013. This is the final and approved form of the dissertation.

Contribution of Calnexin to HIV-1 Nef effects on ABCA1

Lucas Trent Jennelle

Dissertation Research Committee:

Michael I. Bukrinsky, Professor of Microbiology/Tropical Medicine and Biochemistry/Molecular Biology, Dissertation Director

Ajit Kumar, Professor of Biochemistry and Molecular Biology, Committee Member

David Leitenberg, Associate Professor of Microbiology, Immunology & Tropical Medicine, Committee Member

© Copyright 2013 by Lucas Trent Jennelle
All rights reserved

Dedication

To my wife Liza, my daughter Georgia, and my son Felix who have supported me every step of the way and for whom I work so diligently every day. To my mother, father, and brother whose pride and assistance has provided everything else I've ever needed. And to each and every teacher I've ever had at any level, yours is a thankless job always done with love. It is my pleasure to personally dedicate this thesis to Dr. Peter Kennelly, Dr. David Bevan, Dr. Eugene M. Gregory, and Dr. Muriel Lederman of Virginia Tech for helping me realize that I am, and always will be, a scientist.

Acknowledgments

I would like to thank Dr. Michael Bukrinsky for his fantastic mentorship, patience, support, and the opportunity to pursue my thesis research in his lab. He has always been my biggest champion and I could never thank him enough for his assistance and encouragement. I would like to thank my committee members: Dr. Norman Lee, Dr. David Leitenberg, Dr. Ajit Kumar, Dr. Timothy McCaffrey, and Dr. Steven Zeichner who provided valuable guidance during the pursuit of my studies and critical review of my research. My sincerest thanks to all of the past and present members of the Bukrinsky laboratory throughout my tenure: Angela Grant, Zahedi Mujawar, Matthew Morrow, Tatiana Pushkarsky, Sergey Iordanskiy, Ruth Hunegnaw, Steven Santos, and Larisa Dubrovsky. I must also thank Dr. Peter Hotez, for his invaluable service as Department Chair. Thanks to Dr. Anamaris Colberg-Poley and all members of her lab for a wonderful rotation experience and continued support.

I must thank all members of the Microbiology, Immunology, and Tropical Medicine Department who have accepted me as a member of the community for the past six years. Very special thanks are also due to Anastas Popratiloff and Theresa Hawley for expert guidance in microscopy and flow cytometry, without which my research would not have been possible. Additionally, Dr. Kristy Brown and Dr. Yetrib Hathout provided expert assistance in mass spectrometry and proteomics technologies at Children's National Medical Center. Dr. Christine Bianchini from Leica Microsystems was also instrumental in capturing and analyzing images for Confocal Microscopy at Super-Resolution.

Abstract of Dissertation

Contribution of Calnexin to HIV-1 Nef effects on ABCA1

HIV-infected patients are at increased risk of developing atherosclerosis, in part due to an altered HDL profile exacerbated by downmodulation and impairment of ATP-Binding Cassette Transporter A1 (ABCA1) activity by the HIV-1 protein Nef. Nef has been shown to increase delivery of cholesterol to lipid rafts, sites of viral assembly and egress, by inhibition of ABCA1 cholesterol efflux functionality and reduction of ABCA1 protein levels through lysosomal degradation. Important mechanistic details of ABCA1 inactivation and degradation by Nef, and whether these two processes are intimately linked or separable are still to be defined. The studies presented here were designed to identify cellular co-factors for ABCA1-mediated cholesterol efflux that may be targeted by Nef to achieve ABCA1 inactivation. In these studies, a novel cellular factor, the ER-resident lectin chaperone calnexin, was shown to be involved in a physical interaction with ABCA1 that is disrupted by Nef. Nef was found to bind and redistribute calnexin and reduce binding and co-localization of ABCA1 with calnexin. In vitro knockdown of calnexin via RNAi reproduced several previously described biochemical effects of Nef, including redistribution of ABCA1, increased ABCA1 membrane localization, and reduced ABCA1 recycling. Importantly, knockdown of calnexin also resulted in reduced ABCA1-mediated cholesterol efflux, but without the Nef-mediated reduction in ABCA1 protein levels, suggesting that Nef utilizes a bipartite mechanism to inactivate and degrade ABCA1 and that these functions may be separable. Despite the lack of effect of calnexin knockdown on

ABCA1 protein levels, interference with the ABCA1-calnexin interaction was critical for Nef-mediated functional impairment of ABCA1. This was shown with a Nef mutant defective in interaction with calnexin which was incapable of preventing ABCA1-calnexin interaction and was also defective in impairing ABCA1-mediated cholesterol efflux activity. Thus, these studies identified a novel mechanism by which HIV-1 Nef impairs functional activity of cholesterol transporter ABCA1 by blocking its interaction with calnexin. Calnexin acts as an ABCA1 functional chaperone, limiting total and cell surface ABCA1 expression while increasing ABCA1-mediated cholesterol efflux. Combined with the demonstration that Nef increases delivery of ABCA1 to lysosomes, these results suggest the Nef-mediated impairment of ABCA1 function involves reduced interaction with calnexin followed by delivery of ABCA1 to lysosomes for degradation.

Table of Contents

Dedication iv

Acknowledgments v

Abstract of Dissertation vi

Table of Contents viii

List of Figures x

List of Tables xi

List of Abbreviations xii

Chapter 1: Introduction 1

I: Cardiovascular Disease 1

A: Role of HDL 1

C: Cholesterol Efflux and ABCA1 3

II: HIV, Atherosclerosis, and Nef 8

A: HIV and Lipids 8

B: HIV, Atherosclerosis, and Metabolic Syndrome 14

C: Nef and ABCA1 20

III: Calnexin 26

A: Calnexin and its Substrates 26

B: Viruses and Calnexin 29

Chapter 2: Specific Aims 30

Chapter 3: Materials and Methods 33

Chapter 4: Identification of ABCA1-interacting proteins affected by Nef 49

Chapter 5: ABCA1 physically interacts with calnexin 51

Chapter 6: Nef reduces physical interaction of calnexin and ABCA1 58

Chapter 7: Nef physically interacts with calnexin.....78

Chapter 8: Nef expression or calnexin knockdown redistribute ABCA1.....87

Chapter 9: Calnexin contributes to ABCA1 Function 91

Chapter 10: Discussion 101

Bibliography 116

List of Figures

Figure 1. Contribution of cholesterol to the HIV life cycle…….…….....10

Figure 2. Nef binds, redistributes, and degrades ABCA1…….…….....22

Figure 3. ABCA1 Interacts with Calnexin……...…….…….....52

Figure 4. ABCA1 interaction with calnexin is Glycan-Independent..…….....55

Figure 5. Nef disrupts ABCA1 interaction with Calnexin..……...……..59

Figure 6. Nef diminishes ABCA1 and Calnexin interaction during infection....….....62

Figure 7. Nef does not alter cellular localization or solubility of calnexin....….....65

Figure 8. Nef Does Not Alter Raft Partitioning of Calnexin…….....…….....69

Figure 9. Nef induces segregation of calnexin and ABCA1...…….....…….72

Figure 10. Nef increases calnexin surface expression and PACS-2 interaction.....76

Figure 11. Nef Co-Localizes with ER...…….…….....79

Figure 12. Nef Physically Interacts with Calnexin..……..82

Figure 13. Membrane association is required for Calnexin-Nef interaction……85

Figure 14. Calnexin knockdown allows ER escape of ABCA1...……88

Figure 15. Calnexin contributes to ABCA1 Function…….....92

Figure 16. Calnexin knockdown increases total and surface ABCA1 expression…...95

Figure 17. Calnexin knockdown reduces ABCA1 recycling…….....99

Figure 18. Nef effects on ABCA1 and Calnexin……...104

List of Tables

Table 1 ABCA1 Interacting Proteins Identified by MS/MS…….50

List of Abbreviations

1.	ABCA1	ATP-binding cassette transporter A1
2.	ABCG1	ATP-binding cassette transporter G1
3.	AME	amphotericin B methyl ester
4.	ApoA-I	apolipoprotein A1
5.	ARL7	ADP-ribosylation factor (ARF)-like 7
6.	ART	antiretroviral therapy
7.	CA	capsid, viral protein
8.	CE	cholesteryl esters
9.	CETP	cholesteryl ester transfer protein
10.	CNX	calnexin
11.	cIMT	carotid intima-media thickness
12.	CRP	c-reactive protein
13.	CVD	cardiovascular disease
14.	DC	dendritic cell
15.	EC	endothelial cell
16.	EndoH	endoglycosidase H
17.	*env*	envelope, gene of retroviruses
18.	EPC	endothelial progenitor cell
19.	FRAM	Study of Fat Redistribution and Metabolic Change in HIV Infection
20.	*gag*	group antigen, gene of retroviruses
21.	GPL	glycerophospholipid

22. GPX	glutathione peroxidase
23. GSL	glycosphingolipid
24. HDL	high density lipoprotein
25. HDL-C	high density lipoprotein cholesterol
26. HIV-I	human immunodeficiency virus type 1
27. HL	hepatic lipase
28. HMG-CoA	hydroxymethyl glutaryl coenzyme A
29. HTGL	hepatic triglyceride lipase
30. ICAM-1	intercellular adhesion molecule 1
31. IFNγ	interferon gamma
32. IL-1	interleukin 1
33. IL-6	interleukin 6
34. IN	integrase, viral protein
35. LCAT	lecithin:cholesterol acyl transferase
36. LDL	low density lipoprotein
37. LDL-C	low density lipoprotein cholesterol
38. LDLr	LDL receptor
39. Lp(a)	lipoprotein(a)
40. LPL	lipoprotein lipase
41. LRP	LDL receptor-related protein
42. LXR	liver x receptor
43. MA	matrix, viral protein

44. MACS Multicenter AIDS Cohort Study

45. MCP-1 monocyte chemoattractant protein 1

46. MCSF macrophage colony-stimulating factor

47. MDM monocyte-derived macrophage

48. MHC-I major histocompatibility complex class I

49. MI myocardial infarction

50. MMP matrix metalloproteinase

51. NC nucleocapsid, viral protein

52. Nef negative factor, viral protein

53. NIH National Institutes of Health

54. NO nitric oxide

55. NPC1 Niemann-Pick type C1 protein

56. oxLDL oxidized LDL

57. PAF platelet activating factor

58. PAF-AH platelet activating factor acetyl-hydrolase

59. PBL peripheral blood lymphocyte

60. PBMC peripheral blood mononuclear cell

61. PC phosphatidylcholine

62. PGI_2 prostaglandin I_2, prostacyclin

63. $PI(4,5)P_2$ phosphatidylinositol-4,5-bisphosphate

64. PIC pre-integration complex

65. PLTP phospholipid transfer protein

66. PNGase peptide: n-glycosidase F

67. *pol* polymerase, gene of retroviruses

68. PON paraoxonase

69. PR protease, viral protein

70. RCT reverse cholesterol transport

71. REV regulator of virion expression, viral protein

72. RNAi rna interference

73. RT reverse transcriptase, viral protein

74. RXR retinoid x receptor

75. S1P sphingosine-1-phosphate

76. SAA serum amyloid A

77. siRNA short interfering rna

78. SM sphingomyelin

79. SMART Strategies for Management of AntiRetroviral Therapy

80. SMC smooth muscle cell

81. SR-A scavenger receptor, class A

82. SR-BI scavenger receptor, class B, type I

83. TAT trans-activator of transcription, viral protein

84. TGFβ transforming growth factor beta

85. TNFα tumor necrosis factor alpha

86. tPA tissue plasminogen activator

87. TR transferrin receptor

88. VLDL	very low density lipoprotein
89. VSMC	vascular smooth muscle cell
90. VCAM-1	vascular cell adhesion molecule 1
91. Vif	viral infectivity factor, viral protein
92. Vpr	viral protein R, viral protein
93. Vpu	viral protein U, viral protein
94. WT	wild-type

Chapter 1: Introduction

I. Cardiovascular Disease

Cardiovascular disease (CVD) has been on an unprecedented march up the tabulation of human disease burden and morbidity and mortality statistics since the beginning of the 20th century. At the beginning of the century, 10 percent of all deaths were caused by CVD; by 2001 the number had risen to 30 percent (1). Often considered a disease of the developed-world, 80 percent of CVD disease burden actually occurs in low- to middle-income countries (1) where CVD disease burden overlaps most significantly with disease burden of all infectious diseases, including upper respiratory- and sexually transmitted-infections. In 1996, estimates suggested that by 2020, CVD would be the leading cause of death and disability in both the developed- and developing-world. However, as of 2012, this estimate has been eclipsed and today CVD is recognized as the leading cause of death worldwide.

A. Role of HDL

In humans the atherosclerotic disease process reflects an imbalance in tissue cholesterol delivery needs and excess cholesterol removal focused at the cellular level of arterial macrophages, tasked with removing cholesterol from atherosclerotic lesions. This balance is itself reflected in the ratio of the major lipid classes in the circulation. Studies such as the Framingham Heart Study have demonstrated that total- and Low Density Lipoprotein-cholesterol (LDL-C) correlate directly with CVD risk while an inverse relationship exists between CVD mortality and High Density Lipoprotein

Cholesterol (HDL-C) (2). Thus, the concept of a balance between HDL, the so-called "good" cholesterol species and LDL, the "bad" cholesterol species has emerged. While entirely too simple, as both HDL and LDL species are highly heterogeneous functionally and structurally (3-5), the concept does capture the essence of current opinions on the influence of HDL and LDL on CVD risk. Among the multitude of CVD risk factors defined by studies such as Framingham, cholesterol level has proven especially critical as elevated cholesterol can cause CVD in humans and animals in the absence of other traditional risk factors (6). The positive association of HDL-C with atheroprotection has fostered research into the atheroprotective function of HDL and treatments to increase HDL levels as an avenue to treat established CVD (7, 8).

HDL is thought to originate from the liver where apolipoprotein A1 (ApoA-I) containing lipoprotein species are minimally lipidated by hepatic ATP-Binding Cassette Transporter A1 (ABCA1) (9, 10, 10). Lipid-poor ApoA-I in the circulation can remove cholesterol and phospholipids directly from peripheral tissues (mainly macrophages) through the action of macrophage ABCA1 to form discoidal pre-β HDL which is converted to mature spherical α-HDL through esterification of free cholesterol by lecithin:cholesterol acyl transferase (LCAT) (7, 9, 10). Additional proteins, including ATP-Binding Cassette Transporter G1 (ABCG1), can efflux cholesterol to mature HDL but ABCA1 appears to be unique in the ability to efflux cholesterol and phospholipids to lipid poor ApoA-I to generate mature HDL (11, 12). The ApoA (mainly ApoA-I) containing HDL-like particles contain relatively low cholesterol, phospholipid, and triglyceride and are antiatherogenic while the ApoB (mainly ApoB-100) containing LDL-

like particles enriched in cholesterol, phospholipid, and triglyceride tend to cycle through cholesterol exchange between VLDL→IDL→LDL→Lp(a) and remain in the circulation where they exert proatherogenic effects. From this information, it can be appreciated that HDL and LDL levels are interdependent and reflect a balance between tissue cholesterol delivery needs (LDL) and excess cholesterol removal (HDL) and this balance can be altered by an atherogenic diet, genetic factors, and traditional CVD risk factors. This model defines reverse cholesterol transport (RCT) as a perpetual cycle in which cholesterol acceptors (pre-β-1 and apoA-I) are continuously loaded with cholesterol in the periphery, traffic to sites of cholesterol deposit, and are regenerated by cholesterol removal at these sites (7). Several atheroprotective functions have been ascribed to HDL including; enhancement of EC function and inhibition of LDL oxidation (7) but the major atheroprotective function of HDL is participation in RCT (4, 5).

B. Cholesterol Efflux and ABCA1

Cholesterol Efflux

With atherosclerosis now one of the leading causes of morbidity and mortality worldwide, understanding the biogenesis of HDL and mechanisms contributing to atheroprotection by increasing the content of circulating HDL are of paramount importance to global health. It is widely accepted that the primary anti-atherogenic function of HDL is participation in the process of Reverse Cholesterol Transport (RCT) or "cholesterol efflux" (3-5, 9, 10, 13). Succinctly RCT is "*the transfer of cholesterol from nonhepatic cells to the liver*" (7). The fundamental elements of current models of RCT were described over 50 years ago by Glomset and Wright (14). Today, RCT is

viewed as a dynamic process involving cell surface transporters, plasma lipid acceptors, plasma proteins and enzymes, and hepatic cholesterol acceptors (5).

The major atheroprotective contribution of HDL appears to be the removal of cholesterol from macrophages in the artery wall, the initiating event in RCT (3). Cholesterol efflux to HDL occurs through three main pathways; passive diffusion, active efflux by ABCA1 and ABCG1, and bidirectional cholesterol exchange by SR-BI (5). Despite the minimal contribution of macrophage cholesterol to the total pool of HDL-C, active cholesterol efflux to HDL by ABCA1 and ABCG1 contributes as much as 70% of cholesterol effluxed from macrophages upon cholesterol loading (5, 15). Recently, animal models constituting a "macrophage-to-feces" approach and allowing specific measurement of RCT have demonstrated that RCT correlates more favorably than HDL-C with measures of atherosclerosis and suggest that these approaches may be specifically investigating a dynamic atheroprotective process rather than the static outlook provided by total HDL-C measurements (5). A critical role for RCT in atheroprotection has also been suggested by the decreased atherosclerotic sequalae observed in several clinical trials involving infusion of pre-β HDL (apoA-I) (5). Further supporting the atheroprotective function and clinical relevance of RCT, recently developed methodologies to measure specific macrophage cholesterol efflux capacity of patient serum have reported efflux capacity and RCT to be inversely associated with carotid intima-media thickness (cIMT) and CAD likelihood independently of total HDL-C (16). Thus, while the contribution of RCT-derived cholesterol to total HDL-C may be small, specific measurements of RCT appear to confirm the role of arterial macrophage-derived

cholesterol in atherosclerosis and the role of RCT in prevention and reversal of the atherosclerotic process.

ABCA1

Perhaps the most important mediator of circulating HDL in the periphery is the ATP-binding cassette transporter A1 (ABCA1). ABCA1 is a full-size transporter of the ABC superfamily whose members include a number of membrane transport proteins that hydrolyse ATP to efflux a variety of substrates including sugars, proteins, lipids, and drugs (12, 17). ABCA1 is the major component of the cellular process of RCT. The pivotal discovery of ABCA1 as the product of the gene mutated in Tangier disease (18-22) has given rise to a steadily growing body of literature concerning the biogenesis, activity, regulation and recycling of this key cholesterol transporter. *In vitro* studies of ABCA1 mutants that occur naturally in certain Tangier lineages have defined a pathway whereby; ABCA1 expression, cycling through the vesicular network, trafficking to the plasma membrane, and ApoA-I binding and internalization are all required for maximal cholesterol efflux (23, 24). Importantly, several ABCA1 mutants appear to exhibit abnormal folding and are retained within the ER resulting in decreased cholesterol efflux (23-26). Several significant aspects of ABCA1 biology remain poorly characterized and controversial, among them are; elements of the interaction between ABCA1 and the primary circulating acceptor of cellular cholesterol, ApoA-I (11), mechanisms regulating ABCA1 turnover, and identification of components involved in regulation of ABCA1-mediated efflux (27). The emerging outlook suggests an integrated view of ABCA1

function that links intracellular trafficking and protein turnover in function and regulation of ABCA1.

While intracellular trafficking and turnover of ABCA1 are known to contribute to regulation of cholesterol efflux, the elements of the two pathways have most often been described as separable phenomena. In Raw264.7 cells, treatment with Cyclosporin A "traps" ABCA1 at the plasma membrane and leads to defective cholesterol efflux but increases total and cell surface ABCA1 levels (28). Likewise, the PEST sequence in ABCA1 mediates internalization and degradation by an unknown calpain protease, whereas deletion of this sequence markedly increases cell surface expression and cholesterol efflux functionality of ABCA1 (29-31).

ABCA1 as a Cholesterol Efflux Receptor

In addition to functions encoded in the sequence of ABCA1 itself, such as ATP-hydrolysis and ApoA-I binding, ABCA1 interacting proteins also contribute to maximal cholesterol efflux and contribute to a model of ABCA1 as a functional "receptor" for cholesterol efflux. *In vitro*, cholesterol efflux is a multi-determinant process involving regulation by cholesterol metabolites, trafficking and turnover of ABCA1, and intracellular signaling (27). Cholesterol efflux is initiated by interaction between ABCA1 and "ligands" such as Phospholipid Transfer Protein (PLTP) or ApoA-I (32, 33). The Liver X Receptor β isoform (LXRβ) binds and regulates ABCA1 and is suggested to tune ABCA1 function to cellular demand for cholesterol (34, 35). A variety of PDZ domain containing- and associated scaffolding proteins including α- and β-syntrophins, Utrophin, and Dystrophin affect trafficking, distribution, and corresponding functional activity, of

ABCA1 (36-39). Extending the analogy of ABCA1 as a functional "receptor" molecule for cholesterol efflux, cholesterol acceptor interaction with ABCA1 initiates a series of intracellular signaling cascades involving a variety of kinases and GTPases including PKA (40), PKC (41, 42), Cdc42 (43) and Casein Kinase II (CKII) (44).

Members of the ABC superfamily are large, multi-domain proteins with a complex architecture. Topologically, ABCA1 is arranged as a full transporter with two functionally similar ABC transporter motifs each containing, in sequence; a short N-terminal Cytoplasmic sequence, a large extracellular loop (ECL), an extensive transmembrane region (TM), and a C-terminal cytoplasmic domain with several regulatory sites (NBD) (33, 45). Proper lectin-assisted domain folding is proposed to contribute to the stability of several ABC family members (46, 47). Two well-studied ABC transporters, CFTR and P-glycoprotein, interact with the ER lectin chaperone calnexin, and folding mutants of these transporters are retained within the ER by calnexin and eventually degraded (48, 49). Importantly, mutants that cannot escape calnexin binding do not achieve mature glycosylation and these mutations result in reduced transporter function (48, 49).

The position of ABCA1 as a "gatekeeper" in the biogenesis of HDL makes biological interactions influencing the biogenesis, stability, and functionality of ABCA1 of paramount importance to interventions in atherosclerosis (50). While many ABCA1 interaction partners have been described, relatively few proteins that directly affect ABCA1 biogenesis have been identified. Recently, an ER Serine Palmitoyltransferase (SPTLC1) was shown to bind and retain ABCA1 in the ER resulting in inhibition of

cholesterol efflux that could be overcome by inhibiting SPTLC1 with myriocin (51). The biological role of the negative regulation by SPTLC1 is unclear but is proposed to allow cells to react to states of high lipid demand, i.e. during membrane bilayer synthesis (17, 51). While SPTLC1 is an informative example of a negative regulator of ABCA1 biogenesis, proteins and pathways that positively affect this process, which may represent better therapeutic targets because they target ABCA1 directly, have remained elusive.

II. HIV, Atherosclerosis and Nef

A. HIV and Lipids

HIV

Acquired Immune Deficiency Syndrome (AIDS) was originally described as an epidemiological clustering of cases of opportunistic infections in male homosexuals in North America in 1981 (52). Subsequently, AIDS was defined as a disease of profound immunodeficiency characterized by specific opportunistic infections and neoplasms and the causative agent was identified as a retrovirus, now known as Human Immunodeficiency Virus Type 1 (HIV-1), by several groups in 1983-84 (52). Today HIV-1 is a pandemic scourge infecting an estimated 60 million people and responsible for a mounting death toll of at least 25 million (52).

HIV-1 belongs to the lentivirus genera of the *Retroviridae* family and is thought to have arisen from a cross-species introduction of a similar retrovirus occurring naturally in chimpanzees in West Africa (52). The *Retroviridae* are divided into two categories, simple and complex, based on their genome complexity. All retroviruses encode

structural (*gag*), enzymatic (*pol*), and receptor-binding (*env*) protein-coding genes while the complex retroviruses also encode a variety of additional proteins (53). Mature HIV virions include a 9 kilobase genome and 15 distinct proteins (**Fig. 1A**) (53). The *gag* and *pol* genes encode the GagPol precursor polyprotein which is cleaved by viral protease in mature virions to liberate Gag and Pol precursor polyproteins. Gag polyprotein is cleaved by viral protease into Matrix (MA), Capsid (CA), Nucleocapsid (NC), and p6 proteins (53). The *pol* gene encodes the Pol polyprotein that is cleaved by viral protease into Protease (PR), Reverse Transcriptase (RT), and Integrase (IN) proteins (53). The *env* gene encodes the Env (gp160) preprotein that is cleaved by cellular Furin protease (54) into surface (SU, gp120) and transmembrane (TM, gp41) proteins (53). In addition to the major proteins common to all retroviruses, HIV-1 also encodes regulatory (Tat and Rev) and accessory (Vpu, Vpr, Vif, and Nef) proteins (53).

HIV-1 exclusively infects T-cells, macrophages, and dendritic cells (and specialized subsets of these cell types i.e. Kupffer cells) through host cell receptor CD4. HIV infection begins with CD4 binding by the viral envelope protein SU/gp120 and subsequent engagement of co-receptors CXCR4 or CCR5 by gp120 (**Fig. 1B**) (53). Receptor binding and virus-cell fusion are mediated by SU/gp120 and TM/gp41, respectively. Upon fusion the virus undergoes "uncoating," reverse transcription, trafficking to the nucleus, and trans-location through the nuclear pore. Inside the nucleus, viral DNA integrates into the host cell genome. Proviral DNA is transcribed into mRNA using host cell machinery and viral mRNAs and full-length genomic RNAs are

A.

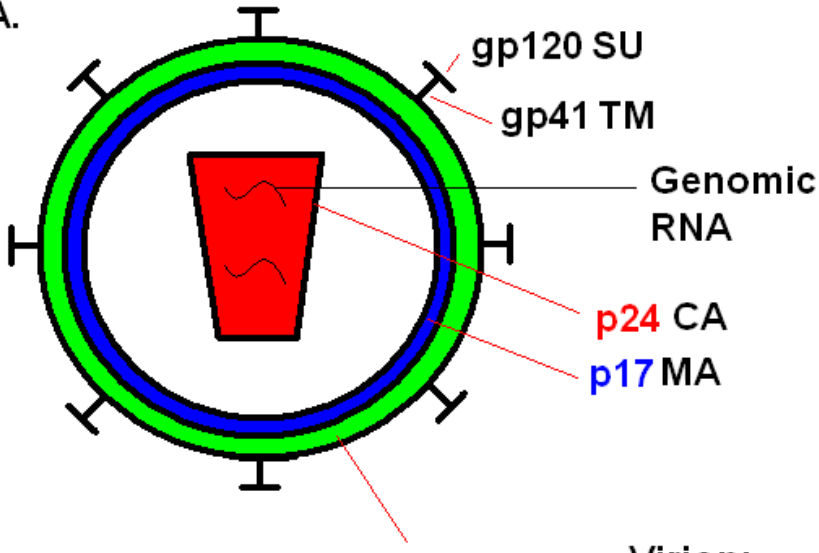

Viral Core:

RT IN
Vpr PR
NC p6

Virion:

Vif Nef

B.

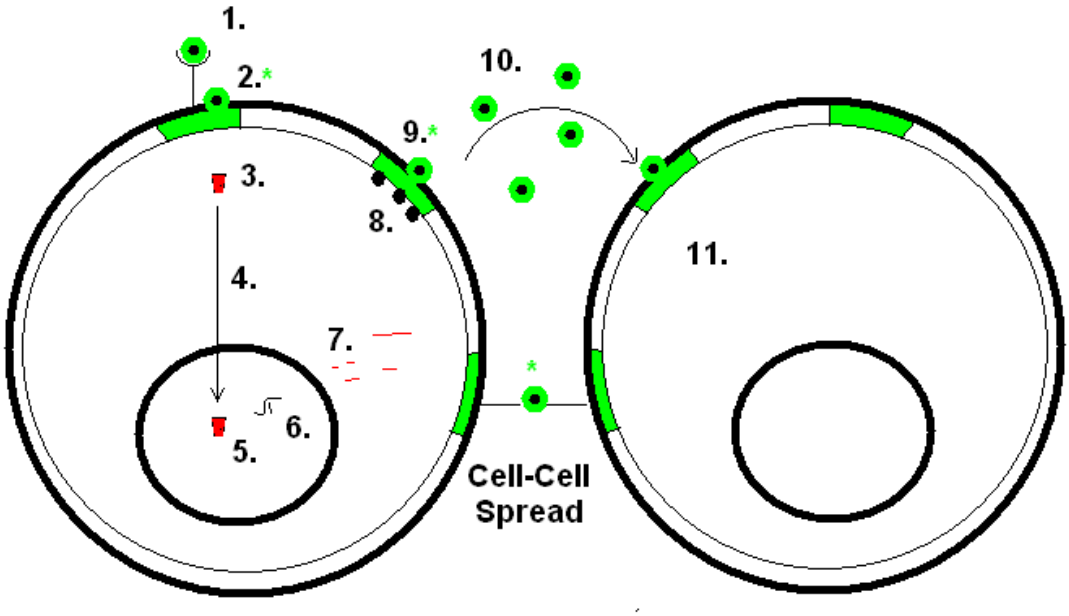

Figure 1. Contribution of cholesterol to the HIV life cycle

A. **Depiction of a mature HIV virion**. Proteins depicted are gp120 (Surface, SU), gp41 (Transmembrane, TM), p24 (Capsid Antigen, CA), p17 (Matrix Antigen), Reverse Transcriptase (RT), Integrase (IN), Viral Protein R (Vpr), p7 (Nucleocapsid, NC), p6 (Vpr-binding protein), Protease (PR), Nef, and Vif. B. **The HIV replication cycle** involves: receptor (CD4) binding (1), virus-cell fusion (2), "uncoating" (3), reverse transcription and trafficking to the nucleus (4), trans-location through the nuclear pore (5), and viral DNA integration into the host cell genome (6). Proviral DNA is transcribed into mRNA using host cell machinery and viral mRNAs and full-length genomic RNAs are transported from the nucleus to the cytoplasm (7). Upon translation, Gag, GagPol, and Env proteins are transported to plasma membrane assembly sites along with full-length viral genomes (8). Assembling virions bud from the host cell plasma membrane (9). Once released, virions undergo maturation (10) and mature virus can infect new target cells to repeat the life cycle (11). Steps in the life cycle sensitive to cholesterol depletion are indicated with a green asterisk and are described in the text. Cell-cell spread is depicted in the minimal space between the producer and target cell. Viral envelope in A. is green to indicate cholesterol enrichment as a result of budding through lipid rafts (green patches) as depicted in B.

transported from the nucleus to the cytoplasm with the aide of the viral Rev protein. Upon translation, Gag, GagPol, and Env proteins are transported to plasma membrane assembly sites along with full-length viral genomes. Assembling virions bud from the host cell plasma membrane. Once released, virions undergo maturation, involving a series of cleavages by the viral protease (observed ultrasctucturally as core condensation) and become fully infectious. Upon encountering a target cell expressing CD4, virus can infect to repeat the life cycle.

HIV and Lipids

Viruses are obligate intracellular pathogens that require host-derived components for their replication. Many types of viruses have been studied scientifically and among them are viruses, like HIV-1, that are coated in a host cell-derived layer of cholesterol and lipids, known as enveloped viruses, and others that do not have an envelope, so-called naked viruses. Since viruses themselves have no means to produce cholesterol and lipids, these components must be commandeered from infected cells during viral replication. Thus, the composition of virus envelopes can provide important information about producer cells and the viral life cycle. Recent advances in lipidomics technologies have allowed investigation of the composition of purified HIV-1 viral envelopes which has informed contemporary models of HIV-1 fusion, assembly, and budding. The lipidome of purified HIV-1 virions is enriched in saturated phosphatidylcholines (PCs) and cholesterol, similar to cellular membrane domains termed “lipid rafts”, suggesting that HIV-1 buds from these microdomains (53) (**Fig. 1B**). Further, HIV-1 has evolved

mechanisms to ensure specific interactions with lipids and drugs that target these interactions have provided many clues about the HIV-1 life cycle and viral pathogenesis.

Lipid species, particularly cholesterol, contribute to HIV-1 entry, assembly/budding, and cell-cell transmission. Cholesterol in virions is required for HIV-1 entry as depletion of virion or producer cell cholesterol with β-cyclodextrin, 2-hydroxypropyl-β-cyclodextrin, nystatin, or amphotericin B methyl ester (AME) significantly reduces viral infectivity and this effect has been shown to involve reduced virus cell membrane fusion (53). Cholesterol in target cells is also required for HIV-1 infectivity as treating cells with cyclodextrins to deplete cholesterol, statins to inhibit cholesterol biosynthesis, or nystatin or filipin to modulate cholesterol organization also inhibits HIV-1 entry, an effect that may be mediated by disruption of lipid rafts (53). For HIV-1 particle assembly to occur, Gag proteins must interact with the plasma membrane and organize into multimers which occurs within lipid rafts. Disruption of lipid rafts in producer cells through cholesterol modulation with cyclodextrins, statins, or AME reduces HIV-1 particle production (53). Lipids in lipid rafts also contribute to a highly efficient mechanism of HIV-1 viral particle exchange between infected and uninfected cells known as cell-cell transmission. In the process of cell-cell transmission, Env proteins cluster at a specific pole of an infected T-lymphocyte that is oriented towards an uninfected cell, thereby causing CD4 to cluster in the opposing pole in the uninfected cell and drawing the two cellular membranes into proximal juxtaposition (53). Virus can rapidly traverse the limited extracellular space at the “virological synapse” and initiate infection in the uninfected cell. Lipid rafts and cholesterol, in particular, have been

shown to contribute to this phenomenon as cholesterol depletion can prevent the necessary polarization of Env in infected cells and CD4 in uninfected cells (53). In support of the concept that lipids are critical in the HIV-1 replication cycle, the HIV Nef protein has been shown to have activity in ensuring availability of lipids during this process. Nef has been shown to increase biosynthesis of cholesterol, bind cholesterol directly, and increase cholesterol in lipid rafts and virions (53, 55). Nef has also been shown to down-regulate ABCA1 and reduce efflux of excess cholesterol, thereby increasing the cellular cholesterol pool (discussed in detail later in this document) (56).

The requirement for cholesterol (particularly as a component of lipid rafts) as an integral component of the viral life cycle and the existence of viral programs targeting cellular cholesterol metabolism machinery suggests that increasing cellular cholesterol in the principle cell targets of HIV infection, T-cells and macrophages, may define a viral strategy to ensure availability of cholesterol for nascent virion production. A logical extension of this concept is that defects in opposing cholesterol removal pathways induced by viral proteins at the cellular level may have unintended consequences at a cardiovascular level as a result of imbalance in cholesterol delivery and removal systems. In turn, the defects at a systems level may be propagated to the organismal level in the form of increased CVD pathology.

B. HIV, Atherosclerosis, and Metabolic Syndrome

The introduction of antiretroviral therapy (ART) has transformed HIV from an acutely fatal disease of immunodeficiency and fulminant opportunistic infections into a manageable condition with near normal life expectancy. However, as larger numbers of

HIV-infected patients age, it has become clear that certain co-morbidities are prevalent in this population; including cancer, liver disease, renal disease, dementia, and bone disease (57). The existence of an AIDS-defining wasting syndrome and an associated metabolic syndrome has long been appreciated and mounting evidence suggests that these factors on a background of HIV infection may increase the risk of CVD (58). In particular, HIV-infected patients have higher rates/risk of atherosclerosis, vascular dysfunction, myocardial infarction, heart failure, and other vascular diseases (57). The HIV-associated metabolic syndrome is characterized by dyslipidemia (including hypertriglyceridemia and cholesterol abnormalities), insulin resistance, and altered fat distribution (peripheral lipoatrophy and increased central adiposity) (58), each of which are independent traditional CVD risk factors. Hypertriglyceridemia in untreated HIV infection involves increases in plasma triglycerides and free fatty acids while cholesterol abnormalities in this context involve decreased total and HDL-C (58, 59) and increased (60) or decreased LDL-C (61). Importantly, these changes are associated with the extent and duration of viremia (60) and low total and HDL-C occur early in infection, prior to the initiation of ART (59), implying a direct viral effect. While total and LDL-C normalize or increase upon ART initiation (58-60), a consistent finding at all stages of HIV disease is low HDL-C (58, 59, 62). Many confounding factors in the HIV-infected population including; higher traditional CVD risk factors (particularly smoking and the lipid abnormalities listed above) (61, 62), risks associated with ART, and the low number of acute events even in large cohort studies have made it difficult to determine if HIV infection *per se* increases CVD risk.

Three seminal studies, the National Institutes of Health (NIH) Strategies for Management of AntiRetroviral Therapy (SMART) study, the Multicenter AIDS Cohort Study (MACS), and the Study of Fat Redistribution and Metabolic Change in HIV Infection (FRAM) allow some interpretation of the impact of HIV infection itself on CVD risk. The SMART study randomized HIV-infected patients to receive either continuous ART through the duration of the study or intermittent ART to maintain CD4 cell counts (>250 cells/mm^3). Intermittent treatment with viral rebound was associated with a dramatic increase in CVD events and mortality (57, 59-62) that associated directly with the duration of uncontrolled viral replication (62). SMART demonstrated reduced total, HDL-C, and LDL-C upon treatment interruption but the reduction in HDL-C was more precipitous leading to an unfavorable, proatherosclerotic increase in the total to HDL-C ratio (59, 61, 63). The MACS study compared HIV seronegative controls to recent HIV seroconverters and demonstrated reduced total, HDL-C and LDL-C upon infection with restoration of normal total and LDL-C levels upon ART initiation but persistently low HDL-C (61). The FRAM study evaluated cIMT in HIV-infected patients compared to uninfected controls (64). After adjusting for traditional CVD risk factors, HIV infection was found to be an independent risk factor for atherosclerosis similar in magnitude to traditional risk factors such as smoking and diabetes (64). Thus, whether HIV infection *per se* increases CVD risk is debatable but there are multiple empirical and observational associations of HIV infection *per se* with negative measures of CVD.

With collective observations suggesting that HIV can, at the very least, exacerbate CVD, research has begun to focus on mechanisms of HIV-specific contributions to this

process. HIV has been suggested to contribute to CVD through; direct effects of viral replication and viral proteins, CD4 T-cell depletion, increased systemic inflammation, monocyte and T-cell activation, T-cell exhaustion and senescence, co-infections, cytokine dysregulation, altered vascular/endothelial function, platelet dysfunction, and microbial translocation (57, 63).

HIV effects on monocyte/macrophages appear to play a significant role in HIV-associated atherosclerosis. Macrophages are uniquely positioned at the intersection between disease states of atherosclerosis and HIV infection and are thus a critical focal point in mechanisms of HIV effects on atherosclerosis development in patients. CD163 is a macrophage scavenger receptor and soluble CD163 (sCD163) is a cleavage product released upon monocyte/macrophage activation (63). Importantly sCD163 is a biomarker of HIV disease and is positively associated with non-calcified coronary plaque (63). Non-calcified plaque is likely more unstable and prone to rupture than calcified plaque associated with traditional CVD risk factors, suggesting that HIV may contribute to increased CVD risk through monocyte/macrophage activation (63). Thus, sCD163 is one example of a macrophage-specific determinant of HIV effects on atherosclerosis.

Examining HIV-associated CVD in the era of HAART is complicated by the dynamic interplay of viral-, genetic-, and treatment-associated factors that are present in treated HIV patients. In this regard, it must be noted that upon initiation of HAART, active viral replication and viral protein expression are significantly reduced and the most numerous infected cells in the circulation transition from productively infected cells during acute viremia to latently infected cells during suppressive anti-viral regimens.

During suppressive HAART, as few as 100 cells per million resting CD4+ T-cells carry integrated proviral DNA, producing a total of ~50 copies of unspliced viral genomic RNA, and essentially undetectable multiply-spliced viral RNAs (necessary for viral protein expression) in some studies (65). Thus, while HIV infection *per se* may make a significant contribution to CVD parameters, particularly during active viral replication, during viral latency and HAART the direct effect of HIV-associated factors is likely mitigated. In this circumstance, other indirect viral effects such as; persistent low-level inflammation, CD4 T-cell depletion, low-level immune activation, T-cell senescence, co-infections, and microbial translocation likely make a more significant contribution. Likely the most significant contribution to lipid imbalance and metabolic disease in treated HIV patients occurs as a result of the metabolic toxicities of antiretrovirals themselves. In particular; the protease inhibitors ritonavir, indinavir, nelfinavir, saquinavir, and lopinavir, the nucleoside RT inhibitors stavudine, didanosine, and abacavir, and the non-nucleoside RT inhibitor efavirenz have each been associated to various degrees with adverse metabolic effects (59, 60, 62). Mitochondrial toxicity, increases in serum lipid levels, insulin resistance, and inihibiton of ApoB degradation have all been suggested to contribute to metabolic effects of antiretroviral agents (59). Given that the proportion of HDL in the circulation that contributes to RCT is a minority and that during latency, viral proteins (including Nef) are expressed at low levels it is likely that other factors contribute to the decrease in total HDL observed in long-term, virally suppressed patients.

A potential role for HIV infection *per se* and Nef in CVD during viral latency and pharmacological viral suppression is still possible however as certain culture models suggest that even in the restrictive environment of, in particular pre-integration latency, viral regulatory proteins (including Nef) are still expressed (66). Additionally, monocytes/macrophages are a proposed reservoir for HIV during latency and HAART as infected monocytes can be detected in the blood of treated patients and infected cells of the specialized macrophage subsets such as microglia and dendritic cells are detectable outside of the circulation (67). However, the strongest support for a direct role of HIV-associated factors in CVD during viral latency and HAART comes from several reports consistently demonstrating detection of early spliced HIV transcripts in PBMCs and Resting CD4+ T-cells from patients on suppressive HAART (68, 69). More precise analysis of early HIV transcription products through RT-PCR techniques was able to specifically confirm the presence of Nef transcripts in PBMCs of HAART-treated patients (69). Surprisingly, while HAART is associated with a mosaic of adverse metabolic side-effects, the specific decrease of HDL consistently observed in treated long-term HIV-infected patients is potentially unrelated to HAART (70). Combined with the demonstration that Nef can be detected in patient sera where the viral protein can exert apparent bystander effects (71), it is reasonable to postulate that Nef may establish a defect in HDL metabolism in infected or bystander cells, either during acute viremia or upon viral suppression, which contributes to a systemic metabolic syndrome affecting CVD. In this scenario, Nef may play the role of catalyst in an HDL defect that is then propagated and exacerbated by more indirect pathological mediators in cells with a more

direct role in HDL metabolism (72). Therefore, while unlikely to affect measures of total HDL directly, it is possible that Nef expression in a limited number of cells could contribute to systemic effects on HDL metabolism as well as specific effects on the minimal population of HDL that contributes to RCT even in the context of viral suppression in the circulation.

C. Nef and ABCA1

HIV infection is associated with high risk of developing atherosclerosis and a consistent finding at all stages of HIV disease, including among treatment-naïve patients, is a low level of circulating HDL-C (58, 59, 62, 64). As discussed previously, ABCA1 contributes to HDL biogenesis through the process of RCT and lipidation of pre-β HDL. Thus, the decreased HDL levels found during HIV infection suggest a possible disturbance of RCT, and a possible mechanism by which HIV infection *per se* may contribute to the development of atherosclerosis, by targeting ABCA1-mediated cholesterol efflux.

Based on the observation that HIV infection causes a reduction in circulating HDL, Bukrinsky & colleagues originally sought to determine if HIV effects ABCA1-mediated cholesterol efflux. Mujawar *et al.* showed that HIV infection impairs RCT from macrophages and T-cells and this effect correlates with the level of viral replication and requires the viral Nef protein (56, 73) (**Fig. 2A**). Mujawar *et al.* also found that Nef, in isolation, impairs cholesterol and phospholipid efflux to ApoA-I (**Fig. 2B**) and this effect requires ABCA1 (56). The effect of Nef was specific for ABCA1 and did not significantly affect efflux to mature HDL including that mediated by ABCG1 (56). HIV

infection or Nef expression reduced ABCA1 protein levels (**Fig. 2C**) but not ABCA1 mRNA (56, 73). A mutant Nef protein lacking a conserved myristoylation signal (G2A) that fails to associate with membranes was defective in reducing ABCA1 protein levels (56, 74) (**Fig. 2C**) and it has been demonstrated that the G2A mutant is ineffective in reducing cholesterol efflux (56, 75) (**Fig. 2B**). Mechanistically, Nef was found to physically interact with ABCA1 (**Fig. 2D**) and to cause redistribution of ABCA1 from intracellular sites to the plasma membrane (**Fig. 2E-G**) with a concomitant increase in cellular ApoA-I binding and a reduction in ApoA-I internalization (56).

HIV-infection also caused significant phenotypic changes in macrophages, inducing a highly atherogenic "foam cell" like state *in vitro*. Significant lipid changes likely contributing to development of foam cells during HIV infection *in vitro* including increased; cholesteryl ester formation, triglyceride and phospholipid biosynthesis, AcLDL uptake, and free cholesterol content were also induced by Nef in isolation, as was the development of foam cells themselves. Having discovered that HIV infection reduces cholesterol efflux, the Bukrinsky group sought to determine if increasing cholesterol efflux from infected cells through pharmacological means could produce an anti-viral effect. Mujawar *et al.* and Morrow *et al.* showed that induction of ABCA1 through Liver X Receptor (LXR) agonists, such as TO-901317, restores ABCA1 protein levels and increases cholesterol efflux from infected cells resulting in reduced virus production, infectivity, and cholesterol content (56, 73). The effects of LXR agonist treatment on

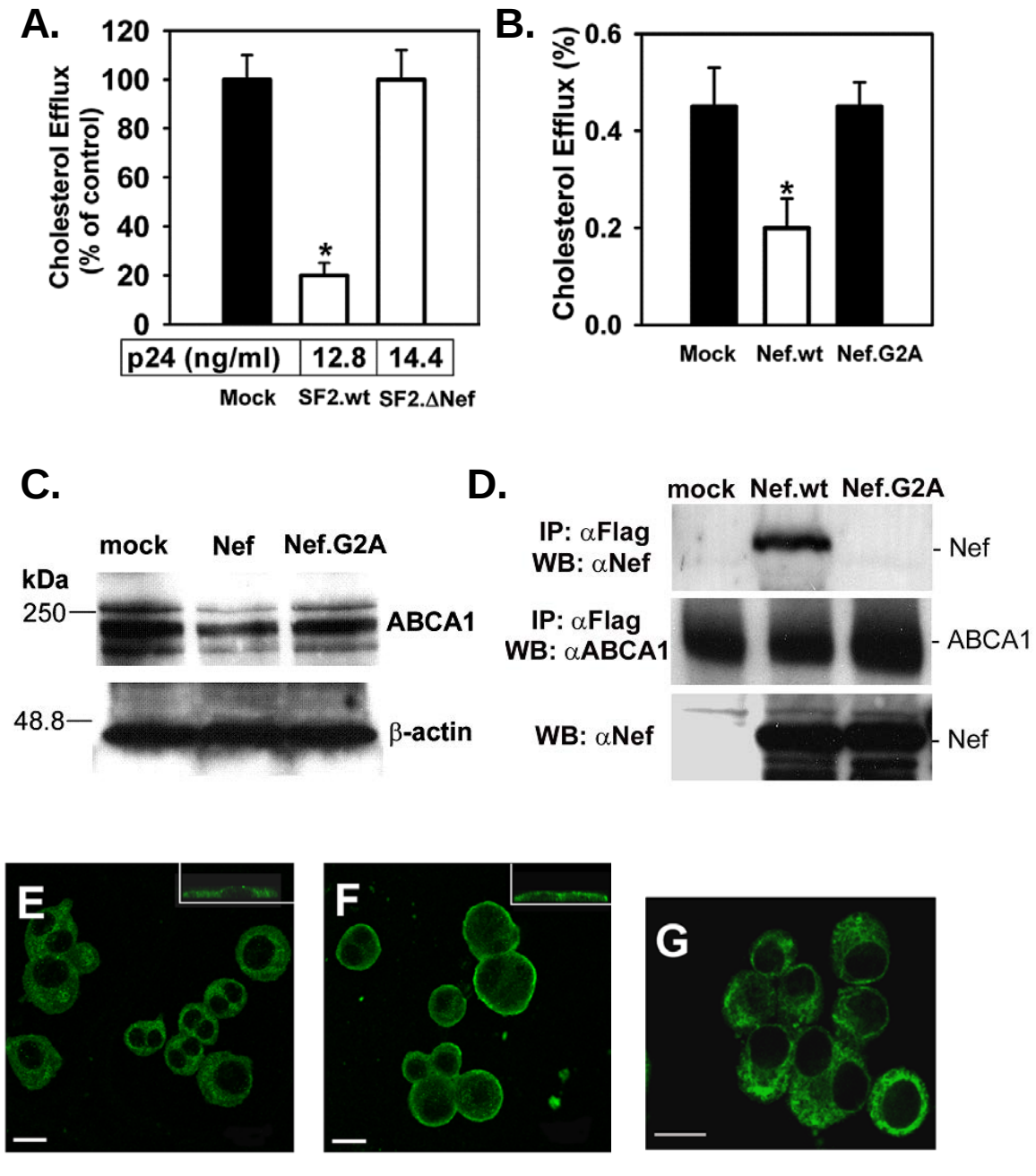
A.
Cholesterol Efflux (% of control)
120
100
80
60
40
20
0
*
p24 (ng/ml)
12.8
14.4
Mock
SF2.wt
SF2.ΔNef
B.
Cholesterol Efflux (%)
0.6
0.4
0.2
0.0
*
Mock
Nef.wt
Nef.G2A
C.
mock
Nef
Nef.G2A
kDa
250
ABCA1
48.8
β-actin
D.
mock
Nef.wt
Nef.G2A
IP: αFlag
WB: αNef
- Nef
IP: αFlag
WB: αABCA1
- ABCA1
WB: αNef
- Nef
E
F
G

Figure 2. Nef binds, redistributes, and degrades ABCA1.

A. MDMs were inoculated with VSV-G-pseudotyped HIV-1 SF2 either deficient in Nef (SF2.ΔNef) or carrying WT Nef (SF2.wt). Specific cholesterol efflux to apoA-I (30 μg/ml) was analyzed on day 6 after inoculation. B. RAW 264.7 cells were transfected with plasmids expressing indicated Nef variants or an empty vector (mock-transfection). Twenty-four hours after transfection, LXR agonist, TO-901317 (1 μmol/L), was added. Cholesterol efflux to apoA-I (30 μg/ml) was performed for 3 h with cells 48 h after transfection. C. RAW 264.7 cells were transfected with vector expressing HIV-1 SF2-derived Nef (either WT or carrying a G2A mutation) or empty vector (mock). Twenty-four hours after transfection, cells were stimulated with TO-901317 (1 μM) and 24 h later, were analyzed by Western blotting for ABCA1 and β-actin (loading control). D. ABCA1 was immunoprecipitated using anti-FLAG M2 affinity gel from HeLa cells co-transfected with ABCA1-FLAG and an empty vector (mock), WT SF2 Nef (Nef.wt), or myristoylation-defective mutant Nef.G2A. IPs were analyzed by Western blotting for Nef (upper panel) or ABCA1 (middle panel) using specific antibodies. Bottom panel shows Nef expression in lysates of cells used for IP. E-G. Distribution of ABCA1 revealed by staining with monoclonal anti-ABCA1 antibody and FITC-conjugated anti-mouse IgG in RAW 264.7 cells transfected with empty vector (E), WT Nef derived from SF2 HIV-1 (*Nef.wt*, panel [F]), or SF2 Nef carrying a G2A mutation (*Nef.G2A*, [G]). Insets in (E and F) show cross-section of the image reconstituted from serial sectioning. Scale bars represent 20 μm. Re-printed from (56), Copyright © 2006 Mujawar et al.

virion cholesterol content and infectivity were reversible by incubation with cholesterol-loaded cyclodextrins suggesting that the anti-viral effect specifically involves cholesterol depletion (73). Treatment with LXR agonist significantly reduced HIV replication *in vitro* and in *ex vivo* cultured lymphoid tissue and in an *in vivo* humanized mouse model of infection (73). The anti-viral effect of LXR agonists in this study was comparable to that of the potent and well described anti-HIV drug AZT (73). Mechanistically, virus produced from cells transfected with ABCA1, to mimic LXR agonist treatment, was specifically deficient in the membrane fusion step of the viral life cycle furthering the notion that the anti-viral effect of LXR agonists involves changes to the cholesterol content of viral membranes (73). More recently, another group has confirmed the demonstration of anti-viral effects of LXR agonists on HIV in T-cells and extended these findings to agonists of the heterodimeric partner of the LXRs, the retinoic acid receptor (RXR) (76).

Recent studies have begun to uncover the contribution of Nef effects on ABCA1 to viral biology and to assess the effects of the Nef-mediated inhibition of RCT on CVD determinants at the level of the host. Nef-mediated downmodulation of ABCA1 enriches cells in cholesterol, increasing the abundance of lipid rafts (sites of HIV assembly) and elevating cholesterol content in cell and viral membranes, thus increasing HIV production and infectivity (56, 73, 77). As an 'unintended' consequence of this activity, Nef impairs HDL maturation in SIV-infected macaques (72) and may be responsible for low HDL levels in HIV-infected patients. Indeed, a key finding in SIV-infected, atherogenic diet fed macaques is the exacerbation of a pro-atherogenic profile characterized by increased

pre-β-1 HDL and an increased pre-β-1/α-4 HDL ratio (72). High pre-β-1 levels indicate a problem with HDL maturation or remodelling as would be expected with a defect in RCT (3). Importantly, in these studies HIV-infected macrophages are observed in atherosclerotic plaques from HIV positive patients, suggesting a possible role of HIV infection in the initiation of atherosclerotic lesion formation.

Nef downmodulates a number of cell surface transmembrane proteins, such as; CD4, MHC-I, MHC-II, transferrin receptor, mannose receptor, CD80, CD86, CD8, and CCR5, by modifying their intracellular trafficking and targeting them to various degradation pathways (78, 79). Indeed, CD4 and MHC-I down-regulation are considered to be the principle pathogenic activities of Nef during HIV infection and likely contribute to viral replication and immune escape *in vivo*. The common mechanism behind this activity of Nef is direct binding to the target protein and connecting it to transport proteins which direct the complex to lysosomes or proteasomes. While Nef has been shown to interact with ABCA1 (**Fig. 2D**) (56), this interaction was shown to be dispensable for Nef-mediated ABCA1 downmodulation and functional impairment (74), suggesting that an alternative indirect mechanism is responsible for target protein downmodulation in this case. Nef also induces a prominent trapping of ABCA1 in the ER, leading to a model of Nef-mediated ER-associated degradation of ABCA1 (74).

Identifying cellular co-factors for ABCA1-mediated cholesterol efflux is of obvious research and clinical interest as a potential means of increasing RCT and effecting the generation of atheroprotective HDL species. Additionally, identifying positive regulators of ABCA1 biogenesis may inform understanding of the process of

RCT itself, and the role of ABCA1 and ABCA1 protein modifications in RCT. Identification of cellular proteins that are targeted by Nef to achieve reduction in RCT has the potential to identify novel anti-viral targets and strategies. Drugs that effect such a pathway would be expected to have the advantage that they target cellular factors rather than viral targets and may thus be less prone to development of resistant virus.

III. Calnexin

A. Calnexin and its Substrates

Calnexin is an integral ER membrane calcium-binding lectin-like chaperone that binds immature glycoproteins destined for the plasma membrane and stabilizes these proteins during folding. Calnexin and its soluble analog, calreticulin, function as chaperones and components of the ER quality control machinery. As chaperones, calnexin and calreticulin are thought to delay protein folding, consequently decreasing aggregation and increasing folding efficiency and domain assembly (80). Calnexin and calreticulin also function in quality control by binding misfolded proteins and targeting them for degradation through the process of ER-associated degradation (ERAD) (80). In addition to its well-defined role in the ER, a minor population of calnexin is also present on the Plasma Membrane (81) though its function at this site has not been described.

As an integral ER membrane protein, calnexin is topologically arranged with an ER lumenal segment, a transmembrane (TM) segment, and a short cytoplasmic segment (Cyt) (82, 83). Consistent with its function, the domain architecture of calnexin includes a globular domain containing the major glycoprotein- and calcium- binding sites, an arm

domain containing proline-rich repeats (sometimes referred to as the p-domain) which may form a cleft for glycoprotein binding, and a c-terminal segment implicated in binding to the ER thiol-oxidoreductase ERp57 (84). It has been suggested that calnexin may stabilize glycoproteins through a dual-binding mode involving glycosyl residue- and peptide-binding or through either single binding mode (glycosyl residue- or peptide-binding) independently (84). Compelling evidence for both pathways exists and both binding modes may be operative on different substrates or under different conditions (80). While it is well accepted that calnexin binds glycoproteins, evidence of calnexin binding to non-glycosylated substrates, while somewhat controversial, has also been reported, suggesting that calnexin may possess true chaperone ability, perhaps independent or interdependent with its lectin-like glycoprotein-binding properties. Recently, many glycoproteins have been shown to interact with calnexin in, at-least partially, glycan-independent fashion, including; Soybean Agglutinin (85), Charcot-Marie Tooth Disease growth arrest –specific 3/peripheral myelin protein 22 (Gas3/PMP-22) (86), γ-aminobutyric acid (GABA) transporter 1 (GAT1) (87), Vesicular Stomatitis Virus G-Protein (VSV-G) (88), T-Cell Receptor (TCR) ε and α subunits (89, 90), CD3 δ and ε subunits (89, 90), thyroglobulin (91), P-glycoprotein (48), D1 and D2 Dopamine Receptors (92), and MHC-I (93) and –II (94) chains. Additionally, several non-glycoproteins including; proteolipid protein (PLP) (95), citrate synthase (CS) (85), and malate dehydrogenase (MDH) (85) have been shown to interact with calnexin suggesting that calnexin is capable of acting as a true chaperone independent of its lectin-like binding properties.

Calnexin interaction with substrate proteins is subject to several well-defined biochemical requirements including; availability of Ca^{2+} and Zn^{2+} ions and ATP. The most highly-characterized requirements for calnexin interaction are availability of ER calcium stores and activity of glycoprotein processing enzymes of the ER. Several pharmacological compounds are available that block these processes and can, in many cases, prevent interaction between calnexin and particular substrates. Tunicamycin is an inhibitor of ER N-linked glycosylation, whereas, N-butyl deoxynojirimycin (NB-DNJ, miglustat) and castanospermine inhibit various classes of glucosidases, which are responsible for the stepwise removal of terminal glucose residues from *N*-glycan chains attached to nascent glycoproteins. These steps are necessary for interaction between select glycoproteins and calnexin, as calnexin binds exclusively to monoglucosylated glycoproteins, thus, these compounds block interactions requiring the glycan-binding function of calnexin and specifically target proteins that depend on it (96-101). Importantly, alteration of glycosylation or glucose trimming with these compounds has been shown to disrupt interaction between calnexin and other ABC transporters (102-104). Inhibiting ER calcium flux through sarco/endoplasmic reticulum Ca2+-ATPase (SERCA) inhibitors, such as Thapsigargin and A23187, targets the calcium-binding requirement of calnexin and can also block calnexin interaction with substrate proteins (105-107), including other ABC transporters (104).

Members of nearly every subclass of ABC transporters including; ABCB1 (P-glycoprotein, MDR1), ABCB2 (TAP1), ABCB3 (TAP2), ABCC2, ABCC7 (CFTR), and ABCG5/G8 have been demonstrated to interact with calnexin (48, 49, 108) and among

these are examples of glycan-dependent and –independent interactions (48, 102, 108, 109). Calnexin has previously been identified in a large-scale proteomics investigation of ABCA1-interacting proteins (38) though the contribution of calnexin to cholesterol efflux has not been investigated.

B. Viruses and Calnexin

Calnexin chaperones a variety of immunoreceptor glycoproteins including; Major Histocompatability (MHC) Class I and II components, T-cell receptor (TCR) components, and the interferon-γ receptor (110). Additionally, a variety of viral glycoproteins are substrates for calnexin including; influenza hemmagluttinin, cytomegalovirus (CMV) glycoprotein B, vesicular stomatitis virus G protein (VSV-G), Hepatitis C Virus (HCV) E1/E2 glycoproteins and HIV-1 gp160 (110). Additionally, several viral proteins bind calnexin with no apparent chaperone activity suggesting a possible role in the viral life cycle. The p12 protein of HTLV-I, which shares structural similarity with Nef, binds calnexin with an apparent function in Calcium signalling modulation by p12 (111). Recently, the first example of a viral protein that subverts a naturally occurring calnexin-substrate interaction to affect viral survival has been described for the HPV E5 protein and MHC-I (112). HPV E5 requires Calnexin for down-regulation of MHC-I (112) and may also utilize calnexin to down-regulate CD1d (113).

Chapter 2: Specific Aims

HIV infection gives rise to a unique metabolic syndrome in AIDS patients with many features in common with classical atherosclerotic vascular disease. Many virus-intrinsic and –extrinsic factors likely contribute to the development of this syndrome and the contribution of any individual factor and even viral infection itself to this phenomenon is likely to remain an area of controversy. However, investigating virus-induced mechanisms of increased cardiovascular risk is a unique and potentially highly informative research platform to investigate the effects of specific factors on atherosclerosis in the context of HIV-infection as a source of important insights into cardiovascular disease in the uninfected population.

One important factor to the development of cardiovascular disease in the general population that appears to be further altered in the context of HIV infection is the level and functionality of circulating High Density Lipoprotein (HDL). Indeed, a reduction in the content of circulating HDL is one of the principle features of HIV-associated lipodystrophy. Our group has shown that HIV reduces cholesterol efflux from macrophages and T-cells through the actions of the viral Nef protein. Nef reduces cholesterol efflux through several effects on the ATP-Binding Cassette Transporter A1 (ABCA1). Nef interferes with trafficking of ABCA1 causing the transporter to become enriched on the plasma membrane, at the expense of intracellular pools of ABCA1 which are reduced. Nef also increases turnover of ABCA1 protein through increased delivery to lysosomes and proteasomes. While Nef can physically interact with ABCA1, this property is unnecessary for Nef effects on ABCA1, suggesting the involvement of other

cellular factors. **We therefore hypothesize that Nef reduces interaction of ABCA1 with a cellular factor involved in normal trafficking or turnover of the transporter to reduce cholesterol efflux.** We propose the following specific aims to address the hypothesis:

Specific Aim 1. To identify ABCA1-interacting cellular proteins whose interaction with ABCA1 is reduced by Nef. Nef can be detected in association with ABCA1 by co-immunoprecipitation (Co-IP). However, recent studies have demonstrated that physical interaction between Nef and ABCA1 is dispensible for both the Nef-mediated degradation of ABCA1 protein and the Nef-mediated reduction in cholesterol efflux, suggesting that the mechanism of Nef effects on ABCA1 may include unidentified cellular proteins. Additionally, these studies also suggested that Nef effects on ABCA1 may involve the endoplasmic reticulum (ER). Based on this, we hypothesize that Nef alters interaction between ABCA1 and a cellular, ER-resident, ABCA1-interacting protein that modulates ABCA1 stability or function.

Specific Aim 2. Characterize the effect of ABCA1-interacting proteins whose interaction is reduced by Nef on ABCA1 stability, localization, and function. Nef reduces cholesterol efflux through a myriad of effects on ABCA1. Nef reduces ABCA1 protein levels, causes re-localization of ABCA1 to the plasma membrane (PM), and reduces ApoA-I-specific cholesterol efflux mediated by ABCA1. Based on this, we

hypothesize that proteins identified in **Aim 1** should contribute to ABCA1 stability or localization and should contribute to ApoA-I-specific cholesterol efflux.

Chapter 3: Materials and Methods

I. Reagents

The following reagents were purchased from the indicated suppliers: mass spectrometry grade Trypsin Gold (ProMega); Metafectene (Biontex); rabbit anti-calnexin antibody, rabbit anti-HSP-90 antibody, rat anti-Grp94 antibody, and rabbit anti-calreticulin antibody (Assay Designs); rabbit anti-EEA1 antibody and rabbit anti-caveolin antibody (Cell Signaling Technology); mouse and rabbit anti-ABCA1 antibodies (Novus Biologicals); goat anti-HA antibody (Genscript); N-butyldeoxynojirimycin (NB-DNJ) (BIOMOL); mouse anti-LCB1 (SPTLC1) (BD Transduction Laboratories); control siRNA ("a scrambled sequence that will not lead to the specific degradation of any cellular message"), calnexin siRNA (Santa Cruz "siRNA products generally consist of pools of two to five target-specific 19-25 nt siRNAs designed to knockdown gene expression"), siRNA transfection medium, rabbit anti-MHC-I antibody, rabbit anti-calnexin (H-70) antibody, and goat anti-Calnexin (C-20) antibody (Santa Cruz); [1,2-^{3}H]cholesterol (PerkinElmer); human lipid free apolipoprotein A-I (Biodesign); pDsRed2-ER (Clontech); tunicamycin (Calbiochem); Castanospermine (LKT Laboratories); normal rabbit serum (NRS) (Jackson Immunoresearch); cell surface protein isolation kit (Pierce); rabbit anti-Dystrophin antibody (Thermo-Pierce); human calnexin cDNA (Open Biosystems); anti-FLAG M2 affinity agarose gel, EZView Red Protein A affinity agarose gel, murine IgG agarose gel, mouse anti-actin antibody, mouse anti-β COP antibody, rabbit anti-FLAG antibody, rabbit anti-GAPDH antibody, rabbit anti-COX IV Isoform 1 antibody, cycloheximide,

concanavalin A (ConA)-HRP, phorbol 12-myristate 13-acetate (PMA), cholecalciferol (vitamin D_3), fatty-acid free Bovine Serum Albumin (BSA), and all other chemicals were from Sigma. Polyclonal rabbit anti-Nef antisera, mouse monoclonal anti-HIV-1 p24, and HIV+ Human sera were all from the NIH AIDS Research and Reference Reagent Program.

II. Cloning and Expression Construct Development

Human calnexin cDNA vectors with a C-terminal HA-tag were prepared by standard PCR methods from calnexin cDNA clones (Open Biosystems) in the pHCMV3 vector (Genlantis). For DsRed2-CNX, calnexin was subcloned from pHCMV3-CNX into pDsRed2 by standard PCR methods.

Nef expression vectors were prepared from pT7consnefhis6 (NIH AIDS Research and Reference Reagent Program) in pHCMV3 by PCR cloning.

Mutant calnexin constructs were generated by PCR similar to the construction of pHCMV3-CNX. Mutants ΔCyt, ΔCyt,TM, and 1-392 were generated using previously described primers (83) with amendments made for cloning into pHCMV3 in-frame with a C-terminal HA-Tag. The ΔRepeats mutation was made by restriction digest and re-ligation of pHCMV3-CNX. All constructs were verified by sequencing.

III. Cell Culture and Transfection

HeLa-ABCA1-GFP cells stably expressing GFP-tagged ABCA1 (114) were a kind gift of Dr. A. Remaley. HeLa cells were cultured in DMEM-C (10% Fetal Calf Serum (FCS), penicillin, streptomycin, L-glutamine) containing Hygromycin B and G418. HEK 293T

cells were grown in tissue culture flasks or 6-well plates in RPMI-C (RPMI-1640, 10% FCS, penicillin, streptomycin, L-glutamine) and transfected with cDNA or siRNA using Metafectene according to the manufacturer's (Biontex) instructions. Following transfection, cells were incubated for 48 h prior to use in experiments.

A similar protocol with slight modification was used to transfect HeLa-ABCA1-GFP cells with siRNA. Following passage and overnight culture, 1 x 10^6 cells were transfected with control or calnexin siRNA using siRNA:Metafectene complexes (16 μL Metafectene mixed with 8 μL of 10 μM siRNA) prepared in separate 100 μL aliquots of serum-free siRNA Transfection Medium (STM; Santa Cruz). Transfection complexes were incubated for 1 h in the dark, diluted with 800 μL STM for a final siRNA concentration of 80 nM and added to cells pre-washed with serum-free DMEM. Cells were incubated with transfection complexes in serum-free STM for 4 h followed by addition of DMEM-C with 2x serum and further overnight incubation. The following day, media was changed to DMEM-C and cells were incubated for additional 48-72 h prior to use in experiments.

IV. High-Resolution LTQ ESI LC-MS/MS Mass Spectrometry

Total cellular protein (5 mg) from HEK 293T cells co-transfected with ABCA1-FLAG and pcDNA-Nef or ABCA1-FLAG and empty control vector (pcDNA) was immunoprecipitated with M2 anti-FLAG affinity gel and co-purifying proteins were identified by tandem MS/MS. The SeeBlue Plus2 Pre-Stained Standard (Invitrogen) with proteins of known identity was run alongside experimental samples and processed in

similar fashion as an internal control for peptide processing and performance of the mass spectrometer. Following 1D gel electrophoresis and staining with GelCode Blue dye (Thermo Pierce), unique bands were excised and stain removed via incubation in distilled water. Gel pieces were washed via sequential dehydration with Acetonitrile (ACN) and rehydration in 100 mM NH_4HCO_3. Gel slices were dried and hydrated on ice in Promega sequencing grade Trypsin Gold (12.5 ng/µl, 10-20 µL) in 50 mM NH_4HCO_3 for 45 min, then a saturating volume of 50 mM ammonium bicarbonate was added, and the tubes were incubated for 16 h at 37°C. The peptide solutions were extracted with 25 mM NH_4HCO_3 (25 µl, 15 min), an equal volume of acetonitrile (ACN) was then added and incubated a further 15 min. The supernatant was collected and the gel pieces further extracted with two washes with 5% formic acid/ACN (1:1, 30 µL) and all extracts were pooled and lyophilized. The lyophilate was dissolved in 10 µL of TriFluoroAcetic Acid (TFA), further desalted with a C18 ZipTip (Millipore), and loaded onto a C18 trap column followed by a C18 reverse-phase column using an Eksigent nano-HPLC system. Peptides were introduced into the mass spectrometer via a 10 µm silica tip (New Objective Inc., Ringoes, NJ) adapted to a nano-electrospray source (ThermoFisher Scientific). The LTQ-Oribtrap XL (ThermoFisher Scientific) was operated in data-dependent mode with one full-MS (300-2000 m/z) survey scan acquired in the Orbitrap, resolution 30000, and subsequently five MS/MS scans performed in the LTQ using collision-induced dissociation with the collision gas (helium) and normalized collision energy value set at 35%. Each file was searched for protein identification using the Sequest algorithm in the Bioworks Browser software (ThermoFisher Scientific) against

the Uniprot all species database indexed for fully tryptic peptides and 2 missed cleavages. Peptide Tolerance was set at 50 ppm and Fragment Ion Tolerance at 1.0 Da. Variable modifications were oxidation of Methionine and Cysteine (15.995 Da). Results were filtered based on peptide probability score with a p value < 0.01.

V. Immunoprecipitation

Immunoprecipitations were used to confirm the physical interaction of ABCA1 and Calnexin in lysates from THP-1 macrophages and HEK 293T cells. HEK 293T cells were transfected with ABCA1-FLAG or empty vector DNA as described above. 48 h after transfection, cells were washed with ice cold PBS and lysed in NP-40 Lysis Buffer (1% NP-40, 150 mM NaCl, 2 mM EDTA, 50 mM Tris-HCl pH 7.0 containing a protease inhibitor tablet) on ice for 30 min. Lysates were centrifuged to remove debris (10 min, 13000 x g, 4°C), the supernatants were transferred to fresh 1.5 mL eppendorf tubes, and ABCA1 was precipitated with M2 anti-FLAG affinity gel overnight at 4°C with rotation. Murine IgG agarose gel was used in an isotype control precipitation. Precipitates were washed three times with TBS (50 mM Tris-HCl, pH 7.0, 150 mM NaCl) and FLAG-ABCA1 complexes were eluted with FLAG peptide (0.5 mg/ml, 1 h, 4°C). Supernatants were separated on SDS-PAGE gels for immunoblotting or in-gel digestion analysis and MS/MS.

For immunoprecipitation in THP-1 macrophages, cells (1 x 10^7 cells/75 cm^2 Primaria™ flask (Becton Dickinson)) were differentiated for 72 h with 100 nM PMA/100 nM $VitD_3$. Cells were washed with ice cold PBS and lysed in NP-40 Lysis Buffer on ice for 30 min.

Lysates were centrifuged to remove debris (10 min, 13000 x g, 4°C), the supernatants were transferred to fresh 1.5 mL Eppendorf tubes, and pre-cleared by incubation with EZView Red Protein A in the absence of antibody. Resulting supernatants were incubated overnight with rabbit anti-ABCA1, rabbit anti-calnexin, or NRS capture antibodies. Immune complexes were precipitated with EZView Red Protein A affinity gel, washed with lysis buffer, boiled in sample buffer to elute bound protein, and separated on SDS-PAGE gels for immunoblotting with goat anti-calnexin antibody.

To assess the requirement for glycosylation of ABCA1 for physical interaction of ABCA1 and Calnexin, HEK 293T cells were transfected with empty control vector (pcDNA) or ABCA1-FLAG as described above. Glycosylation inhibitors were added immediately prior to transfection and maintained throughout the experiment to ensure that ABCA1 remained deglycosylated throughout. 24 h after transfection, cells were lysed and ABCA1 was precipitated with M2 anti-FLAG affinity gel as described above. Anti-FLAG immunoprecipitates were probed with rabbit antibodies to ABCA1, Calnexin, Dystrophin, or SPTLC1. Separate anti-FLAG immunoprecipitation reactions were probed with ConA-HRP per manufacturer's instructions (Sigma).

To assess the effect of glycosylation inhibitors on calnexin-interacting proteins, HEK 293T cells were transfected with HA-CNX and ABCA1-FLAG as described above. Glycosylation inhibitors were added immediately prior to transfection and maintained throughout the experiment to ensure that glycoproteins remained deglycosylated throughout. 24 h after transfection, cells were lysed and calnexin was precipitated with anti-HA affinity gel as described above for FLAG fusion proteins. Anti-HA

immunoprecipitates were probed with rabbit anti-Calnexin, rabbit anti-MHC-I, or rabbit anti-ABCA1 antibodies.

To assess the effect of co-transfection of Nef on the physical interaction of ABCA1 and Calnexin, HEK 293T cells were transfected with empty control vector (pcDNA), ABCA1-FLAG, pcDNA-Nef, or co-transfected with ABCA1-FLAG and pcDNA-Nef as described above. The same amount of each individual cDNA was used in each transfection, the total DNA in each single transfection was balanced with empty control vector. 48 h after transfection, cells were lysed and ABCA1 was precipitated with M2 anti-FLAG affinity gel as described above. Anti-FLAG immunoprecipitates were probed with rabbit anti-Calnexin. Calnexin was precipitated with rabbit anti-Calnexin using EZView Red Protein A as described above. Anti-calnexin immunoprecipitates were probed with mouse anti-ABCA1 monoclonal antibody.

To assess the effect of Nef+ and Nef- viral infection on the physical interaction of ABCA1 and Calnexin, macrophages were infected as described above, cells were lysed and ABCA1 or calnexin were precipitated with mouse anti-calnexin or rabbit anti-ABCA1 antibodies using EZView Red Protein A as described above. Anti-calnexin immunoprecipitates were probed with rabbit anti-ABCA1 or anti-calnexin antibodies or HIV+ Human sera. Anti-ABCA1 immunoprecipitates were probed with goat anti-calnexin or mouse anti-ABCA1 antibody.

His-Bind purifications were carried out exactly as described for FLAG- or HA-immunoprecipitations with Ni-NTA agarose beads in place of antibody beads.

VI. Subcellular Localization and Solubility Studies

Subcellular Fractionation by detergent was performed with a commercially-available kit (Subcellular Protein Fractionation Kit, Pierce). Briefly, 48 hours post-transfection HeLa-ABCA1-GFP cells were harvested and washed with PBS. Cells were lysed and processed with the kit detergents as directed in the manufacturer's protocol. Protein content of each fraction was determined by DC Protein Assay (Bio-Rad) and equal amounts (by total protein) of each fraction were separated by SDS-PAGE and analysed by immunoblotting for ABCA1, Calnexin, Nef, and β-actin. HSP90 (Cytosol), Calreticulin (Membrane), Transferrin Receptor (Membrane), HDAC2 (Nucleus/Chromatin), and Cytokeratin-18 (Cytoskeleton) were used as marker proteins..

Membrane and Soluble protein isolation was performed with the Mem-Per Membrane Protein Extraction kit (Pierce). Briefly, 48 hours post-transfection HeLa-ABCA1-GFP cells were harvested and washed with PBS. Cells were lysed and processed with the kit reagents as directed in the manufacturer's protocol. Protein content of each fraction was determined by DC Protein Assay (Bio-Rad) and equal amounts (by total protein) of each fraction were separated by SDS-PAGE and analysed by immunoblotting for Calnexin and Nef. Transferrin Receptor was used to demonstrate the effect of Nef on solubility of this receptor. Grp94 (soluble), Flotillin (Membrane), and CoxIVi1 (Membrane) were used as marker proteins.

VII. Raft Flotation

Lipid rafts were isolated using modified lysis conditions and flotation on discontinuous sucrose gradients (115, 116). In brief, cells (10^7) were washed with ice-cold PBS and lysed for 30 min on ice in 800µL 1% Triton X-100 in TNEV containing protease inhibitors (TNEV: 10 mM Tris/HCl, pH 7.5, 150 mM NaCl, mM EDTA, and 1 mM sodium orthovanadate). The lysis solution was further homogenized with ten strokes in a loose-fitting Dounce homogenizer. 50µL of lysate was removed and retained as Whole Cell Lysate and the remaining 750µL was mixed with 750µL of 95% sucrose in TNEV and transferred to the bottom of a Beckman 4mL centrifuge tube. The diluted lysate was overlaid with 2mL 35% sucrose in TNEV and finally 0.5mL 5% sucrose in TNEV. The samples were centrifuged in an SW41 rotor at 200,000 *g* for 16–20 h at 4°C. Eight 0.5-ml fractions were collected from the top of the gradient. Equal volumes of each fraction were initially seperated by SDS-PAGE and blotted for ABCA1, Calnexin, Nef, and Caveolin (Raft) to determine which fractions contained rafts (**Fig. 8**, top). Subsequently equal amounts (by Total Protein determined with Bio-Rad DC Protein Assay) of the raft fraction (fraction 2) and non-raft fraction (pooled fractions 7 and 8) and Whole Cell Lysate were analyzed by blotting for Calnexin and Caveolin (**Fig. 8**, bottom).

VIII. Differential Ulrtracentrifugation Isolation of Heavy and Light Membranes

Heavy and light membranes were isolated as previously described (117). Briefly, 48 hours post-transfection HeLa-ABCA1-GFP cells were harvested in Homogenization Buffer (0.25M Sucrose, 10mM HEPES-NaOH pH:7.4, 1mM EDTA), homogenized for 15 strokes

in a tight-fitting Dounce homogenizer, and post-nuclear supernatants prepared by centrifugation for 10 min at 800 x *g*. Heavy membranes (HM) were prepared by centrifugation of supernatants for 10 min at 10000 x *g*. Finally, centrifugation for 1 hour at 100000 x *g* in a Ti-100 rotor yielded light membranes (LM, pellet) and soluble cytosolic (Cyt, supernatant) fractions. Membrane pellets were solubilized in HSE Lysis Buffer (20mM HEPES pH:7.4, 150mM NaCl, 5mM EDTA, 1mM DTT, 1% Triton X-100). Protein content of each fraction was determined by DC Protein Assay (Bio-Rad) and equal amounts (by total protein) of each fraction were separated by SDS-PAGE and analysed by immunoblotting for ABCA1, Calnexin, and Nef. Calreticulin (ER), CoxIVi1 (mitochondria), β-COP (Golgi) and HSP90 (cytosol) were used as organelle marker proteins. EEA1 (endosomes) and Caveolin (plasma membrane) were used to demonstrate separation of plasma membranes and vesicle components.

IX. Western Blotting

BioRad DC Protein Assay was performed on all lysates prior to electrophoresis to normalize loading onto Tris-HCl gels and equal loading was determined on blots with loading control antibodies β-actin, tubulin, or GAPDH. For ABCA1 analysis, cell lysates were loaded onto a 5% or 7.5% gel and run at 100V constant voltage for 1.5 hours. All other proteins were analysed on 10% or 4-20% gradient TGX gels (Bio-Rad). Protein transfer to PVDF membranes was accomplished using a TransBlot Semi-Dry transfer apparatus (BioRad). Membranes were subsequently blocked in 10% milk, washed with 1x TBS with 0.1% Tween-20, and incubated overnight at room temperature with primary antibodies diluted 3% milk, and then for 2 h with horse radish peroxidase-conjugated

secondary antibodies diluted in 1% milk solution. After washing with Tris-buffered saline/Tween, the membrane was developed using the ECL reagent from Amersham Biosciences. ECL was detected by timed exposure to blue photographic film which was developed in a dark room with a Kodak photoprocessor. Films were scanned with an Epson tabletop flatbed scanner through an Adobe Photoshop desktop interface.

X. Confocal Microscopy

For imaging, HeLa-ABCA1-GFP cells were grown on 35 mm glass-bottom cell culture dishes. Images were captured with a Zeiss LSM 510 Confocal Microscope equipped with integrated on-stage incubator chamber. The chamber provides constant temperature at 37°C and is supplied with humidified 5% CO2. Two-channel confocal time series were captured at pixel resolution of 0.175 μm; image frames measured 512 × 512 pixels. Emission filtering was achieved by inserting on the backward light path high-pass 545 and 490 beam splitters in addition to a high-pass 505 filter. Images were taken by sequential line acquisition.

Quantitative colocalization was assessed using Volocity software (PerkinElmer). For colocalization, the images were first subjected to intensity threshold to eliminate the dark current registered at the image, followed by extracting the product of the differences from the mean (PDM). Positive PDM was determined for a single cell, in which pixel intensities of GFP and DsRed vary synchronously and more positive PDM indicates a stronger degree of colocalization. We used the positive PDM as indicator for colocalizing pixels, as by definition, these pixels represent higher than the main pixel value (over threshold) for both channels and reduce the probability of including adjacent structures in the colocalization

outcome. A third channel representing PDM co-localization was plotted in Volocity in addition to GFP (ABCA1) and DsRed2 (CNX or ER) channels and is presented in a three-color image overlay.

XI. Dynamic Sensitized Emission FRET

Sensitized emission FRET experiments were performed to determine the subcellular domains where ABCA1 and DsRed2-ER were in true proximity. GFP emission can be reduced significantly at sites where it is in close proximity to DsRed2 as, for example, when ABCA1 and DsRed2-ER are present within the same vesicle or membrane microdomain. Thus, FRET may compromise the detection of colocalization when the two fluorochromes are within the FRET distance, so that the extent of ABCA1 and DsRed2-ER colocalization is underestimated. In the present studies, dynamic sensitized emission FRET experiments on live-cell microscopy timeseries: (1) identified whether ABCA1 and ER colocalization was reduced as an artifact due to decreased fluorescence of GFP in the presence of DsRed2, and (2) demonstrated the domains where ABCA1 and DsRed2-ER are concentrated within close proximity. Excitation and emission bleed-through to the sensitized emission FRET image (total FRET) was calculated on the confocal images and the sensitized emission FRET efficiency was determined using a normalized sensitized emission algorithm (118).

To generate the confocal images suitable for FRET analysis involving ABCA1-GFP and DsRed2-ER, a two-step acquisition protocol was applied. In the first step, two images were recorded simultaneously by exciting the samples with 488 nm laser while recording two

emission bandwidths. The bandwidth between 492 and 553 nm was recorded to detect GFP emission (ABCA1; donor excitation/donor emission), while the bandwidth 580-630 nm revealed the total FRET emission (donor emission/acceptor excitation). Altogether, the total FRET image had three components: (1) the emission of DsRed2 due to FRET from GFP, (2) the emission bleed-through from GFP to 580-630 nm bandwidth, and (3) the direct excitation of DsRed2 by 488 laser and its emission (excitation bleed-through). In addition, a sequential confocal image was acquired with excitation of 561 laser and filtering the emission bandwidth 580-630 nm to reveal the DsRed2 emission (acceptor excitation and emission). The gain and offset of all three channels were adjusted to the same values based on pixel saturation to insure similar background noise in all images and to reduce the contribution of different sensitivities when the FRET protocol was applied. FRET protocol was applied using Volocity software, with a priori calculations of the amount of GFP and DsRed2 bleed-through to the FRET channel. Then, a threshold was applied to eliminate the signal from the principal cell bodies. Finally, a calculation of FRET efficiency was determined, and FRET channel was generated and overlaid on the channels containing ABCA1 and DsRed2-ER fluorescence.

XII. Super Resolution Confocal Microscopy

Confocal images for Super-Resolution were acquired on a TCS-SP5 II (Leica) microscope with a 63x magnification, NA 1.4 oil objective using Application Suite Advanced Fluorescence (LAS AF; Leica) software. Excitation was performed sequentially with CFP being excited at 458nm followed by GFP at 488nm both with the visible Argon laser and the STED depletion laser at 592nm active throughout. STED images were acquired on a

Leica TCS STED CW. Images were deconvolved using the built-in deconvolution algorithms of the Leica LAS-AF software. The PSF was generated by using a 2D Lorentz function with the full-width half-maximum set to 70nm (as calculated on the image using the Wiener Filter algorithm). Images are presented as 2D maximum intensity projections of 15 x-y optical sections (z-step = 0.5μm) with GFP (Nef) presented as a Red pseudo-color and the targeted CFP constructs (-ER or –Mito) presented as a Green pseudo-color.

XIII. Cholesterol Efflux

HeLa-ABCA1-GFP cells were seeded in 24-well plates at 1 x 10^5 cells/well and transfected with control or calnexin siRNA using Metafectene. 72 h post-transfection cells were labelled with [^{3}H]cholesterol in DMEM-C for 48 h. To remove non-cell-associated cholesterol, cells were washed extensively with serum-free DMEM followed by several washes with DMEM supplemented with 1% fatty-acid free BSA. To initiate efflux, cells were incubated in DMEM /1% fatty-acid free BSA in the presence or absence of 30 μg/mL apoA-I for 20 h as described (114). Medium was collected from the cells and cleared of cells and debris by an 800 *g* spin for 10 min. Cell layers were dissolved in 0.1 N NaOH. Radioactivity in media and cells was determined by scintillation counting and cholesterol efflux calculated as counts in media divided by total counts (cells + media) and converted to percentage efflux.

XIV. Cell Surface Biotinylation

Cell surface protein isolation was performed with slight modification according to the manufacturer's instructions (Pierce). HeLa-ABCA1-GFP cells were seeded in tissue

culture flasks at 4 x 10^6 cells/flask and transfected with control or calnexin siRNA using Metafectene. 72 h post-transfection cells were washed twice with PBS and incubated in Sulfo-NHS-SS-Biotin for 30 min at 4°C. Quenching solution was added to stop the biotinylation reaction and cells were collected by scraping. Cells were rinsed with TBS (0.025 M Tris, 0.15 M NaCl, pH 7.2) and lysed in NP-40 lysis buffer. Total protein in each lysate was determined by DC Protein Assay (Bio-Rad). A total of 60 μg of each sample was used for total protein assessment and a further 60 μg sample was precipitated with NeutrAvadin Agarose. Bead-bound proteins were eluted by boiling in sample buffer as the surface fraction and bead supernatants were retained as the intracellular fraction.

XV. MDM culture, infection, and drug treatment

Blood was purchased from the Red Cross and collected from donors anonymous to the research staff. Monocyte-derived macrophages (MDM) were prepared from peripheral blood mononuclear cells using adherence to plastic, and differentiated in the presence of macrophage colony-stimulating factor (MCSF) essentially as described (56).

Viral DNA derived from lab-adapted HIV NL4-3 bearing M-tropic (92BR020.4) Env with wild-type or Nef-deleted genomes were obtained from the lab of Dr. Frank Kirchhoff. Infectious HIV viral supernatants were prepared by transfection in HEK293T cells using Metafectene according to the manufacturer's (Biontex) instructions. To increase infection viruses were additionally pseudotyped via co-transfection of VSV-G or MLV envelope proteins to produce particles for single-cycle infection giving rise to spreading infection in prolonged MDM cultures. Viral supernatents were normalized

according to in-house Reverse Transcriptase (RT) Assay and used to infect MDM at approximately 7 days of macrophage differentiation. Infection was monitored by in-house RT Assay and infected MDM lysates were prepared in NP-40 Lysis Buffer at approximately 10 days post-infection. Protein expression in lysates was assessed by Western Blot and IP was performed as described above.

XVI. ABCA1 Recycling Assay

Control or calnexin siRNA treated HeLa-ABCA1-GFP cells were incubated with 10 μM monensin for various times to prevent recycling of the internalized protein back to the plasma membrane. After monensin treatment, cells were cooled down on ice and then biotinylated with sulfo-NHS-SS-biotin (Pierce) at 4°C for 50 min. After washing, cells were lysed with NP-40 lysis buffer and centrifuged. After centrifugation, supernatant of cell lysates, normalized based on total protein as determined by DC Protein Assay, was incubated with streptavidin-agarose beads overnight at 4°C to isolate surface proteins. After centrifugation and washing, the collected agarose beads were eluted by boiling in sample buffer and separated by SDS-PAGE. Cell surface ABCA1 at each time point after monensin treatment was detected by Western blot.

Chapter 4: Identification of ABCA1-interacting proteins affected by Nef

To identify ABCA1-interacting proteins that may be affected by Nef, full-length wild-type ABCA1 with a FLAG tag at the C-terminus (ABCA1-FLAG) was transfected into HEK 293T cells alone or co-transfected with wild-type Nef. Mock-transfected cells served as control. Cell lysates from transfected cells were immunoprecipitated with M2 anti-FLAG affinity gel and subjected to 1-D PAGE followed by MS/MS of differing bands. Peptides from several previously described ABCA1-interacting proteins, including dystrophin and utrophin, were specifically identified in ABCA1-FLAG transfected cells compared to mock transfected cells (**Table 1**). Another protein with significant peptide coverage identified specifically in the ABCA1-FLAG transfected cells was calnexin (**Table 1**). Given that calnexin functions as an ER chaperone, that several other well characterized ABC transporters, in particular P-Glycoprotein (P-gp/MDR/ABCB1) (48) and the Cystic Fibrosis Transmembrane Conductance Regulator (CFTR/ABCC7) (49), interact with calnexin, and calnexin contributes to maturation of these transporters, the following studies focused on the ABCA1-calnexin interaction as a potential target of Nef.

TABLE ONE

Proteins that co-purified with ABCA1 identified by mass spectrometry

Co-Purified Protein	No. of peptide matches	Calculated Molecular Mass	Accession	Coverage (%)
Utrophin	66	394247.4	P46939	26.1
Dystrophin	1	399153.8	Q9VDW6	0.4
Calnexin	21	67526.0	P27824	30.9
Filamin	44	280561.4	P21333	16.6
Kinesin-like protein KIF11	26	119084.9	P52732	24.6

Chapter 5: ABCA1 physically interacts with calnexin

To confirm physical interaction of ABCA1 and calnexin, HEK 293T cells were transfected with ABCA1-FLAG, and anti-FLAG precipitates were analysed for calnexin by Western Blotting. Calnexin specifically precipitated with ABCA1-FLAG and was not precipitated with the FLAG vector alone, nor with an irrelevant control construct expressing the FLAG-tag, the Nuclear Factor 90 (NF90-FLAG) or when the IP was performed with an IgG isotype control antibody (**Fig. 3A, right panels**). While HEK 293T cells represent a convenient model system, they are not relevant to cell types where ABCA1 has physiological significance. Therefore, studies were designed to investigate the interaction between ABCA1 and calnexin in differentiated THP-1 cells, a model of tissue macrophages. Calnexin was highly expressed in THP-1 cells regardless of differentiation status, whereas significant up-regulation of ABCA1 occurred upon cell differentiation after treatment with PMA/vitamin D3 (**Fig. 3B, left panels**). ABCA1-calnexin interaction could be detected upon ABCA1 immunoprecipitation from lysates of differentiated THP-1 macrophages (**Fig. 3B, right panels**). These results indicate that a physical interaction between ABCA1 and calnexin occurs in an *in vitro* model of human macrophages.

To determine whether the interaction between ABCA1 and calnexin occurs through the glycosyl residues present on ABCA1 (23, 24, 26, 119), tunicamycin which inhibits an early step in formation of N-glycans on nascent glycoproteins was used, as well as castanospermine and N-butyl deoxynojirimycin (NB-DNJ) which inhibit glucosidases

A.

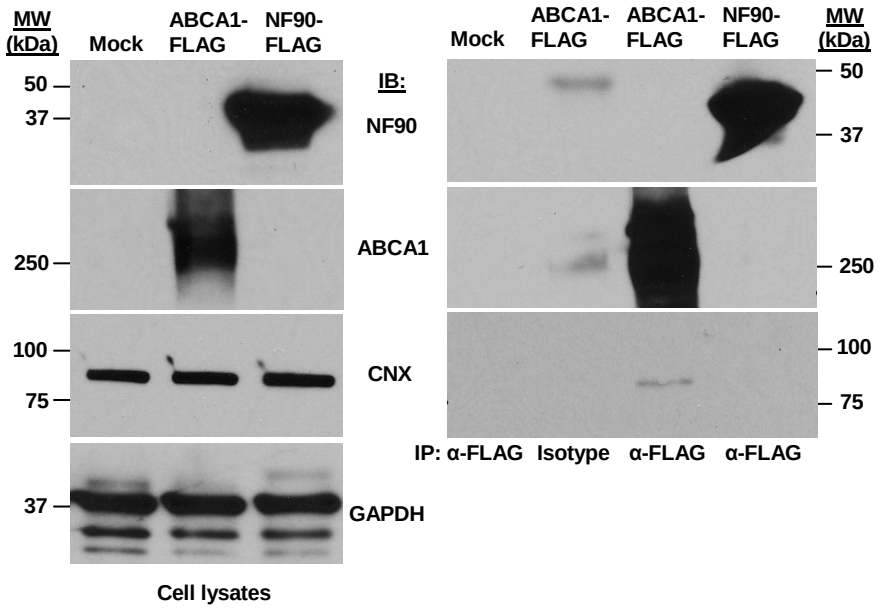
MW (kDa)
Mock
ABCA1-FLAG
NF90-FLAG
IB:
NF90
ABCA1
CNX
GAPDH
50
37
250
100
75
37
Cell lysates
Mock
ABCA1-FLAG
ABCA1-FLAG
NF90-FLAG
MW (kDa)
50
37
250
100
75
IP: α-FLAG
Isotype
α-FLAG
α-FLAG

B.

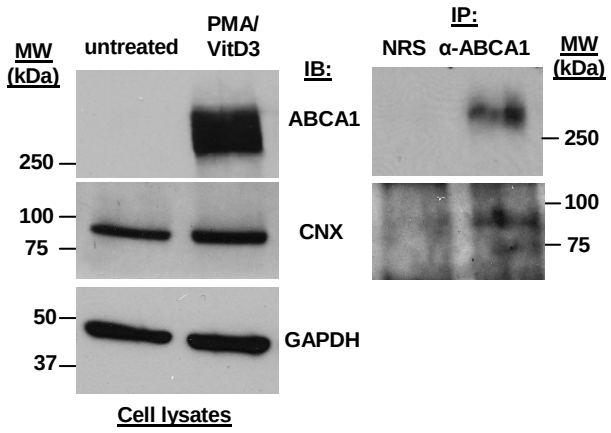
MW (kDa)
untreated
PMA/VitD3
IB:
ABCA1
CNX
GAPDH
250
100
75
50
37
Cell lysates
IP:
NRS
α-ABCA1
MW (kDa)
250
100
75

Figure 3. ABCA1 Interacts with calnexin

A. HEK293T cells were transfected with FLAG-tagged ABCA1 or NF90 (or mock-transfected), lysed and blotted for ABCA1, FLAG (NF90), GAPDH and calnexin (CNX) (left panels). Lysates in (1%) NP-40 Lysis Buffer were immunoprecipitated with anti-FLAG antibody or isotype control, and blotted for FLAG (NF90), ABCA1 and calnexin (right lanes). A representative experiment of three performed is presented. B. THP-1 cells were treated or not with PMA and vitamin D3, lysed and blotted with antibodies to ABCA1, calnexin (CNX) and GAPDH (left panels). Lysates of PMA/vitamin D3-treated THP-1 cells in (1%) NP-40 Lysis Buffer were immunoprecipated with normal rabbit serum (NRS) or rabbit anti-ABCA1 antibody and blotted for ABCA1 and calnexin using monoclonal antibodies. A representative experiment of two performed is presented.

required during later steps in processing and maturation of N-glycans. Following treatment of ABCA1-FLAG transfected HEK 293T cells with tunicamycin, immunoprecipitated ABCA1-FLAG lost major lower molecular weight bands (presumably glycosylated ABCA1) but showed stronger high molecular weight band likely corresponding to multimerized protein (**Fig. 4A, upper panel**). This interpretation was supported by glycosylation analysis using the carbohydrate-binding protein concanavalin-A (ConA). ConA-HRP detected ABCA1 precipitated from DMSO-treated cells (including the upper band), but no reactivity was detected in anti-FLAG IPs from tunicamycin-treated cells, indicating that ABCA1 in these cells was not glycosylated (**Fig. 4A, bottom panel**). Castanospermine and NB-DNJ increased abundance of the multimeric protein without loss of the lower molecular weight bands, suggesting that in this system inhibiting later steps in N-glycan processing is not sufficient to induce observable deglycosylation of ABCA1. Surprisingly, when anti-FLAG IPs were blotted for calnexin, despite the reduction in ABCA1 protein and deglycosylation observed upon tunicamycin treatment, calnexin still co-precipitated with ABCA1 (**Fig. 4A, middle panel**), suggesting that deglycosylation enhanced calnexin-ABCA1 interaction. Castanospermine and NB-DNJ also failed to prevent ABCA1 interaction with calnexin (**Fig. 4A, middle panel**). It is unknown why treatment with the inhibitors caused a significant increase in the amount of calnexin precipitating with ABCA1 but one explanation is that this treatment causes ABCA1 to aggregate which increases calnexin interaction. It is also possible that these treatments increase signaling through the Unfolded Protein Response (UPR), which

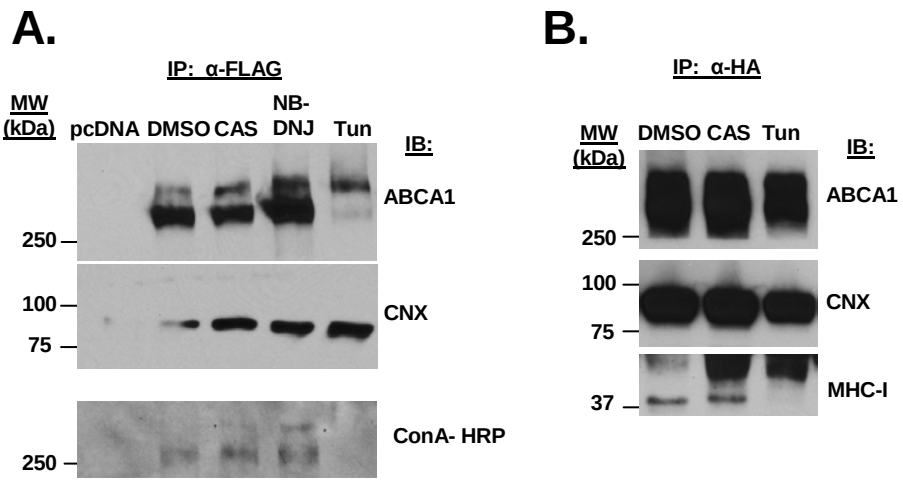
A.
IP: α-FLAG
MW (kDa)
pcDNA
DMSO
CAS
NB-DNJ
Tun
IB:
ABCA1
CNX
ConA- HRP
250
100
75
250
B.
IP: α-HA
MW (kDa)
DMSO
CAS
Tun
IB:
ABCA1
CNX
MHC-I
250
100
75
37

Figure 4. ABCA1 interaction with calnexin is glycan-independent.

A. HEK293T cells were transfected with FLAG-tagged ABCA1 or empty pcDNA vector, treated with DMSO (solvent), castanospermine (Cas), N-butyl deoxynojirimycin (NB-DNJ), or tunicamycin (Tun), immunoprecipitated with anti-FLAG antibody, and blotted for calnexin (CNX) and ABCA1 using monoclonal antibodies (two upper panels), or for glycosylated proteins using HRP-concanavalin A (bottom panel). A representative experiment of three performed is presented. B. HEK293T cells were co-transfected with ABCA1 and HA-tagged calnexin and treated with DMSO, castanospermine or tunicamycin. 48Hrs post-transfection cells were lysed and lysates were immunoprecipitated with anti-HA antibody, and blotted with anti-ABCA1, anti-calnexin, and anti-MHC-I antibodies. A representative experiment of two performed is presented. Of note, the high molecular weight band in the MHC-I blot likely represents non-specific reactivity of the antibody. Also note, the effect of tunicamycin on ABCA1 mobility (decrease of the faster migrating isoform in favor of the slower migrating isoform) is maintained in A. and B. A higher amount of input lysate was required for IP in B. in order to visualize MHC interaction with calnexin.

might be expected to increase calnexin binding to misfolded proteins as well. Similar results were obtained in cells co-transfected with HA-calnexin and ABCA1-FLAG when IP was performed with anti-HA antibody and blotted for ABCA1 (**Fig. 4B, top panel**). Importantly, MHC-I, which has been shown to interact with calnexin in glycan-dependent fashion (120-123), failed to precipitate with calnexin upon 24 h treatment of the cells with tunicamycin (**Fig. 4B, bottom panel**). Thus, it appears that glycosylation of ABCA1 is dispensable for its interaction with calnexin and calnexin binding to ABCA1 is not mediated by the glycosyl residues added to ABCA1 during protein processing.

Chapter 6: Nef reduces physical interaction of calnexin and ABCA1

To determine the effect of Nef on ABCA1 interaction with calnexin, HEK 293T cells were transfected with ABCA1-FLAG and Nef and assessed the relative amounts of proteins precipitating with ABCA1-FLAG by Western Blotting. FLAG precipitates were analyzed for proteins identified in our MS/MS analysis (calnexin and dystrophin) and another previously identified ABCA1-interacting protein, SPTLC1 (51). Co-transfection of ABCA1 and wild type Nef caused the disappearance of a band indicative of calnexin interaction, but did not affect ABCA1 interaction with other partners (**Fig. 5A, right panels**), indicating that Nef specifically disrupts the interaction between ABCA1 and calnexin. A similar result was obtained when calnexin was immunoprecipitated from these lysates and probed with an anti-ABCA1 antibody, though in this case Nef reduced but did not entirely prevent the interaction (**Fig. 5B**). It should be noted that ABCA1 and Nef are being over-expressed in this system, whereas calnexin is present at endogenous levels, likely explaining the overall low amount of calnexin in anti-FLAG IPs compared to the high amount of ABCA1 observed in anti-calnexin IPs.

The effect of Nef on ABCA1 and calnexin co-localization was also assessed. HeLa-ABCA1-GFP cells were co-transfected with a construct expressing DsRed2 labeled calnexin (DsRed2-CNX) and either empty vector (pHCMV3) or wild-type Nef. 48 h post-transfection, cells were imaged (**Fig. 5C**) for GFP (ABCA1) (**Fig. 5C, panels a and d**) and DsRed2 (calnexin) (panels b and e). Under control conditions ABCA1 staining

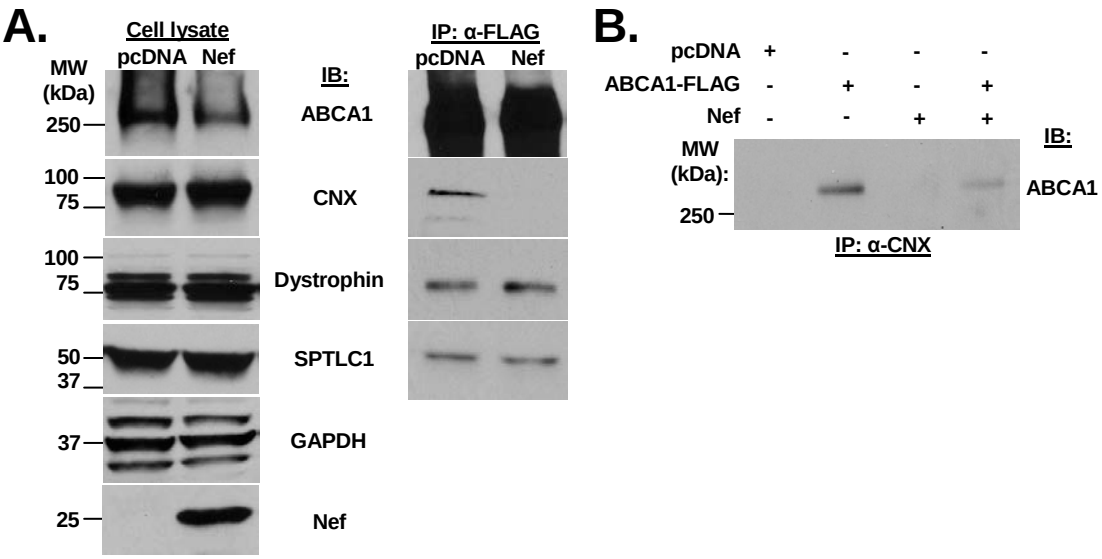
A.
Cell lysate
pcDNA Nef
IP: α-FLAG
pcDNA Nef
MW (kDa)
IB:
250
ABCA1
100
75
CNX
100
75
Dystrophin
50
37
SPTLC1
37
GAPDH
25
Nef
B.
pcDNA + - - -
ABCA1-FLAG - + - +
Nef - - + +
MW (kDa):
IB:
250
ABCA1
IP: α-CNX

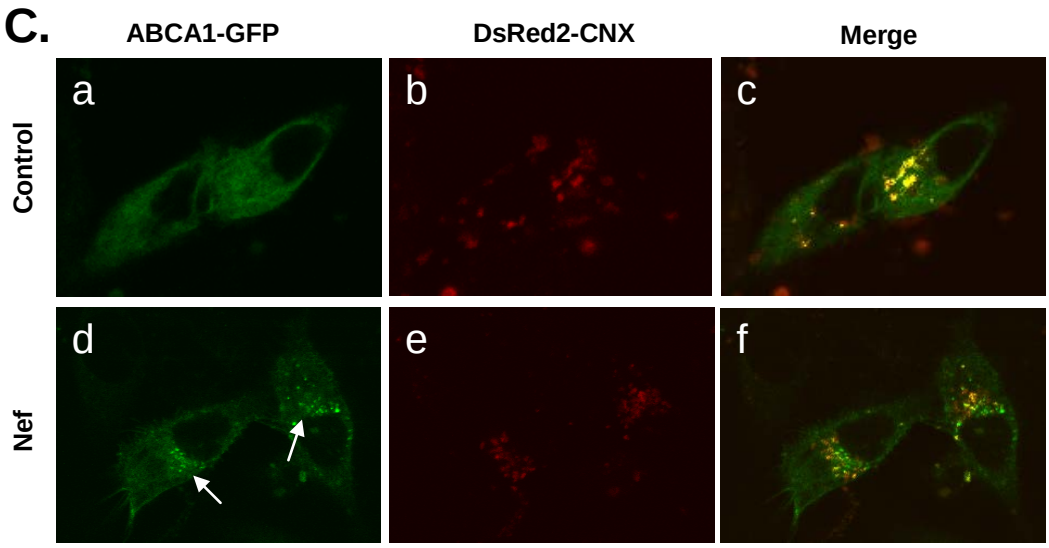
C.
ABCA1-GFP
DsRed2-CNX
Merge
Control
Nef
a
b
c
d
e
f

Figure 5. Nef disrupts ABCA1 interaction with calnexin.

A. HEK293T cells were co-transfected with FLAG-tagged ABCA1 and Nef or empty pcDNA vector, lysed and blotted for ABCA1, calnexin, dystrophin, serine palmitoyltransferase (SPTLC1), GAPDH and Nef (left panels). Following immunoprecipitation with anti-FLAG antibody, immunoprecipitates were blotted for ABCA1, calnexin, dystrophin and SPLTC1 (right panels). A representative experiment of three performed is presented. B. Cell lysates of HEK293T cells transfected with FLAG-tagged ABCA1, Nef, empty pcDNA vector, or co-transfected with FLAG-tagged ABCA1 and Nef were immunoprecipitated with anti-calnexin antibody and blotted for ABCA1. A representative experiment of three performed is presented. C. HeLa-ABCA1-GFP cells were co-transfected with DsRed2 labeled calnexin (DsRed2-CNX) and either empty vector (control) or wild-type Nef. 48 h post-transfection, cells were imaged on a confocal fluorescent microscope for GFP (panels a and d) and DsRed2 (panels b and e). Image overlay is shown in panel c. Arrows point to perinuclear, punctate populations of ABCA1 appearing in Nef-transfected cells. Co-localization was calculated on an image panel including a field of ~10-15 cells from which representative cells are shown.

was diffuse with a significant cytosolic component (**Fig. 5C, panel a**). A three-color image overlay demonstrates that under these conditions ABCA1 and calnexin co-localize in an intracellular, perinuclear region (**Fig. 5C, panel c**). However, in the presence of Nef, co-localization of ABCA1 and calnexin was dramatically reduced (compare **Fig. 5C, panels c and f**) due to a redistribution of intracellular ABCA1 to two clearly distinct plasma membrane and perinuclear, punctate populations (arrows in **Fig. 5C, panel d**).

To determine whether ABCA1-calnexin interaction is impaired during HIV-1 infection, monocyte-derived macrophages were infected with wild-type or Nef-deficient HIV-1 viruses and tested calnexin interaction with ABCA1 and HIV-1 Env (**Fig. 6**). Consistent with previous report (56), the amount of ABCA1 in cells infected with Nef-positive virus was reduced by 36% relative to cells infected with Nef-deficient virus (numbers below upper lane in left panels). ABCA1 co-immunoprecipitated with calnexin in all samples, however, the amount of ABCA1 co-precipitating from cells infected with Nef-positive HIV-1 was reduced over 2-fold relative to cells infected with Nef-deficient HIV-1 (**Fig. 6, top right panels**). A similar result was obtained when immunoprecipitation was performed with anti-ABCA1 antibody and then blotted for calnexin. In this case, the amount of calnexin in the immunoprecipitate from cells infected with Nef-positive HIV-1 was reduced 3.3-fold relative to cells infected with Nef-deficient HIV-1 (**Fig. 6, bottom panel on the right**). Interestingly, interaction between HIV-1 gp160 and calnexin revealed by blotting CNX immunoprecipitate with anti-HIV serum was not affected by the presence of Nef (**Fig. 6, top right panels**). In fact, even more gp160 co-precipitated with calnexin in the presence of Nef. These results support the notion that Nef specifically disrupts

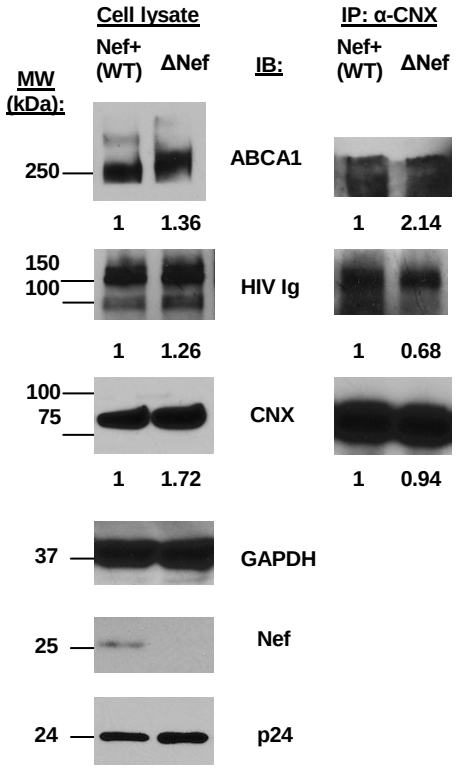
Cell lysate
IP: α-CNX
Nef+ (WT)
ΔNef
IB:
Nef+ (WT)
ΔNef
MW (kDa):
250
ABCA1
1
1.36
1
2.14
150
100
HIV Ig
1
1.26
1
0.68
100
75
CNX
1
1.72
1
0.94
37
GAPDH
25
Nef
24
p24

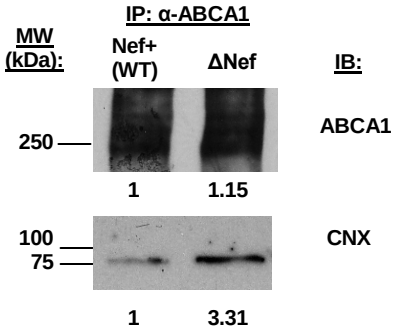
IP: α-ABCA1
MW (kDa):
Nef+ (WT)
ΔNef
IB:
250
ABCA1
1
1.15
100
75
CNX
1
3.31

Figure 6. Nef diminishes ABCA1 and Calnexin interaction during infection

Monocyte-derived macrophages were infected with Nef-positive or Nef-deficient HIV-1 (ΔNef), cultured for 2 weeks, lysed, and immunoblotted using anti-ABCA1 antibody (ABCA1), serum from an HIV-positive patient (HIV), and anti-bodies to calnexin (CNX), GAPDH, Nef and p24 (left panels). Cell lysates were immunoprecipitated using anti-calnexin (top three right panels) or anti-ABCA1 antibody (bottom two right panels) and immunoblotted using anti-ABCA1 antibody (ABCA1), serum from an HIV-positive patient (HIV), and anti-body to calnexin (CNX). A representative experiment of two performed is presented. Density of the bands was quantified using ImageJ program, and results are presented underneath the panels.

interaction between calnexin and ABCA1, but promotes interaction between calnexin and gp160.

Having observed that Nef reduces the interaction between ABCA1 and calnexin, it was hypothesized that Nef may affect calnexin localization. To assess this possibility, HeLa-ABCA1-GFP cells were transfected with Nef or empty control vector and 48 h post-transfection cells were fractionated into cytosolic, membrane, nuclear, chromatin-bound, and cytoskeletal fractions with the Subcellular Fractionation Kit. Marker proteins Hsp90, calreticulin, transferrin receptor, HDAC2, and cytokeratin 18 were used to confirm the identity of each fraction, respectively. In this analysis, calnexin was detected exclusively in the membrane fraction in both control DNA- and Nef-transfected cells (**Fig. 7A**). ABCA1 was also recovered exclusively in the membrane fraction, while Nef was distributed throughout all cellular compartments with particular enrichment in the membrane and in association with cytoskeleton. Thus, Nef does not alter the global sub-cellular distribution of calnexin, and Nef, ABCA1, and calnexin are all enriched in membranes suggesting that membrane association may be involved in the dynamics of interaction between these three proteins.

Nef has been shown to alter the membrane character and solubility of various transmembrane proteins. In particular, Nef is thought to modify the protein content of discreet, ordered areas of membranes variously termed lipid rafts or detergent-resistant membranes (DRM). Nef increases the solubility of certain proteins by excluding them from lipid rafts, exemplified by the ubiquitin conjugating enzyme UbcH7 (124). Nef likewise decreases the solubility of a variety of proteins including Cdc42, βPix, Cbl-b,

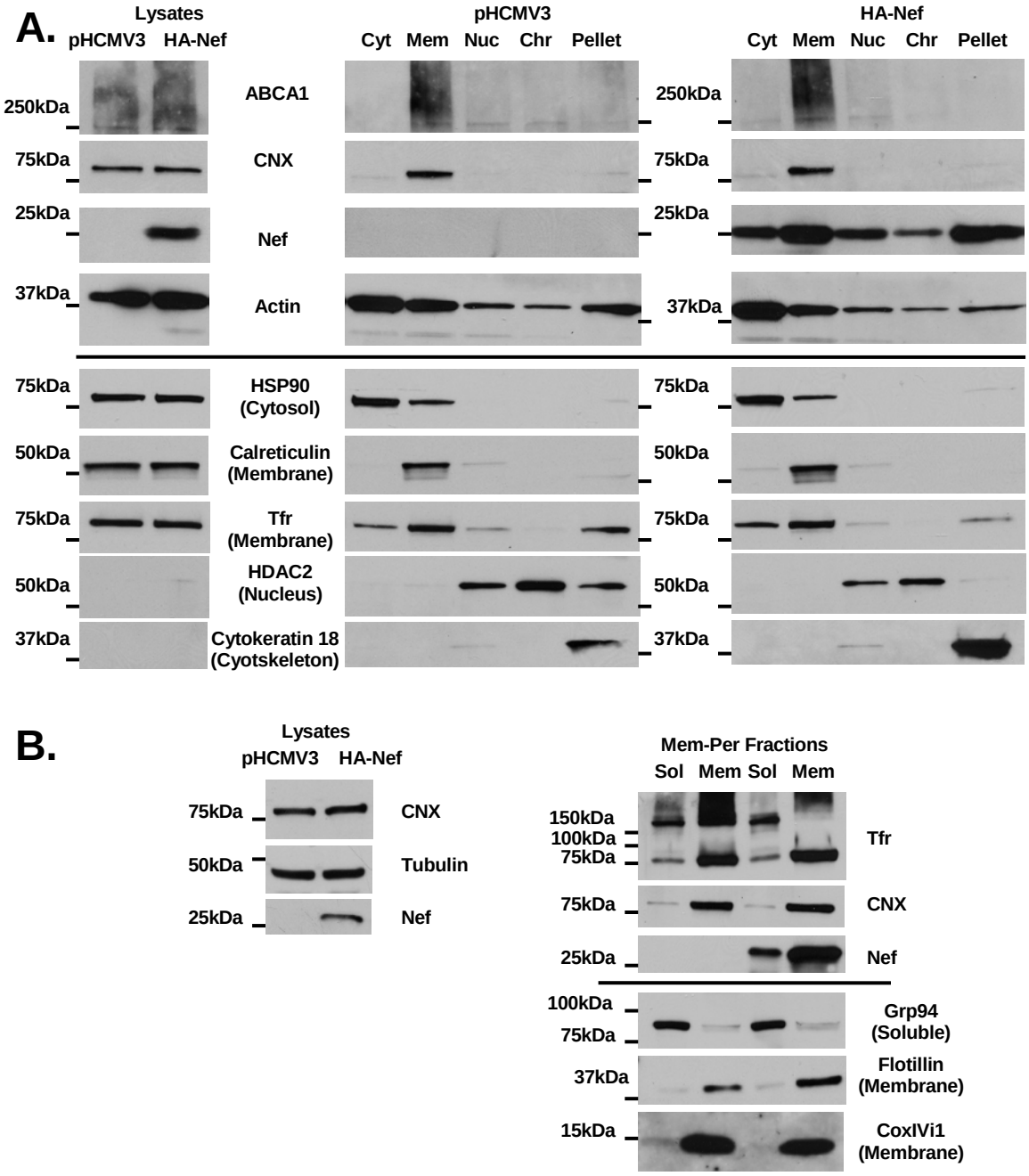
A.
Lysates
pHCMV3
HA-Nef
pHCMV3
Cyt
Mem
Nuc
Chr
Pellet
HA-Nef
Cyt
Mem
Nuc
Chr
Pellet
250kDa
ABCA1
250kDa
75kDa
CNX
75kDa
25kDa
Nef
25kDa
37kDa
Actin
37kDa
75kDa
HSP90 (Cytosol)
75kDa
50kDa
Calreticulin (Membrane)
50kDa
75kDa
Tfr (Membrane)
75kDa
50kDa
HDAC2 (Nucleus)
50kDa
37kDa
Cytokeratin 18 (Cyotskeleton)
37kDa

B.
Lysates
pHCMV3
HA-Nef
75kDa
CNX
50kDa
Tubulin
25kDa
Nef
Mem-Per Fractions
Sol
Mem
Sol
Mem
150kDa
100kDa
75kDa
Tfr
75kDa
CNX
25kDa
Nef
100kDa
75kDa
Grp94 (Soluble)
37kDa
Flotillin (Membrane)
15kDa
CoxIVi1 (Membrane)

Figure 7. Nef does not alter cellular localization or solubility of calnexin

A. HeLa-ABCA1-GFP cells were transfected with pHCMV3 or HA/His-Nef and 48Hr post-transfection were lysed and processed for subcellular fractionation with the Subcellular Protein Fractionation Kit (Pierce). Equal amount of Total Protein from Whole Cell Lystaes and from each fraction were separated by SDS-PAGE and blotted for ABCA1, calnexin, Nef, and actin. HSP90 (cytosol), calreticulin (membrane), transferrin receptor (membrane), HDAC2 (nucleus/chromatin), and cytokeratin-18 (cytoskeleton) marker proteins were used to assess the purity of fractions. B. HeLa-ABCA1-GFP cells were transfected with pHCMV3 or HA/His-Nef and 48Hr post-transfection were lysed and processed for membrane and soluble protein fractionation with the Mem-Per Membrane Protein Extraction Kit (Pierce). (Left panels) Equal amount of total protein from whole cell lysates were separated by SDS-PAGE and blotted for calnexin, tubulin, and Nef. (Right panels) Equal amounts of each fraction (soluble and membrane) were separated by SDS-PAGE and blotted for transferrin receptor, calnexin, and Nef. Grp94 (soluble), Flotillin (membrane), and CoxIVi1 (membrane) marker proteins were used to assess the purity of fractions.

p21-activated kinase (Pak), a palmitoylated mutant G-protein G_0C3S, PKCθ, and Vav1 by recruiting these signaling proteins into DRM (124-128). Additionally there are reports that Nef may alter the solubility of transferrin receptor (Tfr) (116, 129) though this appears to involve altered Tfr recycling rather than DRM (130). Considering that Nef does not appear to alter calnexin localization to membranes, it was hypothesized that Nef may be influencing the interaction between ABCA1 and calnexin by altering the solubility of calnexin. To address this issue, HeLa-ABCA1-GFP cells were transfected with Nef or empty control vector and 48 Hr post-transfection membrane and soluble protein extracts were prepared using the Mem-Per Membrane Protein Extraction Kit (Pierce) (**Fig. 7B**). Grp94 was used to confirm the extraction of soluble proteins while flotillin and CoxIVi1 were used to confirm the extraction of membrane proteins. These marker proteins revealed clear separation of soluble and membrane fractions (**Fig. 7B, bottom right panels**). Whereas a Nef-mediated increase in solubility of the high molecular weight dimeric Tfr was apparent, Nef did not alter the distribution of calnexin between the soluble and membrane fractions (**Fig. 7B, top right panels**).

Having observed that Nef does not affect subcellular localization or solubility of calnexin, the effect of Nef on partitioning of calnexin into lipid rafts was investigated. As described above, Nef has a wide range of effects on the protein composition of lipid rafts through both recruitment and exclusion of target proteins. While calnexin is not traditionally considered a raft-associated protein, various groups have reported the recovery of calnexin in rafts (131, 132). Additionally it has been reported that calnexin may also be present on ER-derived raft-like domains (133). Minor populations of

ABCA1 can also be recovered in rafts and it has been shown that Nef reduces ABCA1 in rafts in favor of non-rafts in RAW macrophages (77). Given these considerations, it was hypothesized that Nef may recruit calnexin into rafts while excluding ABCA1, thereby achieving reduction in ABCA1-calnexin interaction by biophysical segregation of the two proteins. To test the effects of Nef on calnexin partitioning into rafts, HeLa-ABCA1-GFP cells were transfected with pHCMV3 or HA/His-Nef and rafts prepared by flotation on sucrose gradients as described in Materials and Methods. Nef expression had little effect on raft partitioning of either ABCA1 or calnexin as both proteins were predominantly recovered in non-raft fractions in HeLa cells (**Fig. 8**). While Nef appears to induce a consistent reduction in the minor population of calnexin in rafts, this reduction is unlikely to contribute to disruption of the ABCA1-calnexin interaction as the vast majority of calnexin is recovered in non-rafts along with ABCA1.

Nef has been shown to significantly affect subcellular fractionation of multiple proteins at the level of the ER and Golgi. In particular, Nef causes a shift of T-cell signaling complex molecules Lck, p-Lck505, and N-Ras from the plasma membrane to the TGN/ER network (134). Similarly, Nef causes a shift of the macrophage specific signaling kinase Hck from the plasma membrane to the TGN/ER network (135). Nef also disturbs the structure of the TGN as evidenced by a shift of GM130 from heavy membrane fractions (ER-derived) into light membrane fractions (Golgi-derived) (136). Importantly, in certain experiments Nef caused a portion of calnexin to shift from the heavy membranes into lighter membranes (135). In order to determine if Nef re-organization of the ER/Golgi

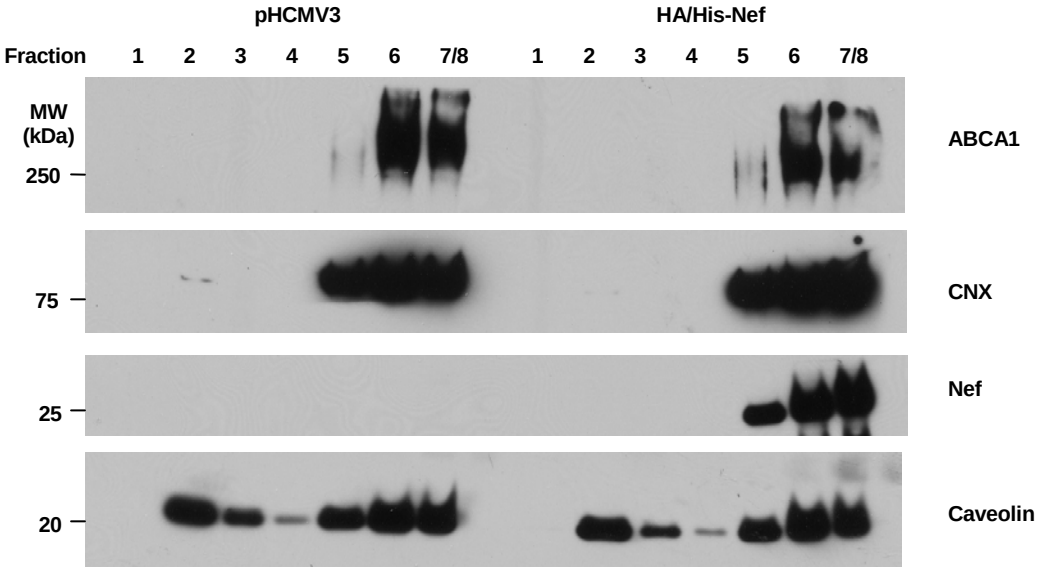
pHCMV3
HA/His-Nef
Fraction 1 2 3 4 5 6 7/8 1 2 3 4 5 6 7/8
MW (kDa)
250
75
25
20
ABCA1
CNX
Nef
Caveolin

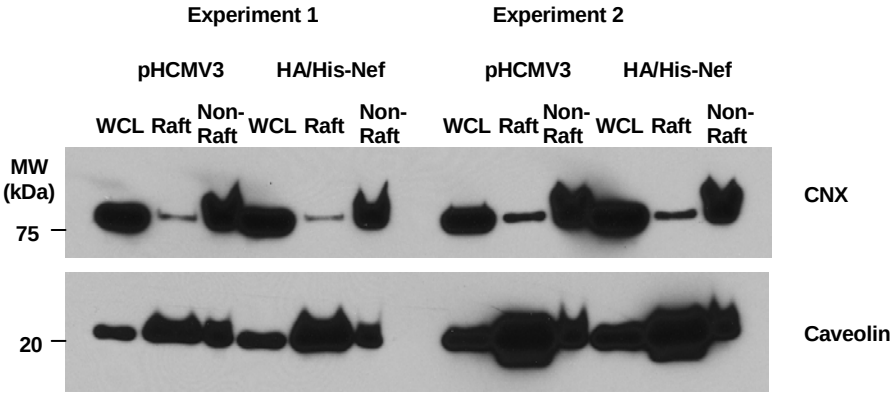
Experiment 1
Experiment 2
pHCMV3
HA/His-Nef
pHCMV3
HA/His-Nef
WCL Raft Non-Raft WCL Raft Non-Raft WCL Raft Non-Raft WCL Raft Non-Raft
MW (kDa)
75
20
CNX
Caveolin

Figure 8. Nef does not alter raft partitioing of calnexin

Top panels-HeLa-ABCA1-GFP cells were transfected with pHCMV3 or HA/His-Nef and 48 h post-transfection were lysed and processed for raft flotation on sucrose gradients as described in Materials and Methods. Eight fractions were recovered from the top of the gradient and equal volumes of each fraction were separated by SDS-PAGE and blotted for ABCA1, calnexin, and Nef. Caveolin, a well-characterized marker of rafts, was used to determine raft flotation into the gradient. Bottom panels- HeLa-ABCA1-GFP cells were processed as in the top panels and equal amounts (by total protein as determined by Bio-Rad DC Protein Assay) of the raft fraction (fraction 2), pooled non-raft fraction (fractions 7/8), and whole cell lysate were separated by SDS-PAGE and blotted for calnexin and caveolin. *Note enrichment of caveolin in raft fractions in bottom panels confirming flotation of rafts to this fraction.

network may contribute to the reduction in interaction of ABCA1 and calnexin HeLa-ABCA1-GFP cells were transfected with Nef or empty control vector and 48 h post-transfection were fractionated into Heavy (HM) and Light (LM) membrane fractions and a soluble cytosolic (Cyt) fraction by differential ultracentrifugation. This method separates membrane organelles based on size such that heavy membranes include ER- and mitochondria-derived proteins, light membranes contain Golgi- and secretory-vesicle derived proteins, and the cytosolic fraction contains mainly non-membrane associated soluble proteins (117). Using this method, plasma membrane proteins (caveolin) fractionated with heavy membranes and Golgi- (β-COP) and endosomal-proteins (EEA1) fractionated with light membranes and the soluble fraction, respectively (**Fig. 9A, lower panels**). Thus, this procedure provides a simple method to separate the most prominent populations of ABCA1 observed in cells: ER- and PM-derived ABCA1 should fractionate into heavy membranes and ABCA1 derived from smaller membranes of the Golgi and vesicular network should fractionate into light membranes. Calreticulin, COXIV Isoform 1, β-COP and HSP90 were used as control markers for ER, mitochondria, Golgi, and cytosolic proteins, respectively. As expected, this analysis showed enrichment of mitochondria and ER markers in heavy membrane fractions, whereas the Golgi marker β-COP was isolated almost exclusively in light membrane pellets (**Fig. 9A, lower panels**). When control transfected cells were fractionated by this method, ABCA1 partitioned into both the HM and LM fractions, being particularly enriched in the LM fraction, but was excluded from the Cyt fraction (**Fig. 9A, upper panels**). Calnexin was distributed throughout both HM and LM nearly equally under control conditions, and was also

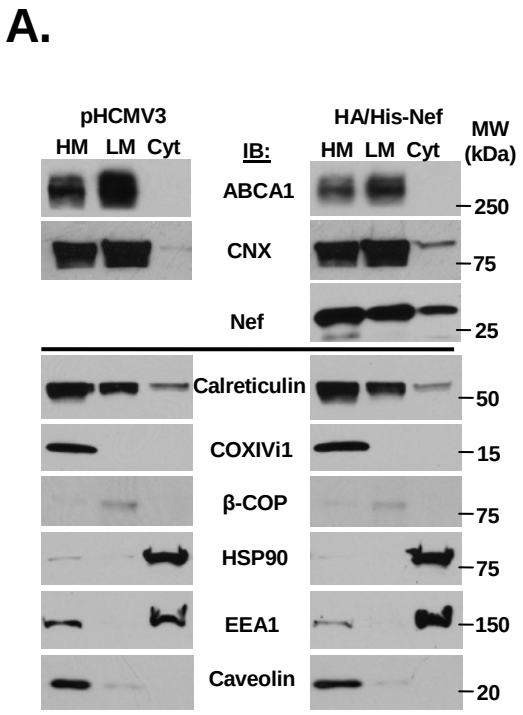
A.
pHCMV3
HM LM Cyt
IB:
HA/His-Nef
HM LM Cyt
MW (kDa)
ABCA1
250
CNX
75
Nef
25
Calreticulin
50
COXIVi1
15
β-COP
75
HSP90
75
EEA1
150
Caveolin
20

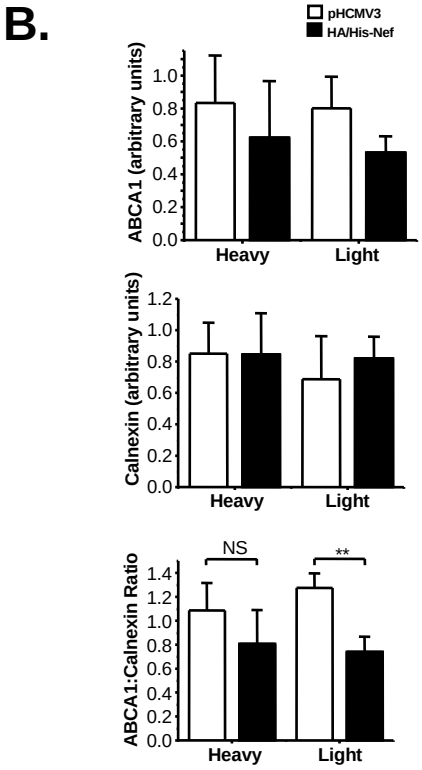
B.
pHCMV3
HA/His-Nef
ABCA1 (arbitrary units)
1.0
0.8
0.6
0.4
0.2
0.0
Heavy
Light
Calnexin (arbitrary units)
1.2
1.0
0.8
0.6
0.4
0.2
0.0
Heavy
Light
ABCA1:Calnexin Ratio
NS
**
1.4
1.2
1.0
0.8
0.6
0.4
0.2
0.0
Heavy
Light

Figure 9. Nef induces segregation of calnexin and ABCA1.

A. HeLa-ABCA1-GFP cells were transfected with HA/His-tagged Nef or empty vector (pHCMV3), lysed, fractionated into heavy membranes (HM), light membranes (LM) and cytosol (Cyt) by sucrose gradient centrifugation, and fractions were blotted for ABCA1, calnexin and Nef, as well as marker proteins calreticulum, COXIVi1, β-COP, HSP90, EEA1 and caveolin. B. ABCA1 (left graph) and calnexin (middle graph) bands were quantified using ImageJ program, the right graph presents ABCA1 to calnexin ratio. NS – not significant, **$p<0.01$. Graphs in D. represent density determinations of three independent experiments.

practically excluded from the Cyt fraction. Upon Nef expression, ABCA1 was reduced in all fractions, as expected, but was particularly decreased from the LM fraction (**Fig. 9B**). In contrast, calnexin was increased in the late-secretory pathway, in particular in the Cyt fraction, by Nef expression. This relative re-distribution of ABCA1 and calnexin induced by Nef resulted in a reduced ratio of ABCA1-calnexin in both compartments but most particularly and significantly on light membranes of the late-secretory pathway (**Fig. 9B**). Together, these observations provide biochemical confirmation for segregation of ABCA1 and calnexin to two distinct locations in the presence of Nef: ABCA1 is reduced in recycling compartments in the Golgi and vesicular network, whereas a significant portion of calnexin is found in these very compartments.

Although calnexin localizes predominantly to ER membranes, its distribution between ER, mitochondria-associated membrane, and plasma membrane can vary upon different treatments (117). It was hypothesized that Nef may alter calnexin distribution between membranes, thus affecting calnexin functional activity. To assess this possibility, HeLa-ABCA1-GFP cells were transfected with Nef or empty control vector and 48 h post-transfection cells were subjected to cell surface biotinylation to isolate plasma membrane proteins. Under control conditions in the absence of Nef, the majority of calnexin was intracellular (**Fig. 10A**). Upon Nef expression, the amount of calnexin accessible to biotin, indicative of plasma membrane expression, was noticeably increased. Nef decreased total ABCA1, however, consistent with previous results in RAW macrophages (56) and HeLa cells (77), ABCA1 on the cell surface was relatively stable while intracellular ABCA1 was greatly reduced.

The distribution of calnexin between ER, mitochondria-associated membrane, and plasma membrane has been reported to be controlled by sorting protein PACS-2 (117). Given that Nef also interacts with PACS-2 (137), it was hypothesized that Nef may alter calnexin localization by altering binding of calnexin and PACS-2. Interaction between calnexin and PACS-2 was increased upon Nef expression (**Fig. 10B**). This result contradicts previous report that binding to PACS-2 increased ER retention of calnexin (117) and suggests that increased interaction between PACS-2 and calnexin in the presence of Nef may contribute to the relocalization of calnexin away from the ER (**Fig. 9**) with ultimate delivery of calnexin to the plasma membrane (**Fig. 10A**), thus preventing calnexin from assisting in ABCA1 maturation.

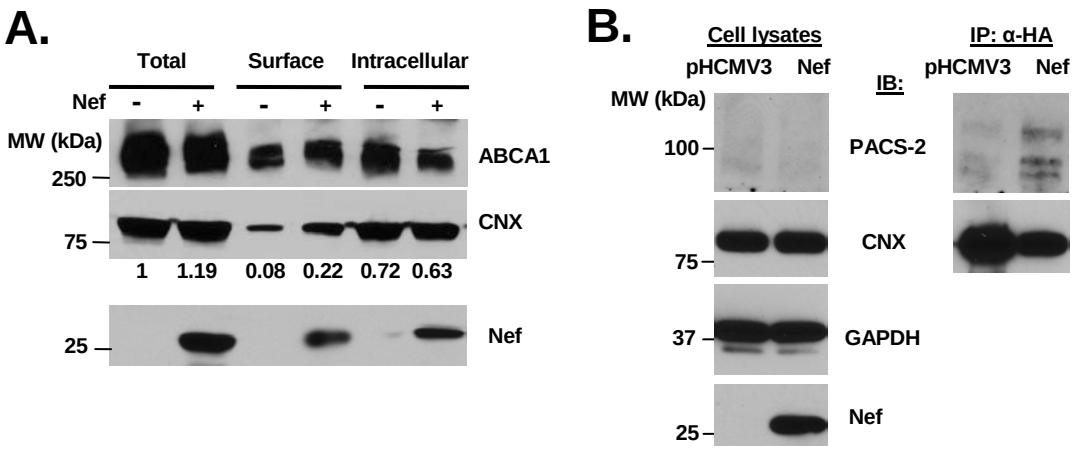
A.
Total
Surface
Intracellular
Nef
- + - + - +
MW (kDa)
250
ABCA1
75
CNX
1 1.19 0.08 0.22 0.72 0.63
25
Nef
B.
Cell lysates
pHCMV3 Nef
IP: α-HA
pHCMV3 Nef
IB:
MW (kDa)
100
PACS-2
75
CNX
37
GAPDH
25
Nef

Figure 10. Nef increases calnexin surface expression and PACS-2 interaction.

A. HeLa-ABCA1-GFP cells were transfected with Nef (+) or empty control vector (-) and subjected to cell surface biotinylation. Cell lysate was probed with antibodies to ABCA1, calnexin, and Nef either before fractionation (lanes marked total), or after precipitation with streptavidin beads into the pellet (lanes marked surface) and supernatant (lanes marked intracellular). Numbers below calnexin blot indicate calnexin density relative to calnexin density from Total column of cells transfected with pHCMV3 as determined by ImageJ. A representative experiment of two perfored is presented. B. HeLa-ABCA1-GFP cells were co-transfected with HA-tagged calnexin and Nef or empty vector pHCMV3, lysed, and immunoblotted for PACS-2, calnexin, GAPDH and Nef (left panels). Following immunoprecipitation with anti-HA antibody, immunoprecipitates were blotted with antibodies to PACS-2 and calnexin (right panels).

Chapter 7: Nef physically interacts with calnexin

Calnexin is an essential protein of the Endoplasmic Reticulum and is largely confined to the ER due to numerous ER-retention signals. However, ER localization of Nef has not been reported. To determine whether Nef localizes to ER, confocal microscopy was performed at super-resolution on HeLa cells transfected with WT Nef-GFP and CFP with a mitochondrial localization signal (CFP-Mito) or an ER localization signal (CFP-ER) (**Fig. 11, panels A-F**). CFP-Mito was chosen for comparison purposes because Nef has been reported to be largely excluded from mitochondria (138). Nef-GFP demonstrated a consistent fluorescent signature enriched on the plasma membrane and diffuse throughout the intracellular space with punctuate concentrations in putative cellular organelle and vesicle membranes (**Fig. 11, panels B and E**). When compared to the fluorescent signature of the targeted CFP constructs, Nef showed little co-localization with mitochondria-targeted CFP (**Fig. 11, panels D-F**), as individual mitochondria could be observed arranged as a "cap" around an intracellular concentration of Nef-GFP perinuclear to the "cap" of mitochondria. In contrast, the perinuclear Nef-GFP appeared to co-localize to a great extent with CFP-ER (**Fig. 11, panels A-C**). This analysis suggests that a proportion of the intracellular population of Nef co-localizes with ER. Together with fractionation data demonstrating predominantly membrane localization of Nef (**Fig. 7**), this result indicates that a fraction of Nef localizes to ER membrane.

Given localization of a proportion of Nef to ER membranes, it was hypothesized that Nef may physically associate with calnexin. To test this possibility, HEK 293T cells were transfected with HA-tagged wild-type or mutant Nef (G2A mutation), precipitated

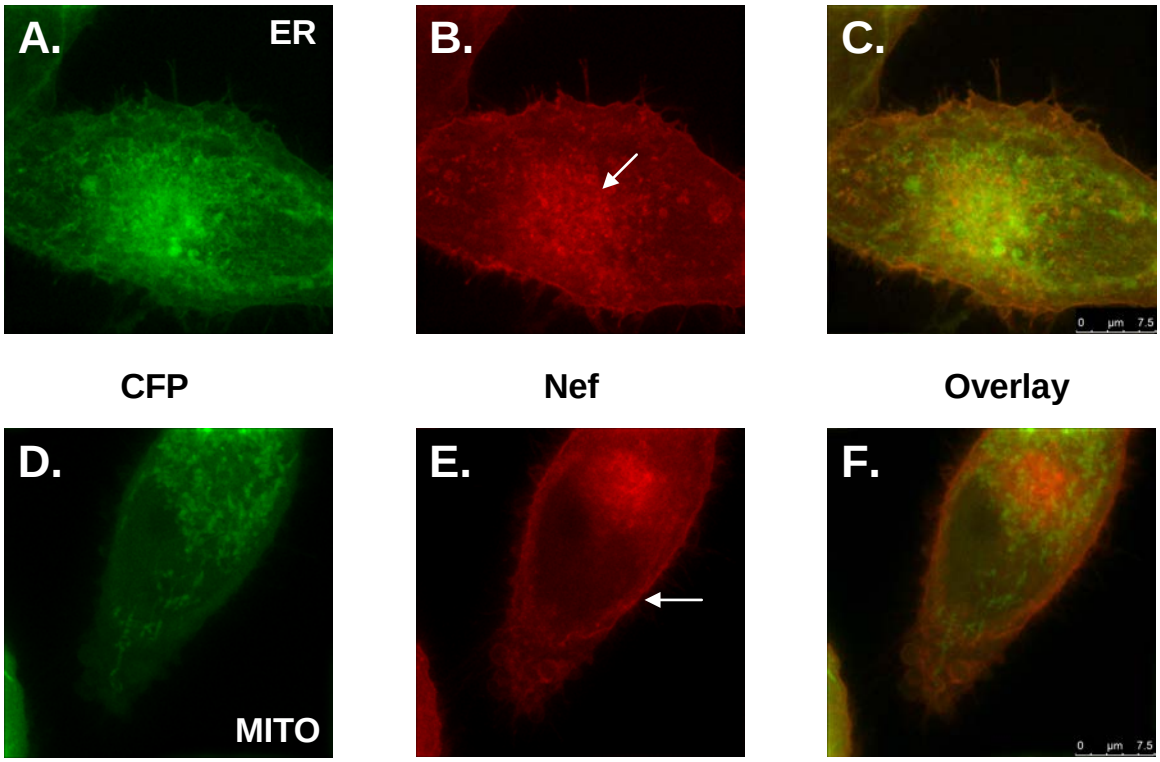
A.
ER
B.
C.
CFP
Nef
Overlay
D.
MITO
E.
F.

Figure 11. Nef co-localizes with ER marker.

Confocal microscopy at super-resolution of HeLa cells co-transfected with Nef-GFP (panels B and E) and CFP with either an ER (CFP-ER) (panel A) or a mitochondrial localization signal (CFP-Mito) (panel D). Arrows point to punctate (panel B) and membrane (panel E) localization of Nef. Panels C and F show overlay of the images.

with agarose-immobilized anti-HA antibody and blotted for calnexin. NefG2A does not associate with membranes due to a myristoylation defect (**Fig. 12B**). Whereas the IP from cells transfected with HA-tagged Nef clearly identified a band corresponding to calnexin, no such band was observed in IPs from NefG2A transfected cells, suggesting that membrane association of Nef was required for the Nef-calnexin interaction (**Fig. 12A**).

Having observed that Nef physically interacts with calnexin and that the NefG2A mutant fails to associate with calnexin, studies were designed to determine if association of Nef with calnexin was required for Nef interference with the ABCA1-calnexin interaction. In order to test this possibility, HEK 293T cells were transfected with ABCA1-FLAG and either WT Nef or NefG2A, and anti-FLAG IPs were analysed for calnexin. According to this analysis, ABCA1 showed little interaction with calnexin in the presence of WT Nef, whereas in the presence of NefG2A ABCA1 precipitated calnexin at normal levels (**Fig. 12C**). Combined with the observation that the NefG2A mutant was consistently defective in impairing ABCA1-mediated cholesterol efflux activity (56), this result suggests that Nef interaction with calnexin is required for Nef-mediated disruption of ABCA1-calnexin interaction and functional impairment of ABCA1.

Based on the evidence presented thus far, it was hypothesized that Nef reduces the interaction between ABCA1 and calnexin by binding to calnexin and physically redistributing calnexin to membranes that may be inaccessible to ABCA1 or may be too late in the secretory pathway for calnexin to perform necessary chaperone function, thus explaining the reduction in ABCA1 activity in the presence of Nef. A key component of this hypothesis is the involvement of membranes and the requirement for Nef and

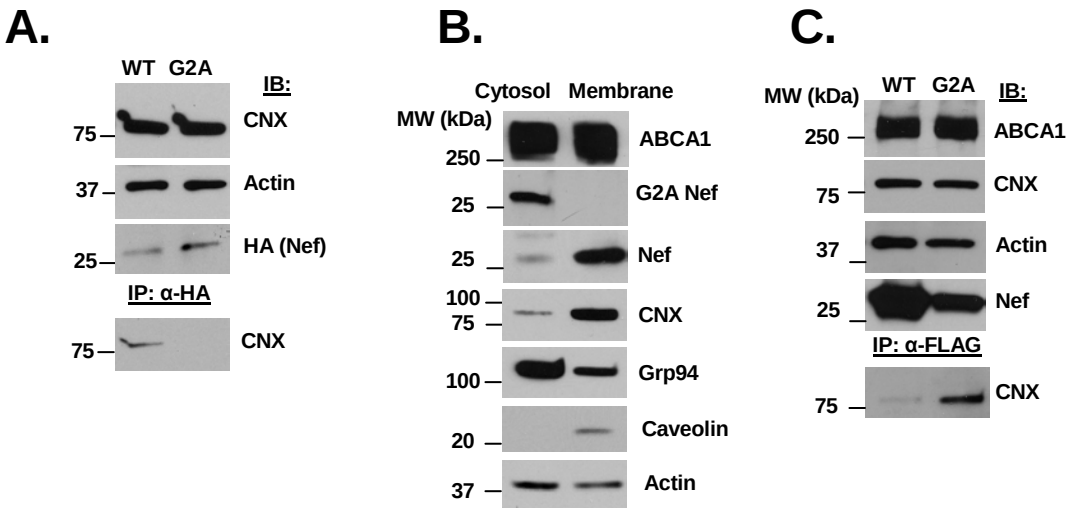
A.
WT G2A
IB:
75
CNX
37
Actin
25
HA (Nef)
IP: α-HA
75
CNX
B.
Cytosol Membrane
MW (kDa)
250
ABCA1
25
G2A Nef
25
Nef
100
75
CNX
100
Grp94
20
Caveolin
37
Actin
C.
MW (kDa)
WT G2A
IB:
250
ABCA1
75
CNX
37
Actin
25
Nef
IP: α-FLAG
75
CNX

Figure 12. Nef physically interacts with calnexin.

A. HEK293T cells were transfected with HA-tagged wild-type Nef (WT) or G2A mutant defective in myristoylation. Cell lysates in (1%) NP-40 Lysis Buffer were blotted for calnexin, actin, and HA (upper panels), and immunoprecipitate obtained using anti-HA antibody was blotted for calnexin (bottom panel). A representative experiment of two performed is presented. B. HeLa-ABCA1-GFP cells were transfected with WT or G2A Nef and 48 hr post-transfection cells were lysed. Cytosol and membrane fractions were prepared with the Mem-Per Membrane Protein Extraction Kit (Pierce). Equal amounts (by total protein determined with Bio-Rad DC Protein Assay) of each fraction were separated by SDS-PAGE and blotted with anti-ABCA1 (Novus Biologicals), anti-Calnexin (Stressgen), Anti-Grp94 (Stressgen), anti-Caveolin (Millipore), or anti-β actin (Sigma) antibodies, or anti-Nef antisera (NIH AIDS Reagent Program). Grp94 (Soluble fraction) and Caveolin (Membrane fraction) were used as marker proteins to assess purity of each fraction. C. HEK293T cells were transfected with ABCA1-FLAG and either WT Nef or NefG2A. Cell lysates in (1%) NP-40 Lysis Buffer were analyzed for ABCA1, calnexin, actin and Nef using monoclonal antibodies (upper panels), and anti-FLAG immunoprecipitates were analyzed for calnexin (bottom panel). A representative experiment of two performed is shown.

calnexin interaction on membranes. Having seen that membrane association of Nef is required for interaction with calnexin (**Fig. 12A**) studies were designed to determine what structural features in calnexin were required for the interaction. Therefore, a series of calnexin mutants were generated that delete individual structural domains (**Fig. 13A**) and determined their capacity to interact with Nef by His-Bind purification of His-Nef (**Fig. 13B**). Calnexin C-terminal truncations targeting the cytoplasmic domain (ΔCyt), both the cytoplasmic and transmembrane domain (ΔCyt, TM), or the entire C-terminal domain (1-392 were analyzed along with a deletion mutant targeting the P-domain which is involved in peptide and calcium binding. The 1-392 construct deletes the portion of calnexin sequence that is non-homologous to calreticulin and generates a soluble species with glycoprotein binding preference similar to that of calreticulin. In this analysis, both constructs that disrupted the transmembrane region of calnexin (ΔCyt, TM and 1-392) abrogated binding to His-Nef (**Fig. 13B**). Thus, membrane association of calnexin is required for interaction with Nef.

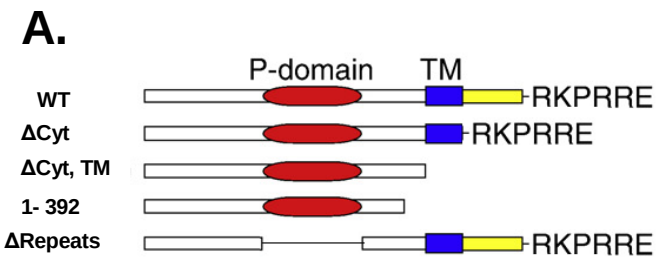
A.
P-domain
TM
WT
RKPRRE
ΔCyt
RKPRRE
ΔCyt, TM
1- 392
ΔRepeats
RKPRRE

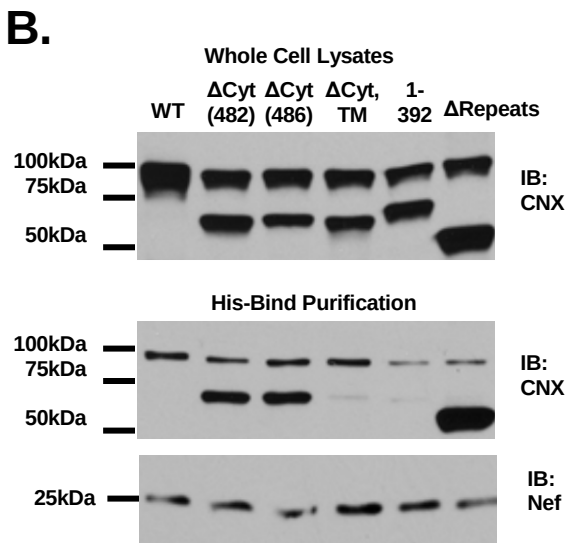
B.
Whole Cell Lysates
WT
ΔCyt (482)
ΔCyt (486)
ΔCyt, TM
1- 392
ΔRepeats
100kDa
75kDa
50kDa
IB: CNX
His-Bind Purification
100kDa
75kDa
50kDa
IB: CNX
25kDa
IB: Nef

Figure 13. Membrane association is required for Calnexin-Nef interaction.

A. Calnexin constructs used to determine requirements for association with Nef. Each construct was generated by standard PCR cloning methods and inserted into pHCMV3 to maintain an in-frame C-terminal HA-Tag. Figure adapted from (139). Copyright © 2008, with permission from Elsevier. B. HEK293T cells were transfected with the indicated calnexin constructs (note that two ΔCyt mutants differ in the residue of termination as indicated below the mutant designation) and His-Nef. 48 h post-transfection cells were lysed and Nef was isolated by His-Bind purification. Co-purifying calnexin was identified with an anti-Calnexin antibody (note that the upper band in calnexin blots of His-Bind purifications likely represents the endogenous calnexin).

Chapter 8: Nef expression or calnexin knockdown redistribute ABCA1

Calnexin is primarily localized to ER and it has been suggested that calnexin interaction with mutants of the ABC transporters P-glycoprotein and CFTR may be responsible for retaining mutants of these proteins in the ER and away from their primary functional location at the plasma membrane (48, 140). In order to test the effect of calnexin on ABCA1 localization, ABCA1 localization relative to a fluorescent construct that labels ER (DsRed2-ER) was monitored via live-cell confocal microscopy of cells transfected with control or calnexin siRNA. 72 h post-transfection, cells were imaged for GFP (ABCA1) (**Fig. 14A, panels a and d**) and DsRed2 (ER) (**Fig. 14A, panels b and e**). Co-localization was determined as described in Materials and Methods (**Fig. 14A, panels c and f**). In cells treated with control siRNA, ABCA1 fluorescence demonstrated a membrane and vesicular staining pattern similar to that described previously (114). A significant portion of ABCA1 in control siRNA treated cells demonstrated co-localization with DsRed2-ER in a perinuclear region, as well as throughout the periphery of a structure with diffuse reticular character stained predominantly with DsRed2-ER as was expected of ER (**Fig. 14A, panel c**). In cells where calnexin was knocked down with siRNA, ABCA1 still demonstrated considerable peripheral staining but the intracellular portion of ABCA1 was greatly reduced and no longer co-localized with ER (**Fig. 14A, panel f**). This result suggests that upon calnexin knock down, a portion of ABCA1 escapes the ER. In summary, these results support the notion that under normal conditions calnexin serves to retain a portion of ABCA1 (supposedly in the process of folding maturation) away from the PM in the ER.

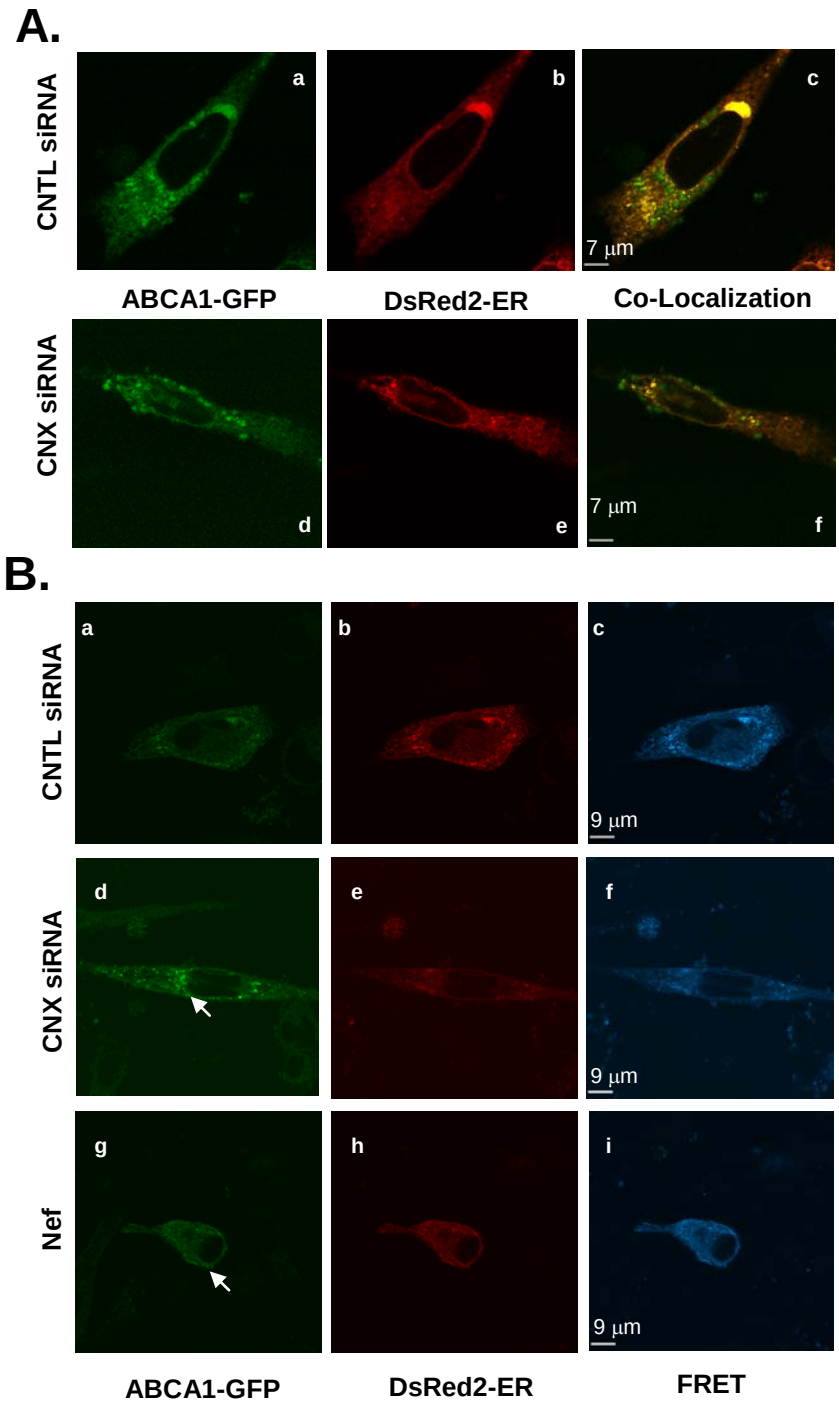
A.
CNTL siRNA
a
b
c
7 μm
ABCA1-GFP
DsRed2-ER
Co-Localization
CNX siRNA
d
e
7 μm
f
B.
CNTL siRNA
a
b
c
9 μm
CNX siRNA
d
e
f
9 μm
Nef
g
h
i
9 μm
ABCA1-GFP
DsRed2-ER
FRET

Figure 14. Calnexin knockdown allows ER escape of ABCA1.

A. HeLa-ABCA1-GFP cells were co-transfected with a fluorescent construct that labels ER (DsRed2-ER) and control (CNTL) or calnexin-specific (CNX) siRNA and monitored via live-cell confocal microscopy. Panels c and f show co-localization of the GFP and DsRed images. B. HeLa-ABCA1-GFP cells were co-transfected with DsRed2-ER and either control (CNTL) siRNA, calnexin (CNX) siRNA or Nef, and spatial proximity of GFP with DsRed2 was determined by FRET (panels c, f, i).

HeLa-ABCA1-GFP cells were then co-transfected with DsRed2-ER and either control siRNA, calnexin siRNA or Nef, imaged GFP (ABCA1) (**Fig. 14B, panels a, d, g**) and DsRed2 (ER) (**Fig. 14B, panels b, e, h**), and determined spatial proximity of GFP with DsRed2 by FRET (**Fig. 14B, panels c, f, i**). In agreement with our other experiments, under control conditions ABCA1 demonstrated membrane and vesicular staining (**Fig. 14B, panel a**) and a high degree of physical proximity to ER as determined by FRET from GFP to DsRed2 (**Fig. 14B, panel c**). Close physical association between ABCA1 and ER observed under control conditions was decreased as evidenced by significantly diminished FRET upon calnexin knockdown (**Fig. 14B, panel f**). Upon Nef expression, a similar reduction in FRET occurred to a level that was intermediate between control and calnexin siRNA treated cells (**Fig. 14B, panel i**). Taken together, these results demonstrate that the organelle where ABCA1-calnexin interaction takes place and is targeted by Nef is ER.

Chapter 9: Calnexin contributes to ABCA1 Function

Having demonstrated that Nef reduces the interaction between ABCA1 and calnexin, experiments were designed to determine if interaction with calnexin contributes to ABCA1 function. To determine if the interaction between ABCA1 and calnexin has an impact on apoA-I specific cholesterol efflux, calnexin was knocked down in HeLa-ABCA1-GFP cells with small-interfering RNA (siRNA) and cholesterol efflux was measured. In the absence of cholesterol acceptor, calnexin knock-down had no effect on diffusional cholesterol efflux (**Fig. 15A**, compare left bar for each sample). However, calnexin knock-down reduced apoA-I specific cholesterol efflux, a portion of efflux mediated by ABCA1, by greater than 50 percent (**Fig. 15B**). Inhibition of apoA-I specific cholesterol efflux is a consistent hallmark of the Nef effect on ABCA1 (56, 73-75, 77). This result supports the notion that blockade of the interaction between ABCA1 and calnexin contributes to the effect of Nef on apoA-I specific cholesterol efflux.

ApoA-I specific cholesterol efflux correlates with gross ABCA1 protein expression as well as ABCA1 membrane localization. Considering the decrease in ApoA-I specific cholesterol efflux observed upon calnexin knock-down, it was hypothesized that interaction with calnexin may stabilize ABCA1 protein and promote efflux in this fashion. To assess the impact of calnexin on ABCA1 expression, calnexin was knocked out in HeLa-ABCA1-GFP cells with calnexin-specific siRNA and ABCA1 turnover was measured by incubating cells with cycloheximide for varying times to inhibit protein synthesis. Calnexin knock-down and ABCA1 turnover were followed by

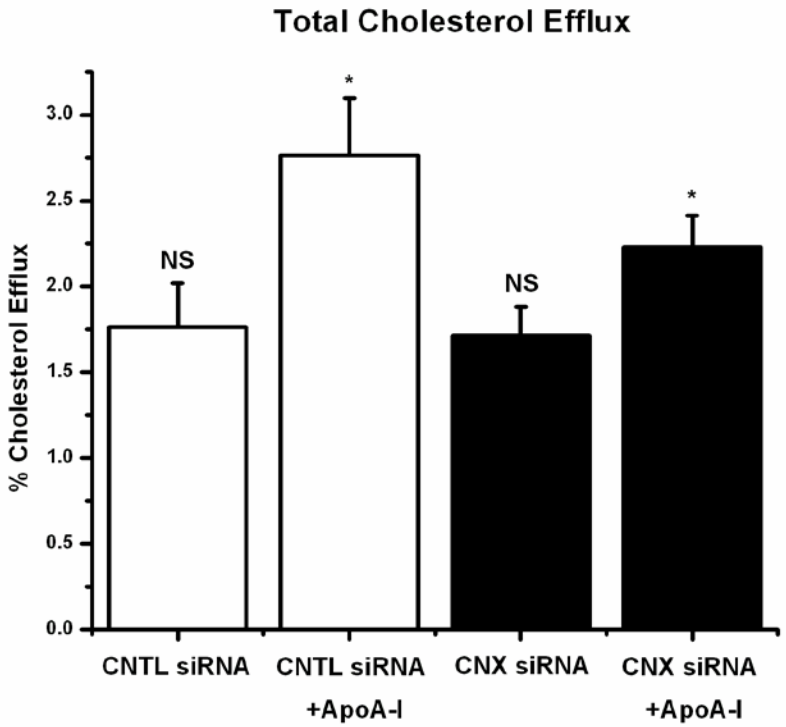
Total Cholesterol Efflux
% Cholesterol Efflux
3.0
2.5
2.0
1.5
1.0
0.5
0.0
NS
*
NS
*
CNTL siRNA
CNTL siRNA +ApoA-I
CNX siRNA
CNX siRNA +ApoA-I

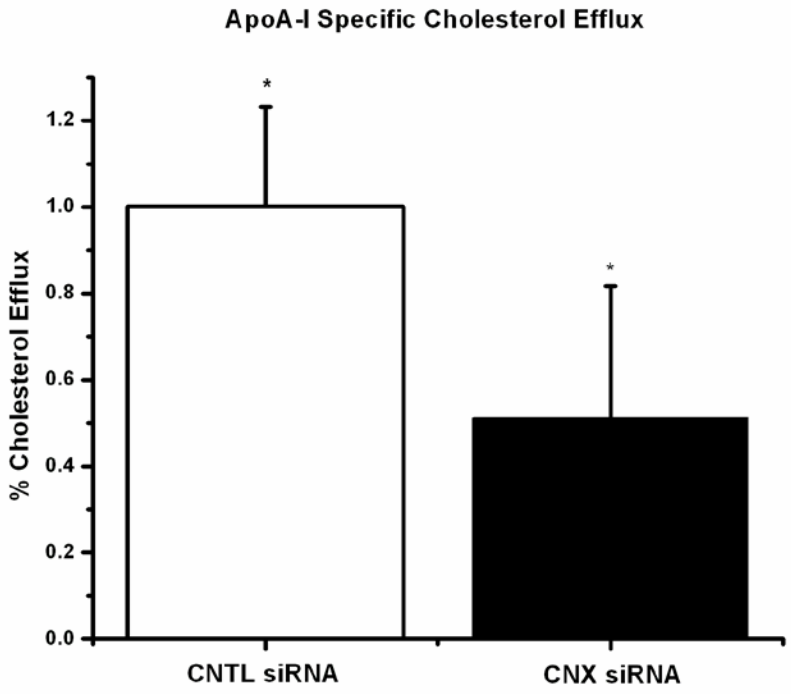
ApoA-I Specific Cholesterol Efflux
% Cholesterol Efflux
1.2
1.0
0.8
0.6
0.4
0.2
0.0
*
*
CNTL siRNA
CNX siRNA

Figure 15. Calnexin contributes to ABCA1 Function.

A. Cholesterol efflux was analyzed in HeLa-ABCA1-GFP cells transfected with control (CNTL) or calnexin (CNX)-specific siRNA. B. ApoA-I specific efflux obtained after subtraction of efflux to BSA. *$p<0.05$. One representative experiment out of two performed is shown. Statistics were calculated on three replicate wells of a 24 well plate for each condition.

Western blotting (**Fig. 16A**). Surprisingly, calnexin knock-down increased the half-life of ABCA1 in contrast to the decrease in cholesterol efflux described above (**Fig. 15**). This indicates that the normal function of calnexin in its interaction with ABCA1 serves to increase ABCA1 turnover, and thus limit total ABCA1 protein levels, perhaps by chaperoning misfolded ABCA1 to ER-associated degradation (ERAD).

Maximal cholesterol efflux depends on ABCA1 expression at the plasma membrane and ABCA1 re-cycling from the vesicular network to the plasma membrane (11, 12, 17, 27). Recent studies confirmed that the plasma membrane is the primary site of ABCA1-mediated cholesterol efflux (141-143) and Tangier disease-associated ABCA1 mutants with reduced cell surface expression also demonstrate reduced cholesterol efflux (23-26). Therefore, the effect of calnexin on ABCA1 plasma membrane localization was determined by cell-surface biotinylation. Knocking down calnexin with siRNA in HeLa-ABCA1-GFP cells produced a slight increase in total ABCA1 protein in agreement with the ABCA1 turnover data presented above. Surprisingly, again in contrast to the efflux data, calnexin knock-down also caused an increase in ABCA1 protein on the plasma membrane (**Fig. 16B**). This result suggests that in its normal capacity, calnexin retains a portion of ABCA1 at intracellular sites away from the plasma membrane. Interestingly, the increase in total ABCA1 upon calnexin knock-down is in contrast to the effect of Nef, which causes a significant reduction in ABCA1 protein levels (56, 74, 77). However, the increase in ABCA1 on the plasma membrane relative to intracellular ABCA1 is indeed consistent with effects of Nef described in this study (**Fig. 10A**) and previously (77). Thus, interference with the ABCA1-calnexin interaction likely contributes to some of the

A.

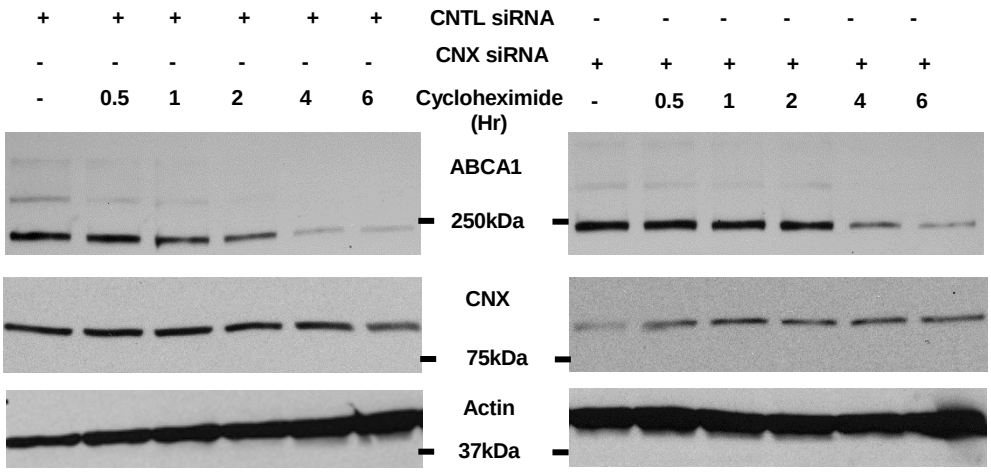
+ + + + + + CNTL siRNA - - - - - -
- - - - - - CNX siRNA + + + + + +
- 0.5 1 2 4 6 Cycloheximide (Hr) - 0.5 1 2 4 6
ABCA1
250kDa
CNX
75kDa
Actin
37kDa

B.

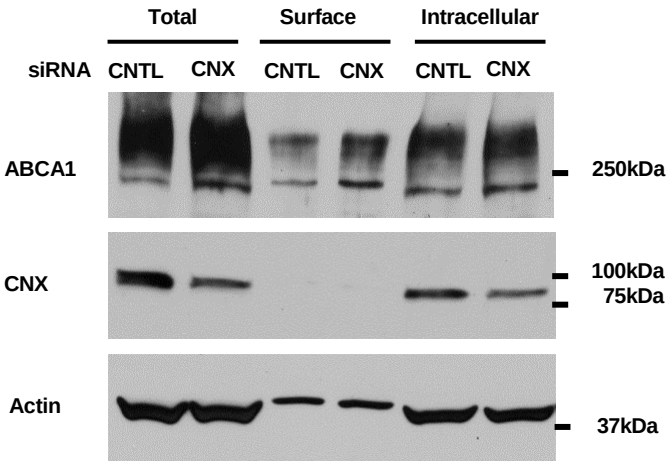
Total
Surface
Intracellular
siRNA CNTL CNX CNTL CNX CNTL CNX
ABCA1
250kDa
CNX
100kDa
75kDa
Actin
37kDa

Figure 16. Calnexin knockdown increases total and surface ABCA1 expression

A. HeLa-ABCA1-GFP cells were transfected with control (CNTL) or calnexin (CNX) siRNA and 72 h post-transfection were treated with cycloheximide as indicated to follow protein turnover. B. HeLa-ABCA1-GFP cells were transfected with control (CNTL) or calnexin (CNX) siRNA and 72 h post-transfection subjected to cell surface biotinylation. Cell lysate was probed with antibodies to ABCA1, calnexin, and actin either before fractionation (lanes marked total), or after precipitation with streptavidin beads into the pellet (lanes marked surface) and supernatant (lanes marked intracellular).

observed Nef effects on ABCA1 but does not explain the decrease in ABCA1 protein levels mediated by Nef. It is feasible that Nef interference with the ABCA1-calnexin interaction renders ABCA1 functionally defective and that this defective ABCA1 becomes a substrate for an accessory degradation pathway mediated by Nef.

Though the exact role of endocytosis in the ABCA1-mediated cholesterol efflux cycle is controversial, there is general agreement that ABCA1 recycling through the vesicular network contributes at least some proportion of cholesterol efflux. Pharmacological treatments that impair ABCA1 intracellular trafficking inhibit cholesterol efflux in vitro and recent reports suggest that recycling of ABCA1 may make a significant contribution to cholesterol efflux when cells accumulate excess cholesterol (12, 29, 144). Given the contribution of ABCA1 recycling to cholesterol efflux, studies were designed to determine whether calnexin might contribute to this process. Calnexin was knocked down in HeLa-ABCA1-GFP cells via siRNA and cells were treated with monensin to follow internalization. Monensin treatment prevents ABCA1 delivery from the Golgi to the plasma membrane (29, 114). When combined with cell-surface biotinylation, this technique allows assessment of ABCA1 turnover on the plasma membrane (29). Under control conditions, ABCA1 disappeared from the cell surface gradually during 2 h monensin treatment with a total reduction of >80% during the chase period (**Fig. 17**). In contrast, ABCA1 was relatively stable in the membrane for over 2 h after monensin treatment in cells treated with calnexin siRNA with a total reduction of ~70%. This indicates that calnexin contributes to retrieval of ABCA1 from the plasma membrane and effects ABCA1 recycling. Combined with our observations that calnexin

knock-down caused redistribution of ABCA1 from the cell interior to the periphery, extended ABCA1 half-life, and reduced cholesterol efflux, this result suggests that interfering with the ABCA1-calnexin interaction caused non-functional ABCA1 to exit the ER and accumulate at the plasma membrane where it cannot be recycled and fails to mediate efflux. Each of the effects described can be equally applied to Nef, reinforcing the contribution of interference with calnexin interaction to Nef effects on ABCA1.

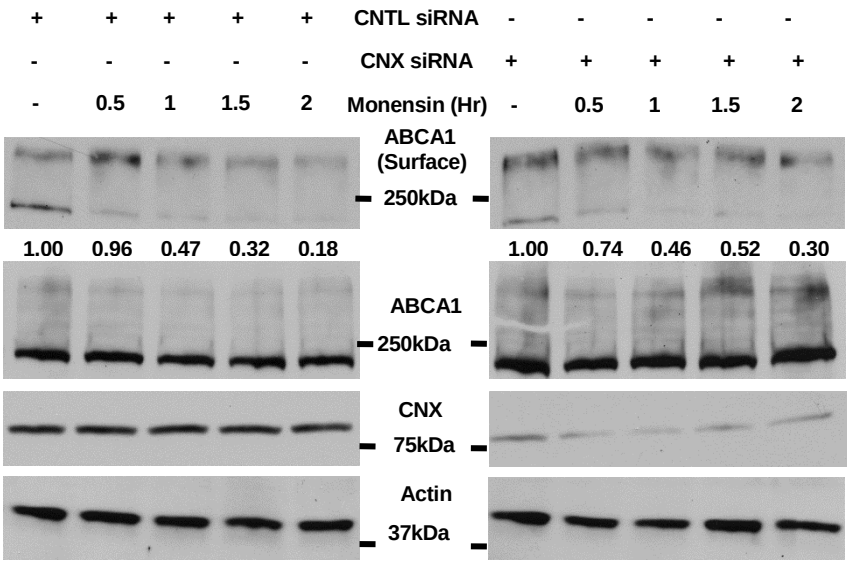
+ + + + + CNTL siRNA - - - - -
- - - - - CNX siRNA + + + + +
- 0.5 1 1.5 2 Monensin (Hr) - 0.5 1 1.5 2
ABCA1 (Surface)
250kDa
1.00 0.96 0.47 0.32 0.18
1.00 0.74 0.46 0.52 0.30
ABCA1
250kDa
CNX
75kDa
Actin
37kDa

Figure 17. Calnexin knockdown reduces ABCA1 recycling.

HeLa-ABCA1-GFP cells were transfected with control (CNTL) or calnexin (CNX) siRNA and 72 h post-transfection were treated with cycloheximide to inhibit protein synthesis and Monensin for the indicated time period to prevent delivery of recycled ABCA1 to the cell surface. Cells were then subjected to cell surface biotinylation and surface ABCA1 was assessed to determine the extent of ABCA1 recycling during the chase period (indicated as Surface). Numbers below the Surface ABCA1 blot indicate ABCA1 density compared to density at T=0 as determined by image analysis with ImageJ. Note the higher molecular weight ABCA1 species recovered as the predominant species on the cell surface likely represents a mature multimeric transporter complex. A representative experiment of two performed is presented.

Chapter 10: Discussion

Findings of the Study

This report describes a novel mechanism by which Nef interferes with activity of host cell protein, cholesterol transporter ABCA1. The endoplasmic reticulum chaperone calnexin was identified as a cellular co-factor for ABCA1-mediated cholesterol efflux and it was demonstrated that Nef binds to calnexin and disrupts its interaction with ABCA1, leading to a release from ER of a non-functional transporter. Importantly, Nef does not indiscriminately disrupt all calnexin interactions, as interaction between calnexin and HIV-1 Env, which is critical for proper Env glycosylation and maturation (145), was not affected by Nef.

Calnexin and calreticulin function as partner lectin-like chaperones in the ER protein production, stabilization, and folding cycle (146). Calnexin is membrane-bound and chaperones predominantly membrane glycoproteins, whereas calreticulin is soluble and chaperones soluble proteins. It has been suggested that calnexin may stabilize glycoproteins through a dual-binding mode involving glycosyl residue and peptide binding or through either single binding mode (glycosyl residue or peptide binding) independently (84). Members of nearly every subclass of ABC transporters, including ABCB1 (P-glycoprotein, MDR1), ABCB2 (TAP1), ABCB3 (TAP2), ABCC2, ABCC7 (CFTR), and ABCG5/G8 have been demonstrated to interact with calnexin and among these are examples of glycan-dependent and -independent interactions (46, 108, 147-149). The data in this study suggest that the interaction between ABCA1 and calnexin is glycan-independent and likely involves a peptide-binding mechanism of calnexin action. Calnexin

has been reported to interact with the ABCB1/P-glycoprotein transporter in a lectin-independent quality control mechanism that involves the transmembrane regions of P-glycoprotein (46). Similarly, results of these studies suggest that Nef interacts with calnexin and disrupts ABCA1-calnexin interaction through a mechanism that requires membrane association of Nef, indicating that membrane association may also be required for the ABCA1-calnexin interaction. The extensive list of ABC transporters that interact with calnexin suggests that calnexin may serve as a prototypical chaperone for membrane glycoproteins of the ABC superfamily and suggests that these proteins may represent heretofore unappreciated targets of Nef.

Calnexin knockdown was used to demonstrate that calnexin contributes to cholesterol efflux, thus Nef interferance with ABCA1-calnexin interaction would be expected to reduce cholesterol efflux as is indeed observed upon Nef expression and during HIV infection. Calnexin knockdown also lead to an increase in the plasma membrane/intracellular ratio of ABCA1 similar to that reported previously for Nef. This increase of ABCA1 on the plasma membrane in the absence of calnexin occurred as a result of ER escape. The major discrepancy between the effect of calnexin knockdown and Nef expression on ABCA1 involves the major decrease in ABCA1 protein levels observed in the presence of Nef that is absent upon calnexin knockdown. This suggests that upon calnexin knockdown a degradative mechanism of ABCA1 is disrupted, while in the presence of Nef an active program of ABCA1 degradation is activated. Calnexin is suggested to play a role in ERAD of many proteins and may perform such a function for misfolded ABCA1, thus upon calnexin knockdown, misfolded ABCA1 is no longer

targeted for degradation and is instead allowed to exit the ER and transit to the cell surface where it is less functional (as indicated by the reduction in cholesterol efflux observed upon calnexin knockdown). Nef on the other hand has been shown to actively increase delivery of ABCA1 to lysosomes (77). Targeting ABCA1 through two, potentially non-redundant, pathways; degradation and inactivation, has many advantages for the virus as a bipartite targeting mechanism is likely much more efficient than either individual activity alone. Indeed the cholesterol efflux defect in the presence of Nef is consistently ~60-80% while that of calnexin knockdown is ~50%.

Nef disrupted the interaction between ABCA1 and calnexin through a mechanism that involves Nef interaction with calnexin, requires membrane targeting of both Nef and calnexin, and results in increased calnexin interaction with PACS-2 and relative re-distribution of ABCA1 and calnexin (**Fig. 18B**). PACS-2 sorts calnexin between the ER, mitochondria-associated membranes and plasma membrane with increased binding to PACS-2 causing increased ER retention of calnexin (117). Thus, it is surprising that Nef increases calnexin binding to PACS-2 but also causes calnexin to localize to the late secretory compartment in our fractionation analysis. In this regard, it has been reported that Nef binds PACS-2 (137) and that Nef and PACS-2 interaction may involve the Golgi and endosomes (137, 150). This is in contrast to the normal localization of PACS-2 to the ER (151). Thus, it appears that increased binding of calnexin to PACS-2 in the presence of Nef may actually cause calnexin to localize to the secretory pathway and away from ER, as observed in our fractionation analysis. Calnexin knockdown or Nef expression also caused

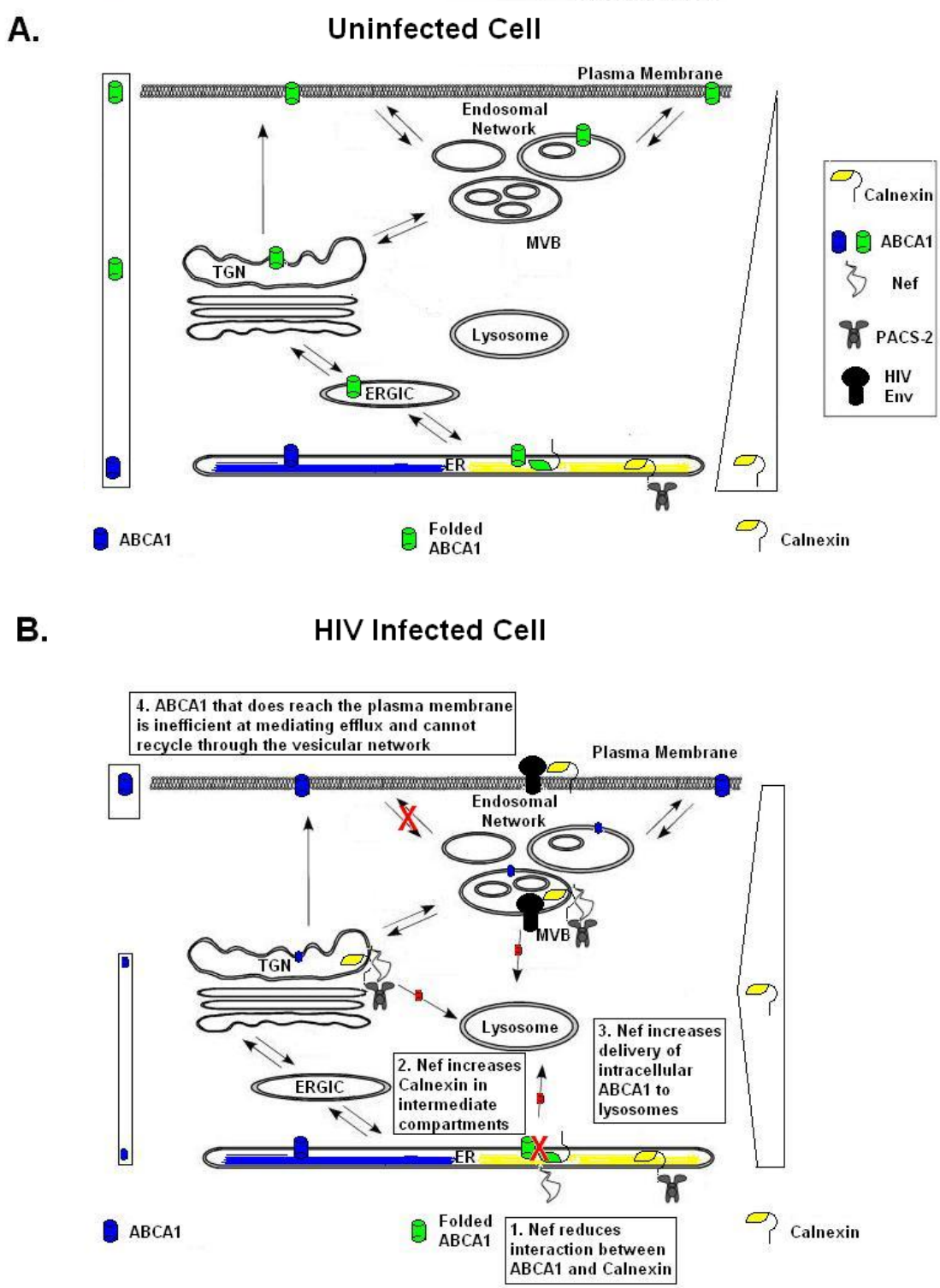
A.
Uninfected Cell
Plasma Membrane
Endosomal Network
MVB
TGN
Lysosome
ERGIC
ER
Calnexin
ABCA1
Nef
PACS-2
HIV Env
ABCA1
Folded ABCA1
Calnexin
B.
HIV Infected Cell
4. ABCA1 that does reach the plasma membrane is inefficient at mediating efflux and cannot recycle through the vesicular network
Plasma Membrane
Endosomal Network
MVB
TGN
Lysosome
3. Nef increases delivery of intracellular ABCA1 to lysosomes
2. Nef increases Calnexin in intermediate compartments
ERGIC
ER
ABCA1
Folded ABCA1
1. Nef reduces interaction between ABCA1 and Calnexin
Calnexin

Figure 18. Nef effects on ABCA1 and calnexin.

A. In the absence of Nef, nascent ABCA1 (blue) and calnexin (yellow) interact in the ER where calnexin assists ABCA1 in achieving a functional folding state (green). Once properly folded, ABCA1 can exit the ER and transverse the ER/Golgi Imtermediate Compartments (ERGIC), Trans-Golgi Network (TGN), and Endosomal Network, finally arriving at the plasma membrane (PM) where the functional transporter can mediate cholesterol efflux and be recycled through the endosomal network. In this scenario, PACS-2 binding retains calnexin in the ER establishing a gradient of calnexin expression (right) which is highest in the ER, moderate in the TGN, vesicles, and endosomes, and minor on the PM. ABCA1 expression in the absence of Nef is nearly uniform in the ER, TGN/endo-vesicular network, and on the PM (left). B. In infected cells, the presence of Nef disrupts interaction between nascent ABCA1 and calnexin (1), perhaps because of the shift of calnexin to intermediate membranes of the TGN/endo-vesicular network (2) in concert with increased calnexin binding to PACS-2. Nef targets the intracellular population of ABCA1 for delivery to lysosomes (3), reducing ABCA1 in the TGN/endo-vesicular network. Nascent (likely misfolded) ABCA1 that does exit the ER can transverse the ERGIC, TGN, and endo-vesicular network for delivery to the PM where it fails to mediate efflux and cannot be recycled (4), leading to a stable population of ABCA1 on the PM. Thus Nef increases calnexin expression later in the secretory pathway (right), perhaps to ensure availability of calnexin to contribute to Env folding, and segregates ABCA1 to two populations; a larger stable pool of ABCA1 on the PM and a smaller intracellular pool of ABCA1 that is steadily diminished by delivery to lysosomes (left).

a re-distribution of ABCA1 relative to ER. Cumulatively, these results suggest that calnexin functions as an ABCA1 quality-control chaperone, limiting total and plasma membrane ABCA1 expression, while increasing ABCA1 cholesterol efflux activity (**Fig. 18A**). HIV-1 Nef exploits this requirement for ABCA1 interaction with calnexin to reduce ABCA1 function (**Fig. 18B**).

Fractionation, biotinylation, and confocal imaging data from these studies may seem to suggest conflicting mechanisms as the fractionation data clearly show that Nef reduces ABCA1 in recycling compartments and restricts ABCA1 to heavy membranes (to include ER-derived membranes) while the confocal imaging data demonstrate that Nef expression, presumably through effects on the ABCA1-calnexin interaction allows ER escape of ABCA1. However, it must be noted that heavy membranes include ER- and plasma membrane-derived membranes. Thus, combining this data with cell surface biotinylation data from these studies suggests that the overall effect of Nef (**Fig. 18B**) is to allow ER escape of immature ABCA1 which is then destined to one of two fates; intracellular ABCA1 is likely delivered to degradative organelles (lysosomes or proteasomes) while ABCA1 that reaches the plasma membrane is comparatively stable and accumulates at this site rather than recycling through the endosomal network. Thus giving rise to the two populations of ABCA1 (plasma membrane and perinuclear) observed in confocal images that are a consistent feature of the Nef effect on ABCA1. Evidence that the perinuclear concentrations of ABCA1 observed upon Nef expression (**Fig. 5C**) in fact represent lysosomes has been presented previously (77).

Nef is a multi-functional accessory protein involved in multiple interactions with host cell proteins (78, 79). These interactions are responsible for a multitude of Nef activities benefiting HIV replication. Most of these activities involve a direct interaction of Nef with the target protein, followed by attraction of specific cellular traffic regulating factors, which mediate transfer of the target protein to the degradation pathway (152-156). Here another mechanism is identified which is used by Nef to downmodulate ABCA1 and impair its cholesterol efflux activity. Nef binds calnexin and promotes its relocalization to plasma and mitochondria-associated membranes, disrupting calnexin association with ABCA1 (**Fig. 5** and **Fig. 6**). Calnexin is a particularly good target for Nef because interfering with chaperone function would allow Nef to modulate membrane expression of a variety of proteins simultaneously to enhance viral survival, infectivity, and immune evasion. The requirement of HIV gp160 for interaction with calnexin suggests that Nef interference with calnexin interactions with cellular proteins may be part of the viral strategy to ensure the availability of calnexin to assist in folding of viral Envelope proteins.

Limitations of the study

Limitations exist in the design of the studies presented in this work and should inform any conclusions to be drawn from them. Interpretation of the studies must include consideration of potential limitations in study design, methodology, and interpretations. In particular, the study relies heavily on the use of immortalized cell lines, siRNA, and immunoprecipitation each of which have specific concerns.

A major limitation in the study design of this work is that much of the mechanistic detail is interpreted from experiments in HeLa-ABCA1-GFP cells. These cells are

immortalized fibroblasts engineered to stably express fluorescent ABCA1. While the studies establishing this cell line (114) investigated many potential concerns with ABCA1 biology, function, and regulation in these cells, it is impossible to rule out that some of the mechanistic detail in the studies presented here result from the nature of this cell line and may not always reflect relevant mechanisms outside of this artificial context. Additionally, experiments investigating protein-protein interactions were performed in HEK293T cells where ABCA1 is overexpressed by transfection. Again, this is unlikely to reflect natural biological regulation of ABCA1. Where possible, to mitigate these limitations, these studies made use of more appropriate cell culture models (THP-1 cells and primary human MDMs). Interpretation of these results must, therefore, include consideration of the fact that conclusions are being drawn from several different cell types and several different modes of ABCA1 expression and regulation (overexpression in HeLa-ABCA1-GFP cells and HEK293T cells and endogenous expression in THP-1 cells and MDMs).

Methodological concerns with these studies relate to the use of glycosylation and glucose trimming inhibitors to investigate the glycan-dependance of ABCA1 interaction with calnexin. This class of inhibitors is subject to significant toxicity and significant off-target effects on unrelated glycoproteins. Indeed, it is evident from the experiments with Tunicamycin that this inhibitor has a significant effect on ABCA1 stability which suggests that caution must be used in interpreting these particular experiments in terms of which effects are truly related to deglycosylation of ABCA1 and which effects may be related to reduced ABCA1 stability. Another limitation of methodologies utilized in these studies is the reliance on calnexin siRNA as a means to assess the contribution of calnexin to ABCA1

expression, localization, and function. In particular, during the experiments with siRNA, calnexin knockdown is not complete and residual calnexin protein can be detected by Western Blotting. In this instance, it is possible that the small fraction of calnexin that remains leads to underestimation of the overall role of calnexin. Further, it is possible that the siRNA used in this study, commercially available from Santa Cruz Biotechnology Inc., has off-target effects that are undetectable in these studies or that on-target effects of the siRNA on targets other than calnexin contribute to the effects observed on ABCA1. In particular, it is possible that calnexin chaperones a regulatory protein that positively regulates ABCA1 function, the function of such a regulatory protein would likely be decreased by calnexin knockdown. Alternatively, calnexin may chaperone a regulatory protein that negatively regulates ABCA1 protein levels, in this case the over-abundance of ABCA1 protein upon the loss of such a regulatory protein may, in turn, reduce ABCA1 functionality. A methodological concern regarding raft flotation in HeLa cells is clearly evident from inspection of **Fig. 8**. Rafts in HeLa cells are overtly dissimilar to rafts in T-cells in that raft markers (Caveolin or GM1) are not restricted to a particular density upon flotation and instead migrate throughout the gradient, indicating significant heterogeneity in rafts in HeLa cells. In contrast, rafts are well-defined in T-cells and tend to cluster at specific densities (124). Studies of Nef effects on lipid rafts are typically performed in T-cell lines where rafts are more homogeneous; however, ABCA1 is expressed at very low levels in unstimulated T-cells and is only upregulated upon prolonged exposure to pharmacological agents (e.g., LXR agonsits, unpublished observations). Therefore, it is possible that Nef effects on calnexin may be different in other cell types, such as T-cells.

An additional methodological concern is that in this study protein-protein interactions are investigated through the use of co-immunoprecipitation and His-Bind purifications, each of which makes use of agarose beads as a capture reagent. Agarose beads in this type of experiment are prone to non-specific interactions with a variety of proteins. While it is unlikely that all of the interactions presented here are the result of non-specific binding it is possible that non-specific binding may contribute to the level of binding observed in some of these experiments. Where possible, isotype antibody controls were used to rule out interference from non-specific interactions.

Alternative Interpretations

Throughout this study the interaction of ABCA1 with calnexin and the mechanism of this interaction were examined. Experiments with siRNA demonstrated that clanexin knockdown reduces cholesterol efflux and increases ABCA1 protein levels. However, this simple interpretation overlooks the possible contribution of other proteins and potentially other biological mechanisms related to these phenomena.

A cell line that lacks calnexin (CEM-NK_R) has been described and these cells are viable for long-term culture (157). This suggests that calnexin is not absolutely required for cell viability and that the multitude of glycoproteins chaperoned by calnexin may be chaperoned by other proteins in the absence of calnexin. The interaction between MHC-I and calnexin has been well-described but does not appear to be required for expression of MHC-I suggesting that interaction with calnexin is not an absolute requirement for some calnexin substrates (157). It is possible that the lack of calnexin engages alternate chaperone machinery potentially including calreticulin. In the experiments with calnexin

siRNA described here, it is impossible to rule out that calreticulin or another chaperone contributes to ABCA1 expression in the absence of calnexin. It is, therefore, possible that alterations in normal ABCA1 function and regulation observed in the absence of calnexin in these studies could be a result of abnormal chaperone activity directed toward ABCA1.

In this study, Nef effects on target proteins were investigated largely outside the context of viral infection. The environment of an HIV-infected cell is undeniably different than the environment of uninfected cells and cells transfected with individual viral proteins. Therefore, caution must be used with interpretation of the results presented here for cells over-expressing Nef alone. These studies were intentionally designed to investigate Nef in isolation due to the previously described association between Nef and ABCA1. At least one other viral protein, the viral Env gp160 protein, has been shown to interact with calnexin (145, 158, 159). It is reasonable to assume that the effects of viral biology on calnexin require interpretation of the combined influence of several viral proteins and virus-induced processes. To be able to determine the predominant effects of HIV-infection on calnexin biology, it will be necessary to reproduce observed phenomena in the context of infection with wild-type, replication-competent virus.

Another important alternative interpretation that must be mentioned is the possibility that calnexin knockdown, overexpression, or HIV infection induce the Unfolded Protein Response (UPR). Indeed, induction of the UPR by Tunicamycin has been reported and is known to have detrimental effects on ABCA1 expression (74). This consideration limits the utility of Tunicamycin in investigating treatments that prevent calnexin interaction with ABCA1 and is a major reason that in these studies Tunicamycin was only

used in a very limited setting. Nonetheless, it cannot be ruled out that several of the treatments described in these studies, such as Nef expression, glucosidase inhibitor treatment, and calnexin knockdown, may have contributed to UPR signaling that was not detected. In several experiments with calnexin siRNA, we did not note induction of CHOP expression nor XBP-1 splicing, but the HeLa cells in which these experiments were performed displayed endogenous low-level UPR activity constitutively (unpublished observations).

An additional concern in interpreting these results is that the effects of Nef on calnexin distribution in the secretory pathway were small (**Fig. 9**). Thus, these effects may not be the principle mechanism through which Nef disrupts the interaction between ABCA1 and calnexin. While the requirement for membrane association of Nef for interaction with calnexin suggests a role for membranes in this process, the G2A mutant of Nef used to prove this point is highly defective and results with this mutant must be interpreted cautiously. It is possible that Nef reduces interaction between ABCA1 and calnexin by directly binding ABCA1 and physically blocking calnexin or alternatively binding calnexin and physically blocking association with ABCA1. The observation that Nef mutants that fail to bind ABCA1 still reduce efflux and ABCA1 protein levels (74) makes the former unlikely, whereas the specificity of the Nef effect on ABCA1 relative to other calnexin substrates, such as Env, makes the latter interpretation more likely. Future experiments will identify mutants of both Nef and ABCA1 that fail to associate with calnexin in similar fashion to the calnexin mutants described in this study.

Future Directions

These studies demonstrated a role for calnexin in Nef effects on ABCA1. Future studies are being designed to investigate the contribution of calnexin to other well-established functions of Nef, investigate the contribution of calnexin to viral infectivity, and define genetic requirement in both Nef and ABCA1 for interaction with calnexin.

Nef induces down-regulation of a multitude of cell surface immunoreceptors and many of these proteins are glycoproteins and known calnexin substrates. MHC-I, MHC-II, Transferrin, CD1d, and components of the T-cell Receptor are all calnexin substrates (110) that are known to be targeted by Nef (78, 79, 160, 161). Future experiments to further the studies presented here will assess the effect of Nef on calnexin substrates in a parental T-cell line (CEM) and the derivative cell line that lacks calnexin ($CEM.NK_R$). If calnexin is required for Nef effects, it is possible that the absence of calnexin in the derivative T-cell line will prevent Nef-induced down-regulation of these calnexin substrates. The adaptation of proteomics technologies to these studies will increase the likelihood that additional targets of Nef whose targeting requires calnexin will be identified. The E5 protein of Human Papillomavirus 16 (HPV-16) has been reported to interact with calnexin and to require calnexin to down-regulate MHC-I in a mechanism that involves a transmembrane domain of E5 (112). The results with E5 and the results presented her with Nef suggest that investigating Nef function in $CEM.NK_R$ is a good strategy to define the contribution of calnexin to MHC-I down-regulation by Nef.

The results of this study indicate that Nef increases Env binding to calnexin (**Fig. 6**). While Env binding to calnexin has been described and extensively characterized (145,

158, 159), the effect of Nef on Env interaction with calnexin is a novel fiding of these studies. In studies using CEM.NK_R cells, it has been reported that these cells are resistant to productive HIV infection, an effect involving reduced virion production and reduced infectivity (162). It was reported that calnexin rescue in this cell line did not rescue viral replication (163). However, given the reported role of calnexin in chaperoning Env, it is unlikely that calnexin has no effect on virus production and infectivity. Future investigations to extend the study presented here will assess the effect of calnexin on virus infectivity and the contribution of Nef to this effect.

Conclusions

These studies describe the novel finding of ABCA1 interaction with molecular chaperone calnexin and the targeting of this interaction by HIV-1 Nef protein. Calnexin was demonstrated to contribute to ABCA1-specific cholesterol efflux. The potential for these findings to be applied for clinical benefit in CVD and HIV are intriguing. Of particular interest, a promising recent clinical development in Cystic Fibrosis, most commonly caused by a mutation (ΔF508) inducing a folding defect in the ABC transporter CFTR (ABCC7), has been the use of Miglustat/Zavesca™ (*N*-butyldeoxynojirimycin) (103, 164-167) (recently in Phase II Clinical Trials) (168). The mechanism of action of Miglustat in mitigating Cystic Fibrosis is postulated to involve modulating the interaction between CFTR and calnexin (169). This same compound has been shown to have broad antiviral activity against multiple primary isolates of HIV by targeting Env folding at the level of the calnexin cycle (170). Thus, modulating calnexin interaction may have dual-

benefit in HIV-infected patients by increasing HDL levels through effects on ABCA1 and reducing virus replication through effects on Env.

As well as the potential benefit in the HIV-infected population, investigating calnexin interaction has the potential to uncover additional insights and details of biological function and regulation of ABCA1 unrelated to HIV infection. Studies to assess the contribution of calnexin and glycoprotein processing to cholesterol efflux independent of HIV infection will be necessary to understand HDL metabolism and the role of ABCA1 folding and regulation in the development of atherosclerosis and CVD. A major research effort at the end of the 20th century devoted to the discovery of pharmacological interventions to reduce LDL-C culminated in the discovery of inhibitors of hydroxymethyl glutaryl coenzyme A (HMG-CoA), known as “statins” (171). Statins have proven to be a remarkable victory for cardiovascular science and have been shown to reduce clinical events by 30-45% (172). The identification and description of mutations in ABCA1 as the predisposing genetic determinant of Tangier Disease has similarly served as a bellwether for research on the expression, function, and regulation of this key mediator of HDL biogenesis as a novel regulator of HDL levels in the circulation. Identification of proteins involved in ABCA1 biogenesis that contribute to cholesterol efflux functionality can potentially inform new therapeutic strategies that may someday augment the statin armamentarium to simultaneously target HDL and LDL in treating developing and established CVD.

Bibliography

References

1. Gaziano TA. Cardiovascular disease in the developing world and its cost-effective management. Circulation. 2005 December 06;112(23):3547-53.

2. Gordon DJ, Rifkind BM. High-density lipoprotein — the clinical implications of recent studies. N Engl J Med. 1989 11/09; 2012/10;321(19):1311-6.

3. Asztalos BF, Tani M, Schaefer EJ. Metabolic and functional relevance of HDL subspecies. Curr Opin Lipidol. 2011 Jun;22(3):176-85.

4. Camont L, Chapman MJ, Kontush A. Biological activities of HDL subpopulations and their relevance to cardiovascular disease. Trends Mol Med. 2011 10;17(10):594-603.

5. Rosenson RS, Brewer HB, Davidson WS, Fayad ZA, Fuster V, Goldstein J, et al. Cholesterol efflux and atheroprotection. Circulation. 2012 April 17;125(15):1905-19.

6. Glass CK, Witztum JL. Atherosclerosis: The road ahead. Cell. 2001 2/23;104(4):503-16.

7. Assmann G, Gotto AM. HDL cholesterol and protective factors in atherosclerosis. Circulation. 2004 June 15;109(23 suppl 1):III-8,III-14.

8. Linsel-Nitschke P, Tall AR. HDL as a target in the treatment of atherosclerotic cardiovascular disease. Nat Rev Drug Discov. 2005 print;4(3):193-205.

9. Brewer HB. Increasing HDL cholesterol levels. N Engl J Med. 2004 04/08; 2012/10;350(15):1491-4.

10. Brewer HB. High-density lipoproteins: A new potential therapeutic target for the prevention of cardiovascular disease. Arteriosclerosis, Thrombosis, and Vascular Biology. 2004 March 01;24(3):387-91.

11. Cavelier C, Lorenzi I, Rohrer L, von Eckardstein A. Lipid efflux by the ATP-binding cassette transporters ABCA1 and ABCG1. Biochim Biophys Acta. 2006 Jul;1761(7):655-66.

12. Boadu E, Bilbey NJ, Francis GA. Cellular cholesterol substrate pools for adenosine-triphosphate cassette transporter A1-dependent high-density lipoprotein formation. Curr Opin Lipidol. 2008 Jun;19(3):270-6.

13. Mineo C, Shaul PW. Novel biological functions of high-density lipoprotein cholesterol. Circulation Research. 2012 September 28;111(8):1079-90.

14. Glomset JA, Wright JL. Some properties of a cholesterol esterifying enzyme in human plasma. Biochimica et Biophysica Acta (BBA) - Specialized Section on Enzymological Subjects. 1964 8/26;89(2):266-76.

15. Yvan-Charvet L, Wang N, Tall AR. Role of HDL, ABCA1, and ABCG1 transporters in cholesterol efflux and immune responses. Arteriosclerosis, Thrombosis, and Vascular Biology. 2010 February 01;30(2):139-43.

16. Khera AV, Cuchel M, de lL, Rodrigues A, Burke MF, Jafri K, et al. Cholesterol efflux capacity, high-density lipoprotein function, and atherosclerosis. N Engl J Med. 2011 01/13; 2012/11;364(2):127-35.

17. Kang MH, Singaraja R, Hayden MR. Adenosine-triphosphate-binding cassette transporter-1 trafficking and function. Trends Cardiovasc Med. 2010 2;20(2):41-9.

18. Brooks-Wilson A, Marcil M, Clee SM, Zhang L, Roomp K, van Dam M, et al. Mutations in ABC1 in tangier disease and familial high-density lipoprotein deficiency. Nat Genet. 1999 print;22(4):336-45.

19. Bodzioch M, Orso E, Klucken J, Langmann T, Bottcher A, Diederich W, et al. The gene encoding ATP-binding cassette transporter 1 is mutated in tangier disease. Nat Genet. 1999 print;22(4):347-51.

20. Rust S, Rosier M, Funke H, Real J, Amoura Z, Piette J, et al. Tangier disease is caused by mutations in the gene encoding ATP-binding cassette transporter 1. Nat Genet. 1999 print;22(4):352-5.

21. Lawn RM, Wade DP, Garvin MR, Wang X, Schwartz K, Porter JG, et al. The tangier disease gene product ABC1 controls the cellular apolipoprotein-mediated lipid removal pathway. J Clin Invest. 1999 Oct;104(8):R25-31.

22. Remaley AT, Rust S, Rosier M, Knapper C, Naudin L, Broccardo C, et al. Human ATP-binding cassette transporter 1 (ABC1): Genomic organization and identification of the genetic defect in the original tangier disease kindred. Proceedings of the National Academy of Sciences. 1999 October 26;96(22):12685-90.

23. Tanaka AR, Abe-Dohmae S, Ohnishi T, Aoki R, Morinaga G, Okuhira K, et al. Effects of mutations of ABCA1 in the first extracellular domain on subcellular trafficking and ATP binding/hydrolysis , Journal of Biological Chemistry. 2003 March 07;278(10):8815-9.

24. Singaraja RR, Visscher H, James ER, Chroni A, Coutinho JM, Brunham LR, et al. Specific mutations in ABCA1 have discrete effects on ABCA1 function and lipid phenotypes both in vivo and in vitro. Circulation Research. 2006 August 18;99(4):389-97.

25. Singaraja RR, Brunham LR, Visscher H, Kastelein JJP, Hayden MR. Efflux and atherosclerosis. Arteriosclerosis, Thrombosis, and Vascular Biology. 2003 August 01;23(8):1322-32.

26. Tanaka AR, Kano F, Ueda K, Murata M. The ABCA1 Q597R mutant undergoes trafficking from the ER upon ER stress. Biochem Biophys Res Commun. 2008 5/16;369(4):1174-8.

27. Oram JF, Heinecke JW. ATP-binding cassette transporter A1: A cell cholesterol exporter that protects against cardiovascular disease. Physiol Rev. 2005 Oct;85(4):1343-72.

28. Le Goff WF, FAU PD, Settle MF, Brubaker G FAU - Morton, Richard,E., FAU MR, Smith JD. Cyclosporin A traps ABCA1 at the plasma membrane and inhibits ABCA1-mediated lipid efflux to apolipoprotein A-I. Arteriosclerosis, thrombosis, and vascular biology JID - 9505803. 0531.

29. Chen W, Wang N, Tall AR. A PEST deletion mutant of ABCA1 shows impaired internalization and defective cholesterol efflux from late endosomes. Journal of Biological Chemistry. 2005 August 12;280(32):29277-81.

30. Wang NF, Chen WF, Linsel-Nitschke P FAU - Martinez, Laurent,O., FAU ML, Agerholm-Larsen B FAU - Silver, David,L., FAU SD, et al. A PEST sequence in ABCA1 regulates degradation by calpain protease and stabilization of ABCA1 by apoA-I. The Journal of clinical investigation JID - 7802877. 0303.

31. Martinez LO, Agerholm-Larsen B, Wang N, Chen W, Tall AR. Phosphorylation of a pest sequence in ABCA1 promotes calpain degradation and is reversed by ApoA-I. Journal of Biological Chemistry. 2003 September 26;278(39):37368-74.

32. Oram JF, Wolfbauer G, Vaughan AM, Tang C, Albers JJ. Phospholipid transfer protein interacts with and stabilizes ATP-binding cassette transporter A1 and enhances cholesterol efflux from cells. Journal of Biological Chemistry. 2003 December 26;278(52):52379-85.

33. Fitzgerald ML, Morris AL, Rhee JS, Andersson LP, Mendez AJ, Freeman MW. Naturally occurring mutations in the largest extracellular loops of = ABCA1 can disrupt its direct interaction with apolipoprotein A-I=20. Journal of Biological Chemistry=20. 2002=20 September 06=20;277=20(36=20):33178=20,33187=20.

34. Hozoji M, Munehira Y, Ikeda Y, Makishima M, Matsuo M, Kioka N, et al. Direct interaction of nuclear liver X receptor-β with ABCA1 modulates cholesterol efflux. Journal of Biological Chemistry. 2008 October 31;283(44):30057-63.

35. Hozoji-Inada M, Munehira Y, Nagao K, Kioka N, Ueda K. Liver X receptor β (LXRβ) interacts directly with ATP-binding cassette A1 (ABCA1) to promote high

density lipoprotein formation during acute cholesterol accumulation. Journal of Biological Chemistry. 2011 June 03;286(22):20117-24.

36. Buechler C, Boettcher A, Maa Bared S, Probst MCO, Schmitz G. The carboxyterminus of the ATP-binding cassette transporter A1 interacts with a β2-syntrophin/utrophin complex. Biochem Biophys Res Commun. 2002 5/3;293(2):759-65.

37. Munehira Y, Ohnishi T, Kawamoto S, Furuya A, Shitara K, Imamura M, et al. A1-syntrophin modulates turnover of ABCA1. Journal of Biological Chemistry. 2004 April 09;279(15):15091-5.

38. Okuhira K, Fitzgerald ML, Sarracino DA, Manning JJ, Bell SA, Goss JL, et al. Purification of ATP-binding cassette transporter A1 and associated binding proteins reveals the importance of β1-syntrophin in cholesterol efflux. Journal of Biological Chemistry. 2005 November 25;280(47):39653-64.

39. Albrecht DE, Sherman DL, Brophy PJ, Froehner SC. The ABCA1 cholesterol transporter associates with one of two distinct dystrophin-based scaffolds in schwann cells. Glia. 2008;56(6):611-8.

40. See RH, Caday-Malcolm RA, Singaraja RR, Zhou S, Silverston A, Huber MT, et al. Protein kinase A site-specific phosphorylation regulates ATP-binding cassette A1 (ABCA1)-mediated phospholipid efflux. Journal of Biological Chemistry. 2002 November 01;277(44):41835-42.

41. Yamauchi Y, Hayashi M, Abe-Dohmae S, Yokoyama S. Apolipoprotein A-I activates protein kinase cα signaling to phosphorylate and stabilize ATP binding cassette transporter A1 for the high density lipoprotein assembly. Journal of Biological Chemistry. 2003 November 28;278(48):47890-7.

42. Wang Y, Oram JF. Unsaturated fatty acids phosphorylate and destabilize ABCA1 through a protein kinase C δ pathway. Journal of Lipid Research. 2007 May 01;48(5):1062-8.

43. Nofer J, Remaley AT, Feuerborn R, Wolinńska I, Engel T, von Eckardstein A, et al. Apolipoprotein A-I activates Cdc42 signaling through the ABCA1 transporter. Journal of Lipid Research. 2006 April 01;47(4):794-803.

44. Roosbeek S, Peelman F, Verhee A, Labeur C, Caster H, Lensink MF, et al. Phosphorylation by protein kinase CK2 modulates the activity of the ATP binding cassette A1 transporter. Journal of Biological Chemistry. 2004 September 03;279(36):37779-88.

45. Bungert S, Molday LL, Molday RS. Membrane topology of the ATP binding cassette transporter ABCR and its relationship to ABC1 and related ABCA transporters. Journal of Biological Chemistry. 2001 June 29;276(26):23539-46.

46. Loo TW, Clarke DM. P-glycoprotein. Journal of Biological Chemistry. 1995 September 15;270(37):21839-44.

47. Rosser MFN, Grove DE, Chen L, Cyr DM. Assembly and misassembly of cystic fibrosis transmembrane conductance regulator: Folding defects caused by deletion of F508 occur before and after the calnexin-dependent association of membrane spanning domain (MSD) 1 and MSD2. Molecular Biology of the Cell. 2008 November 01;19(11):4570-9.

48. Loo TW, Clarke DM. Prolonged association of temperature-sensitive mutants of human P-glycoprotein with calnexin during biogenesis. Journal of Biological Chemistry. 1994 November 18;269(46):28683-9.

49. Pind S, Riordan JR, Williams DB. Participation of the endoplasmic reticulum chaperone calnexin (p88, IP90) in the biogenesis of the cystic fibrosis transmembrane conductance regulator. Journal of Biological Chemistry. 1994 April 29;269(17):12784-8.

50. Oram JF, Lawn RM. ABCA1: The gatekeeper for eliminating excess tissue cholesterol. Journal of Lipid Research. 2001 August 01;42(8):1173-9.

51. Tamehiro N, Zhou S, Okuhira K, Benita Y, Brown CE, Zhuang DZ, et al. SPTLC1 binds ABCA1 to negatively regulate trafficking and cholesterol efflux activity of the transporterâ€ . Biochemistry (N Y). 2008 06/01; 2012/03;47(23):6138-47.

52. Sharp PM, Hahn BH. Origins of HIV and the AIDS pandemic. Cold Spring Harbor Perspectives in Medicine. 2011 September 01;1(1).

53. Waheed AA, Freed EO. The role of lipids in retrovirus replication. Viruses. 2010 May 1;2(5):1146-80.

54. Peterlin BM, Trono D. Hide, shield and strike back: How HIV-infected cells avoid immune eradication. Nat Rev Immunol. 2003 print;3(2):97-107.

55. Zheng Y, Plemenitas A, Fielding CJ, Peterlin BM. Nef increases the synthesis of and transports cholesterol to lipid rafts and HIV-1 progeny virions. Proceedings of the National Academy of Sciences. 2003 July 08;100(14):8460-5.

56. Mujawar Z, Rose H, Morrow MP, Pushkarsky T, Dubrovsky L, Mukhamedova N, et al. Human immunodeficiency virus impairs reverse cholesterol transport from macrophages. PLoS Biol. 2006 10/31;4(11):e365.

57. Hsue PY, Deeks SG, Hunt PW. Immunologic basis of cardiovascular disease in HIV-infected adults. Journal of Infectious Diseases. 2012 June 01;205(suppl 3):S375-82.

58. Grinspoon S, Carr A. Cardiovascular risk and body-fat abnormalities in HIV-infected adults. N Engl J Med. 2005 01/06; 2013/03;352(1):48-62.

59. Carr A. Pathogenesis of cardiovascular disease in HIV infection. Current opinion in HIV and AIDS JID - 101264945 EDAT- 2009/04/18 09:00 MHDA- 2009/04/18 09:01 CRDT- 2009/04/18 09:00 AID - 10.1097/COH.0b013e3282fb7be0 doi] AID - 01222929-200805000-00007 pii] PST - ppublish. 1216(1746-630).

60. Palella FJ,Jr, Phair JP. Cardiovascular disease in HIV infection. Current Opinion in HIV and AIDS. 2011;6(4).

61. Lo JF, Grinspoon S. Cardiovascular disease in HIV-infected patients: Does HIV infection in and of itself increase cardiovascular risk? Current opinion in HIV and AIDS JID - 101264945 EDAT- 2009/04/18 09:00 MHDA- 2009/04/18 09:01 CRDT- 2009/04/18 09:00 AID - 10.1097/COH.0b013e3282fb7ba6 doi] AID - 01222929-200805000-00003 pii] PST - ppublish. 1216(1746-630).

62. Martinez EF, Larrousse M FAU - Gatell, Jose,M., Gatell JM. Cardiovascular disease and HIV infection: Host, virus, or drugs? Current opinion in infectious diseases JID - 8809878. 0728.

63. Lo JF, Plutzky J. The biology of atherosclerosis: General paradigms and distinct pathogenic mechanisms among HIV-infected patients. The Journal of infectious diseases JID - 0413675. 0712.

64. Grunfeld C, Delaney JAC, Wanke C, Currier JS, Scherzer R, Biggs ML, et al. Preclinical atherosclerosis due to HIV infection: Carotid intima-medial thickness measurements from the FRAM study. AIDS. 2009;23(14).

65. Hermankova M, Siliciano JD, Zhou Y, Monie D, Chadwick K, Margolick JB, et al. Analysis of human immunodeficiency virus type 1 gene expression in latently infected resting CD4+ T lymphocytes in vivo. Journal of Virology. 2003 July 01;77(13):7383-92.

66. Wu Y, Marsh JW. Selective transcription and modulation of resting T cell activity by preintegrated HIV DNA. Science. 2001 August 24;293(5534):1503-6.

67. Le Douce V, Herbein G, Rohr O, Schwartz C. Molecular mechanisms of HIV-1 persistence in the monocyte-macrophage lineage. Retrovirology. 2010;7(1):32.

68. Lassen KG, Bailey JR, Siliciano RF. Analysis of human immunodeficiency virus type 1 transcriptional elongation in resting CD4+ T cells in vivo. Journal of Virology. 2004 September 01;78(17):9105-14.

69. Zhang J, Crumpacker CS. Human immunodeficiency virus type 1 RNA in peripheral blood mononuclear cells of patients receiving prolonged highly active antiretroviral therapy. Journal of Infectious Diseases. 2001 November 15;184(10):1341-4.

70. Meynard J, Lacombe K, Poirier J, Massot O, Lefebvre B, Bouchaud O, et al. Sustained increase of HDL cholesterol over a 72-week period in HIV-infected patients exposed to an antiretroviral regimen including lopinavir/ritonavir. Journal of

the International Association of Physicians in AIDS Care (JIAPAC). 2008 December 01;7(6):311-6.

71. James CO, Huang M, Khan M, Garcia-Barrio M, Powell MD, Bond VC. Extracellular nef protein targets CD4+ T cells for apoptosis by interacting with CXCR4 surface receptors. Journal of Virology. 2004 March 15;78(6):3099-109.

72. Asztalos BF, Mujawar Z, Morrow MP, Grant A, Pushkarsky T, Wanke C, et al. Circulating nef induces dyslipidemia in simian immunodeficiency virus-infected macaques by suppressing cholesterol efflux. Journal of Infectious Diseases. 2010 August 15;202(4):614-23.

73. Morrow MP, Grant A, Mujawar Z, Dubrovsky L, Pushkarsky T, Kiselyeva Y, et al. Stimulation of the liver X receptor pathway inhibits HIV-1 replication via induction of ATP binding cassette transporter A1. Molecular Pharmacology. 2010 May 17.

74. Mujawar Z, Tamehiro N, Grant A, Sviridov D, Bukrinsky M, Fitzgerald ML. Mutation of the ATP cassette binding transporter A1 (ABCA1) C-terminus disrupts HIV-1 nef binding but does not block the nef enhancement of ABCA1 protein degradation. Biochemistry. 2010 Sep 28;49(38):8338-49.

75. Lin S, Nadeau PE, Wang X, Mergia A. Caveolin-1 reduces HIV-1 infectivity by restoration of HIV nef mediated impairment of cholesterol efflux by apoA-I. Retrovirology. 2012 Oct 15;9:85,4690-9-85.

76. Jiang HF, Badralmaa YF, Yang JF, Lempicki RF, Hazen AF, Natarajan V. Retinoic acid and liver X receptor agonist synergistically inhibit HIV infection in CD4+ T cells by up-regulating ABCA1-mediated cholesterol efflux. Lipids in health and disease JID - 101147696. 1220(1476-511; 1476-511).

77. Cui HL, Grant A, Mukhamedova N, Pushkarsky T, Jennelle L, Dubrovsky L, et al. HIV-1 nef mobilizes lipid rafts in macrophages through a pathway that competes with ABCA1-dependent cholesterol efflux. Journal of Lipid Research. 2012 January 19.

78. Roeth JF, Collins KL. Human immunodeficiency virus type 1 nef: Adapting to intracellular trafficking pathways. Microbiol Mol Biol Rev. 2006 Jun;70(2):548-63.

79. Leonard JA, Filzen T, Carter CC, Schaefer M, Collins KL. HIV-1 nef disrupts intracellular trafficking of major histocompatibility complex class I, CD4, CD8, and CD28 by distinct pathways that share common elements. Journal of Virology. 2011 July 15;85(14):6867-81.

80. Williams DB. Beyond lectins: The calnexin/calreticulin chaperone system of the endoplasmic reticulum. Journal of Cell Science. 2006 February 15;119(4):615-23.

81. Okazaki Y, Ohno H, Takase K, Ochiai T, Saito T. Cell surface expression of calnexin, a molecular chaperone in the endoplasmic reticulum. Journal of Biological Chemistry. 2000 November 17;275(46):35751-8.

82. Danilczyk UG, Cohen-Doyle MF, Williams DB. Functional relationship between calreticulin, calnexin, and the endoplasmic reticulum luminal domain of calnexin. Journal of Biological Chemistry. 2000 April 28;275(17):13089-97.

83. Tjoelker LW, Seyfried CE, Eddy RL,Jr, Byers MG, Shows TB, Calderon J, et al. Human, mouse, and rat calnexin cDNA cloning: Identification of potential calcium binding motifs and gene localization to human chromosome 5. Biochemistry. 1994 Mar 22;33(11):3229-36.

84. Leach MR, Cohen-Doyle MF, Thomas DY, Williams DB. Localization of the lectin, ERp57 binding, and polypeptide binding sites of calnexin and calreticulin. J Biol Chem. 2002 Aug 16;277(33):29686-97.

85. Ihara Y, Cohen-Doyle MF, Saito Y, Williams DB. Calnexin discriminates between protein conformational states and functions as a molecular chaperone in vitro. Mol Cell. 1999 9;4(3):331-41.

86. Fontanini A, Chies R, Snapp EL, Ferrarini M, Fabrizi GM, Brancolini C. Glycan-independent role of calnexin in the intracellular retention of charcot-marie-tooth 1A Gas3/PMP22 mutants. Journal of Biological Chemistry. 2005 January 21;280(3):2378-87.

87. Korkhov VM, Milan-Lobo L, Zuber B, Farhan H, Schmid JA, Freissmuth M, et al. Peptide-based interactions with calnexin target misassembled membrane proteins into endoplasmic reticulum-derived multilamellar bodies. J Mol Biol. 2008 4/25;378(2):337-52.

88. Cannon KS, Hebert DN, Helenius A. Glycan-dependent and -independent association of vesicular stomatitis virus G protein with calnexin. Journal of Biological Chemistry. 1996 June 14;271(24):14280-4.

89. Rajagopalan S, Xu Y, Brenner M. Retention of unassembled components of integral membrane proteins by calnexin. Science. 1994 January 21;263(5145):387-90.

90. van Leeuwen JEM, Kearse KP. Calnexin associates exclusively with individual CD3 and T cell antigen receptor (TCR) proteins containing incompletely trimmed glycans that are not assembled into multisubunit TCR complexes. Journal of Biological Chemistry. 1996 April 19;271(16):9660-5.

91. Kim PS, Arvan P. Calnexin and BiP act as sequential molecular chaperones during thyroglobulin folding in the endoplasmic reticulum. The Journal of Cell Biology. 1995 January 01;128(1):29-38.

92. Free RB, Hazelwood LA, Cabrera DM, Spalding HN, Namkung Y, Rankin ML, et al. D1 and D2 dopamine receptor expression is regulated by direct interaction with the chaperone protein calnexin. Journal of Biological Chemistry. 2007 July 20;282(29):21285-300.

93. Carreno BM, Schreiber KL, McKean DJ, Stroynowski I, Hansen TH. Aglycosylated and phosphatidylinositol-anchored MHC class I molecules are associated with calnexin. evidence implicating the class I-connecting peptide segment in calnexin association. The Journal of Immunology. 1995 May 15;154(10):5173-80.

94. Arunachalam B, Cresswell P. Molecular requirements for the interaction of class II major histocompatibility complex molecules and invariant chain with calnexin. Journal of Biological Chemistry. 1995 February 10;270(6):2784-90.

95. Swanton E, High S, Woodman P. Role of calnexin in the glycan-independent quality control of proteolipid protein. EMBO J. 2003 06/16;22(12):2948-58.

96. Mehta A, Zitzmann N, Rudd PM, Block TM, Dwek RA. A-glucosidase inhibitors as potential broad based anti-viral agents. FEBS Lett. 1998 6/23;430(1–2):17-22.

97. Zitzmann N, Mehta AS, Carrouée S, Butters TD, Platt FM, McCauley J, et al. Imino sugars inhibit the formation and secretion of bovine viral diarrhea virus, a pestivirus model of hepatitis C virus: Implications for the development of broad spectrum anti-hepatitis virus agents. Proceedings of the National Academy of Sciences. 1999 October 12;96(21):11878-82.

98. Bonen DK, Nassir F, Hausman AML, Davidson NO. Inhibition of N-linked glycosylation results in retention of intracellular apo[a] in hepatoma cells, although nonglycosylated and immature forms of apolipoprotein[a] are competent to associate with apolipoprotein B-100 in vitro. Journal of Lipid Research. 1998 August 01;39(8):1629-40.

99. Mirazimi A, Nilsson M, Svensson L. The molecular chaperone calnexin interacts with the NSP4 enterotoxin of rotavirus in vivo and in vitro. Journal of Virology. 1998 November 01;72(11):8705-9.

100. Zhang JX, Braakman I, Matlack KE, Helenius A. Quality control in the secretory pathway: The role of calreticulin, calnexin and BiP in the retention of glycoproteins with C-terminal truncations. Mol Biol Cell. 1997 Oct;8(10):1943-54.

101. Hammond C, Braakman I, Helenius A. Role of N-linked oligosaccharide recognition, glucose trimming, and calnexin in glycoprotein folding and quality control. Proceedings of the National Academy of Sciences. 1994 February 01;91(3):913-7.

102. Chang X, Mengos A, Hou Y, Cui L, Jensen TJ, Aleksandrov A, et al. Role of N-linked oligosaccharides in the biosynthetic processing of the cystic fibrosis

membrane conductance regulator. Journal of Cell Science. 2008 September 01;121(17):2814-23.

103. Norez C, Noel S, Wilke M, Bijvelds M, Jorna H, Melin P, et al. Rescue of functional delF508-CFTR channels in cystic fibrosis epithelial cells by the α-glucosidase inhibitor miglustat. FEBS Lett. 2006 4/3;580(8):2081-6.

104. Norez C, Antigny F, Becq F, Vandebrouck C. Maintaining low Ca2+ level in the endoplasmic reticulum restores abnormal endogenous F508del-CFTR trafficking in airway epithelial cells. Traffic. 2006;7(5):562-73.

105. Choudhury P, Liu Y, Bick RJ, Sifers RN. Intracellular association between UDP-glucose:Glycoprotein glucosyltransferase and an incompletely folded variant of α1-antitrypsin. Journal of Biological Chemistry. 1997 May 16;272(20):13446-51.

106. Capps GG, Zúñiga MC. Class I histocompatibility molecule association with phosphorylated calnexin. implications for rates of intracellular transport. Journal of Biological Chemistry. 1994 April 15;269(15):11634-9.

107. Schmidt BZ, Perlmutter DH. Grp78, Grp94, and Grp170 interact with α1-antitrypsin mutants that are retained in the endoplasmic reticulum. American Journal of Physiology - Gastrointestinal and Liver Physiology. 2005 September 01;289(3):G444-55.

108. Graf GA, Cohen JC, Hobbs HH. Missense mutations in ABCG5 and ABCG8 disrupt heterodimerization and trafficking. Journal of Biological Chemistry. 2004 June 04;279(23):24881-8.

109. Hammerle MM, Aleksandrov AA, Chang XB, Riordan JR. A novel CFTR disease-associated mutation causes addition of an extra N-linked oligosaccharide. Glycoconj J. 2000 Nov;17(11):807-13.

110. Helenius A, Trombetta ES, Hebert DN, Simons JF. Calnexin, calreticulin and the folding of glycoproteins. Trends Cell Biol. 1997 05/01;7(5):193-200.

111. Ding W, Albrecht B, Luo R, Zhang W, Stanley JRL, Newbound GC, et al. Endoplasmic reticulum and cis-golgi localization of human T-lymphotropic virus type 1 p12I: Association with calreticulin and calnexin. Journal of Virology. 2001 August 15;75(16):7672-82.

112. Gruener M, Bravo IG, Momburg F, Alonso A, Tomakidi P. The E5 protein of the human papillomavirus type 16 down-regulates HLA-I surface expression in calnexin-expressing but not in calnexin-deficient cells. Virol J. 2007 Oct 30;4:116.

113. Miura S, Kawana K, Schust DJ, Fujii T, Yokoyama T, Iwasawa Y, et al. CD1d, a sentinel molecule bridging innate and adaptive immunity, is downregulated by the human papillomavirus (HPV) E5 protein: A possible mechanism for immune evasion by HPV. J Virol. 2010 Nov;84(22):11614-23.

114. Neufeld EB, Remaley AT, Demosky SJ, Stonik JA, Cooney AM, Comly M, et al. Cellular localization and trafficking of the human ABCA1 transporter , Journal of Biological Chemistry. 2001 July 20;276(29):27584-90.

115. Cheng PC, Dykstra ML, Mitchell RN, Pierce SK. A role for lipid rafts in B cell antigen receptor signaling and antigen targeting. The Journal of Experimental Medicine. 1999 December 06;190(11):1549-60.

116. Giese SI, Woerz I, Homann S, Tibroni N, Geyer M, Fackler OT. Specific and distinct determinants mediate membrane binding and lipid raft incorporation of HIV-1SF2 nef. Virology. 2006 11/25;355(2):175-91.

117. Myhill N, Lynes EM, Nanji JA, Blagoveshchenskaya AD, Fei H, Carmine Simmen K, et al. The subcellular distribution of calnexin is mediated by PACS-2. Molecular Biology of the Cell. 2008 July 01;19(7):2777-88.

118. Xia Z, Liu Y. Reliable and global measurement of fluorescence resonance energy transfer using fluorescence microscopes. Biophys J. 2001 10/01;81(4):2395-402.

119. Tanaka AR, Ikeda Y, Abe-Dohmae S, Arakawa R, Sadanami K, Kidera A, et al. Human ABCA1 contains a large amino-terminal extracellular domain homologous to an epitope of sjögren's syndrome. Biochem Biophys Res Commun. 2001 5/25;283(5):1019-25.

120. Zhang Q, Tector M, Salter RD. Calnexin recognizes carbohydrate and protein determinants of class I major histocompatibility complex molecules. Journal of Biological Chemistry. 1995 February 24;270(8):3944-8.

121. Vassilakos A FAU - Cohen-Doyle,,M.F., Cohen-Doyle MF FAU - Peterson,,P.A., FAU PP, FAU JM, Williams DB. The molecular chaperone calnexin facilitates folding and assembly of class I histocompatibility molecules. The EMBO journal JID - 8208664. 0606.

122. Tector M, Zhang Q, Salter RD. B2-microglobulin and calnexin can independently promote folding and disulfide bond formation in class I histocompatibility proteins. Mol Immunol. 1997 4;34(5):401-8.

123. Danilczyk UG, Williams DB. The lectin chaperone calnexin utilizes polypeptide-based interactions to associate with many of its substrates in vivo. Journal of Biological Chemistry. 2001 July 06;276(27):25532-40.

124. Simmons A, Gangadharan B, Hodges A, Sharrocks K, Prabhakar S, García A, et al. Nef-mediated lipid raft exclusion of UbcH7 inhibits cbl activity in T cells to positively regulate signaling. Immunity. 2005 12/01;23(6):621-34.

125. Krautkrämer E, Giese SI, Gasteier JE, Muranyi W, Fackler OT. Human immunodeficiency virus type 1 nef activates p21-activated kinase via recruitment into lipid rafts. Journal of Virology. 2004 April 15;78(8):4085-97.

126. Rauch S, Pulkkinen K, Saksela K, Fackler OT. Human immunodeficiency virus type 1 nef recruits the guanine exchange factor Vav1 via an unexpected interface into plasma membrane microdomains for association with p21-activated kinase 2 activity. Journal of Virology. March 15, 2008 March 15, 2008;82(6):2918-29.

127. Guzzi F, Celano E, Levi G, Parenti M. Interaction between HIV-1 NEF and go proteins in transfected COS-7 cells. Biochem Biophys Res Commun. 2000 4/13;270(2):570-5.

128. Witte V, Laffert B, Gintschel P, Krautkrämer E, Blume K, Fackler OT, et al. Induction of HIV transcription by nef involves lck activation and protein kinase cθ raft recruitment leading to activation of ERK1/2 but not NFκB. The Journal of Immunology. 2008 December 15;181(12):8425-32.

129. Mazzolini J, Herit F, Bouchet J, Benmerah A, Benichou S, Niedergang F. Inhibition of phagocytosis in HIV-1–infected macrophages relies on nef-dependent alteration of focal delivery of recycling compartments. Blood. 2010 May 27;115(21):4226-36.

130. Madrid R, Janvier K, Hitchin D, Day J, Coleman S, Noviello C, et al. Nef-induced alteration of the early/recycling endosomal compartment correlates with enhancement of HIV-1 infectivity. Journal of Biological Chemistry. 2005 February 11;280(6):5032-44.

131. Li N, Mak A, Richards DP, Naber C, Keller BO, Li L, et al. Monocyte lipid rafts contain proteins implicated in vesicular trafficking and phagosome formation. Proteomics. 2003;3(4):536-48.

132. Mao H, Diehl AM, Li Y. Sonic hedgehog ligand partners with caveolin-1 for intracellular transport. Lab Invest. 2009 01/12;89(3):290-300.

133. Sevlever DF, Pickett S FAU - Mann,,K.J., FAU MK, Sambamurti K FAU - Medof,,M.E., FAU MM, Rosenberry TL. Glycosylphosphatidylinositol-anchor intermediates associate with triton-insoluble membranes in subcellular compartments that include the endoplasmic reticulum. The Biochemical journal JID - 2984726R. 0103.

134. Pan X, Rudolph JM, Abraham L, Habermann A, Haller C, Krijnse-Locker J, et al. HIV-1 nef compensates for disorganization of the immunological synapse by inducing trans-golgi network–associated lck signaling. Blood. 2012 January 19;119(3):786-97.

135. Hassan R, Suzu S, Hiyoshi M, Takahashi-Makise N, Ueno T, Agatsuma T, et al. Dys-regulated activation of a src tyroine kinase hck at the golgi disturbs N-glycosylation of a cytokine receptor fms. J Cell Physiol. 2009;221(2):458-68.

136. Hiyoshi M, Takahashi-Makise N, Yoshidomi Y, Chutiwitoonchai N, Chihara T, Okada M, et al. HIV-1 nef perturbs the function, structure, and signaling of the golgi through the src kinase hck. J Cell Physiol. 2012;227(3):1090-7.

137. Dikeakos JD, Thomas L, Kwon G, Elferich J, Shinde U, Thomas G. An interdomain binding site on HIV-1 nef interacts with PACS-1 and PACS-2 on endosomes to down-regulate MHC-I. Molecular Biology of the Cell. 2012 June 01;23(11):2184-97.

138. Bentham M, Mazaleyrat S, Harris M. Role of myristoylation and N-terminal basic residues in membrane association of the human immunodeficiency virus type 1 nef protein. Journal of General Virology. 2006 March 01;87(3):563-71.

139. Okiyoneda T, Niibori A, Harada K, Kohno T, Michalak M, Duszyk M, et al. Role of calnexin in the ER quality control and productive folding of CFTR; differential effect of calnexin knockout on wild-type and ΔF508 CFTR. Biochimica et Biophysica Acta (BBA) - Molecular Cell Research. 2008 9;1783(9):1585-94.

140. Okiyoneda T, Harada K, Takeya M, Yamahira K, Wada I, Shuto T, et al. ΔF508 CFTR pool in the endoplasmic reticulum is increased by calnexin overexpression. Molecular Biology of the Cell. 2004 February 01;15(2):563-74.

141. Chambenoit O, Hamon Y, Marguet D, Rigneault H, Rosseneu M, Chimini G. Specific docking of apolipoprotein A-I at the cell surface requires a functional ABCA1 transporter. Journal of Biological Chemistry. 2001 March 30;276(13):9955-60.

142. Hassan HH, Denis M, Lee DD, Iatan I, Nyholt D, Ruel I, et al. Identification of an ABCA1-dependent phospholipid-rich plasma membrane apolipoprotein A-I binding site for nascent HDL formation: Implications for current models of HDL biogenesis. Journal of Lipid Research. 2007 November 01;48(11):2428-42.

143. Vedhachalam C, Ghering AB, Davidson WS, Lund-Katz S, Rothblat GH, Phillips MC. ABCA1-induced cell surface binding sites for ApoA-I. Arteriosclerosis, Thrombosis, and Vascular Biology. 2007 July 01;27(7):1603-9.

144. Azuma Y, Takada M, Shin H, Kioka N, Nakayama K, Ueda K. Retroendocytosis pathway of ABCA1/apoA-I contributes to HDL formation. Genes to Cells. 2009;14(2):191-204.

145. Papandréou M, Barbouche R, Guieu R, Rivera S, Fantini J, Khrestchatisky M, et al. Mapping of domains on HIV envelope protein mediating association with calnexin and protein-disulfide isomerase. Journal of Biological Chemistry. 2010 April 30;285(18):13788-96.

146. Caramelo JJ, Parodi AJ. Getting in and out from calnexin/calreticulin cycles. Journal of Biological Chemistry. 2008 April 18;283(16):10221-5.

147. Suh WK, Mitchell EK, Yang Y, Peterson PA, Waneck GL, Williams DB. MHC class I molecules form ternary complexes with calnexin and TAP and undergo peptide-regulated interaction with TAP via their extracellular domains. The Journal of Experimental Medicine. 1996 August 01;184(2):337-48.

148. Hagmann WF, Schubert JF, Konig JF, Keppler D. Reconstitution of transport-active multidrug resistance protein 2 (MRP2; ABCC2) in proteoliposomes. Biological chemistry JID - 9700112. 0411.

149. Amaral M. CFTR and chaperones. Journal of Molecular Neuroscience. 2004 02/01;23(1-2):41-8.

150. Atkins KM, Thomas L, Youker RT, Harriff MJ, Pissani F, You H, et al. HIV-1 nef binds PACS-2 to assemble a multikinase cascade that triggers major histocompatibility complex class I (MHC-I) down-regulation: ANALYSIS USING SHORT INTERFERING RNA AND KNOCK-OUT MICE. Journal of Biological Chemistry. 2008 April 25;283(17):11772-84.

151. Simmen T, Aslan JE, Blagoveshchenskaya AD, Thomas L, Wan L, Xiang Y, et al. PACS-2 controls endoplasmic reticulum-mitochondria communication and bid-mediated apoptosis. EMBO J. 2005 02/23;24(4):717-29.

152. Jin Y, Cai CY, Zhang X, Zhang H, Hirst JA, Burakoff SJ. HIV nef-mediated CD4 down-regulation is adaptor protein complex 2 dependent. The Journal of Immunology. 2005 September 01;175(5):3157-64.

153. Chaudhuri R, Lindwasser OW, Smith WJ, Hurley JH, Bonifacino JS. Downregulation of CD4 by human immunodeficiency virus type 1 nef is dependent on clathrin and involves direct interaction of nef with the AP2 clathrin adaptor. Journal of Virology. April 15, 2007 April 15, 2007;81(8):3877-90.

154. Chaudhuri R, Mattera R, Lindwasser OW, Robinson MS, Bonifacino JS. A basic patch on α-adaptin is required for binding of human immunodeficiency virus type 1 nef and cooperative assembly of a CD4-nef-AP-2 complex. Journal of Virology. March 15, 2009 March 15, 2009;83(6):2518-30.

155. Williams M, Roeth JF, Kasper MR, Filzen TM, Collins KL. Human immunodeficiency virus type 1 nef domains required for disruption of major histocompatibility complex class I trafficking are also necessary for coprecipitation of nef with HLA-A2. Journal of Virology. 2005 January 01;79(1):632-6.

156. Wonderlich ER, Williams M, Collins KL. The tyrosine binding pocket in the adaptor protein 1 (AP-1) μ1 subunit is necessary for nef to recruit AP-1 to the major histocompatibility complex class I cytoplasmic tail. Journal of Biological Chemistry. 2008 February 08;283(6):3011-22.

157. Scott J, Dawson J. MHC class I expression and transport in a calnexin-deficient cell line. The Journal of Immunology. 1995 July 01;155(1):143-8.

158. Ou W, Bergeron JJM, Li Y, Kang CY, Thomas DY. Conformational changes induced in the endoplasmic reticulum luminal domain of calnexin by mg-ATP and ca. Journal of Biological Chemistry. 1995 July 28;270(30):18051-9.

159. Li Y, Bergeron JJ, Luo L, Ou WJ, Thomas DY, Kang CY. Effects of inefficient cleavage of the signal sequence of HIV-1 gp 120 on its association with calnexin, folding, and intracellular transport. Proceedings of the National Academy of Sciences. 1996 September 03;93(18):9606-11.

160. Chen N, McCarthy C, Drakesmith H, Li D, Cerundolo V, McMichael AJ, et al. HIV-1 down-regulates the expression of CD1d via nef. Eur J Immunol. 2006 Feb;36(2):278-86.

161. Cho S, Knox KS, Kohli LM, He JJ, Exley MA, Wilson SB, et al. Impaired cell surface expression of human CD1d by the formation of an HIV-1 nef/CD1d complex. Virology. 2005 Jul 5;337(2):242-52.

162. Han Y, Wang X, Dang Y, Zheng Y. Demonstration of a novel HIV-1 restriction phenotype from a human T cell line. PLoS ONE. 2008 07/30;3(7):e2796.

163. Zhou T, Han Y, Dang Y, Wang X, Zheng Y. A novel HIV-1 restriction factor that is biologically distinct from APOBEC3 cytidine deaminases in a human T cell line CEM.NKR. Retrovirology. 2009;6(1):31.

164. Antigny F, Norez C, Becq F, Vandebrouck C. Calcium homeostasis is abnormal in cystic fibrosis airway epithelial cells but is normalized after rescue of F508del-CFTR. Cell Calcium. 2008 2;43(2):175-83.

165. Lubamba B, Lebacq J, Lebecque P, Vanbever R, Leonard A, Wallemacq P, et al. Airway delivery of low-dose miglustat normalizes nasal potential difference in F508del cystic fibrosis mice. American Journal of Respiratory and Critical Care Medicine. 2009 June 01;179(11):1022-8.

166. Noël S, Wilke M, Bot AGM, De Jonge HR, Becq F. Parallel improvement of sodium and chloride transport defects by miglustat (n-butyldeoxynojyrimicin) in cystic fibrosis epithelial cells. Journal of Pharmacology and Experimental Therapeutics. 2008 June 01;325(3):1016-23.

167. Norez C, Antigny F, Noel S, Vandebrouck C, Becq F. A cystic fibrosis respiratory epithelial cell chronically treated by miglustat acquires a non-cystic fibrosis-like phenotype. Am J Respir Cell Mol Biol. 2009 August 1;41(2):217-25.

168. Leonard A, Lebecque P, Dingemanse J, Leal T. A randomized placebo-controlled trial of miglustat in cystic fibrosis based on nasal potential difference. Journal of Cystic Fibrosis. 2012 5;11(3):231-6.

169. Proesmans M, Vermeulen F, De Boeck K. What's new in cystic fibrosis? from treating symptoms to correction of the basic defect. Eur J Pediatr. 2008 Aug;167(8):839-49.

170. Pollock S FAU - Dwek, Raymond,A., FAU DR, FAU BD, Zitzmann N. N-butyldeoxynojirimycin is a broadly effective anti-HIV therapy significantly enhanced by targeted liposome delivery. AIDS (London, England) JID - 8710219. 1204.

171. Libby P, Ridker PM, Hansson GK. Progress and challenges in translating the biology of atherosclerosis. Nature. 2011 05/19;473(7347):317-25.

172. Scandinavian Simvastatin Survival SG. Randomised trial of cholesterol lowering in 4444 patients with coronary heart disease: The scandinavian simvastatin survival study (4S). Lancet. 1994 11/19;344(8934):1383-9.